



COCORA 2017

The Seventh International Conference on Advances in Cognitive Radio

ISBN: 978-1-61208-551-7

April 23 - 27, 2017

Venice, Italy

COCORA 2017 Editors

Calin Vladeanu, University Politehnica of Bucharest, Romania

Shahid Mumtaz, Instituto de Telecomunicações, Portugal

COCORA 2017

Forward

The Seventh International Conference on Advances in Cognitive Radio (COCORA 2017), held between April 23-27, 2017 in Venice, Italy, followed the previous editions dealing with various aspects, advanced solutions and challenges in cognitive (and collaborative) radio networks. It covers fundamentals on cognitive and collaborative radio, specific mechanism and protocols, signal processing (including software defined radio) and dedicated devices, measurements and applications.

Most of the national and cross-national boards (FCC, European Commission) had/have a series of activities in the technical, economic, and regulatory domains in searching for better spectrum management policies and techniques, due to spectrum scarcity and spectrum underutilization issues. Therefore, dynamic spectrum management via cognition capability can make opportunistic spectrum access possible (either by knowledge management mechanisms or by spectrum sensing functionality). The main challenge for a cognitive radio is to detect the existence of primary users reliably in order to minimize the interference to licensed communications. Optimized collaborative spectrum sensing schemes give better spectrum sensing performance. Effects as hidden node, shadowing, fading lead to uncertainties in a channel; collaboration has been proposed as a solution. However, traffic overhead and other management aspects require enhanced collaboration techniques and mechanisms for a more realistic cognitive radio networking

The conference had the following tracks:

- Cognitive radio and emerging technologies
- 5GSPECTRUM: Advanced Spectrum Management in 5G and Beyond Systems
- MEC&mmW: Mobile Edge Computing and Millimeter Waves as Key Technology Enablers

We take here the opportunity to warmly thank all the members of the COCORA 2017 technical program committee, as well as all the reviewers. The creation of such a high quality conference program would not have been possible without their involvement. We also kindly thank all the authors that dedicated much of their time and effort to contribute to COCORA 2017. We truly believe that, thanks to all these efforts, the final conference program consisted of top quality contributions.

We also gratefully thank the members of the COCORA 2017 organizing committee for their help in handling the logistics and for their work that made this professional meeting a success.

We hope that COCORA 2017 was a successful international forum for the exchange of ideas and results between academia and industry and to promote further progress in the field of cognitive radio. We also hope that Venice, Italy provided a pleasant environment during the conference and everyone saved some time to enjoy the unique charm of the city.

COCORA 2017 Committee

COCORA Steering Committee

Ty Znati, University of Pittsburgh, USA

Calin Vladeanu, University Politehnica of Bucharest, Romania

David Haccoun, École Polytechnique de Montréal, Canada

Malgorzata Gajewska, Gdansk University of Technology, Poland

Rogério Dionísio, Instituto Politecnico de Castelo Branco, Portugal

COCORA Industry/Research Advisory Committee

Valerio Frascolla, Intel Deutschland GmbH, Germany

Silvian Spiridon, Broadcom Ltd., USA

Alan A. Varghese, RFMD-TRIQUINT, USA

COCORA 2017 Committee

COCORA Steering Committee

Ty Znati, University of Pittsburgh, USA
Calin Vladeanu, University Politehnica of Bucharest, Romania
David Haccoun, École Polytechnique de Montréal, Canada
Malgorzata Gajewska, Gdansk University of Technology, Poland
Rogério Dionísio, Instituto Politecnico de Castelo Branco, Portugal

COCORA Industry/Research Advisory Committee

Valerio Frascolla, Intel Deutschland GmbH, Germany
Silvian Spiridon, Broadcom Ltd., USA
Alan A. Varghese, RFMD-TRIQUINT, USA

COCORA 2017 Technical Program Committee

Kamran Arshad, Ajman University of Science & Technology, UAE / University of Greenwich, UK
Vivek Bohara, Indraprastha Institute of Information Technology, Delhi, India
Faouzi Bouali, University of Surrey, UK
Daniel B. da Costa, Federal University of Ceará (UFC), Brazil
Rogério Dionísio, Instituto Politecnico de Castelo Branco, Portugal
Ozgur Ergul, Koc University, Turkey
Michael Fitch, British Telecommunications, UK
Valerio Frascolla, Intel Deutschland GmbH, Germany
Malgorzata Gajewska, Gdansk University of Technology, Poland
Slawomir Gajewski, Gdansk University of Technology, Poland
Shimin Gong, Shenzhen Institutes of Advanced Technology, Chinese Academy of Science, China
Sanjeev Gurugopinath, PES University, India
David Haccoun, École Polytechnique de Montréal, Canada
Miguel López-Benítez, University of Liverpool, UK
Irene Macaluso, CONNECT | Trinity College, Dublin, Ireland
R. Muralishankar, CMR Institute of Technology, India
Miia Mustonen, VTT Technical Research Centre of Finland, Finland
Karthick Parashar, IMEC, Leuven, Belgium
Pekka Pirinen, University of Oulu, Finland
Mubashir Husain Rehmani, COMSATS Institute of Information Technology, Pakistan
Tanguy Risset, CITI-INRIA | Insa-Lyon, France
Ali Sadri, Intel Corporation, USA
H. N. Shankar, CMR Institute of Technology, India

Vinod Sharma, Indian Institute of Science, Bangalore, India
Bhabani Sinha, Indian Statistical Institute, India
Silvian Spiridon, Broadcom Ltd., USA
Michal Szydelko, Huawei Technologies, Sweden
Alan A. Varghese, RFMD-TRIQUINT, USA
Calin Vladeanu, University Politehnica of Bucharest, Romania
Seppo Yrjölä, Nokia, Finland
Ty Znati, University of Pittsburgh, USA

Copyright Information

For your reference, this is the text governing the copyright release for material published by IARIA.

The copyright release is a transfer of publication rights, which allows IARIA and its partners to drive the dissemination of the published material. This allows IARIA to give articles increased visibility via distribution, inclusion in libraries, and arrangements for submission to indexes.

I, the undersigned, declare that the article is original, and that I represent the authors of this article in the copyright release matters. If this work has been done as work-for-hire, I have obtained all necessary clearances to execute a copyright release. I hereby irrevocably transfer exclusive copyright for this material to IARIA. I give IARIA permission to reproduce the work in any media format such as, but not limited to, print, digital, or electronic. I give IARIA permission to distribute the materials without restriction to any institutions or individuals. I give IARIA permission to submit the work for inclusion in article repositories as IARIA sees fit.

I, the undersigned, declare that to the best of my knowledge, the article does not contain libelous or otherwise unlawful contents or invading the right of privacy or infringing on a proprietary right.

Following the copyright release, any circulated version of the article must bear the copyright notice and any header and footer information that IARIA applies to the published article.

IARIA grants royalty-free permission to the authors to disseminate the work, under the above provisions, for any academic, commercial, or industrial use. IARIA grants royalty-free permission to any individuals or institutions to make the article available electronically, online, or in print.

IARIA acknowledges that rights to any algorithm, process, procedure, apparatus, or articles of manufacture remain with the authors and their employers.

I, the undersigned, understand that IARIA will not be liable, in contract, tort (including, without limitation, negligence), pre-contract or other representations (other than fraudulent misrepresentations) or otherwise in connection with the publication of my work.

Exception to the above is made for work-for-hire performed while employed by the government. In that case, copyright to the material remains with the said government. The rightful owners (authors and government entity) grant unlimited and unrestricted permission to IARIA, IARIA's contractors, and IARIA's partners to further distribute the work.

Table of Contents

Analysis of Sharing Economy Antecedents for Recent Spectrum Sharing Concepts <i>Seppo Yrjola, Marja Matinmikko, Miia Mustonen, and Petri Ahokangas</i>	1
New Spectrum Sensing based on Goodness of Fit Testing for Cognitive Radio <i>Djamel Teguig and Horlin Francois</i>	11
Spread Spectrum-Based Underlay Cognitive Radio Wireless Networks <i>Saed Daoud, David Haccoun, and Christian Cardinal</i>	20
Experimentation with Radio Environment Maps for Resources Optimisation in Dense Wireless Scenarios <i>Rogério Pais Dionisio, Tiago Ferreira Alves, and Jorge Miguel Afonso Ribeiro</i>	25
X2-Based Handover Performance in LTE Ultra-Dense Networks using NS-3 <i>Sherif Adeshina Busari, Shahid Mumtaz, Kazi Mohammed Saidul Huq, and Jonathan Rodriguez</i>	31
Performance Analysis of Downlink CoMP Transmission in Long Term Evolution-Advanced (LTE-A) <i>Maryem Neyja, Shahid Mumtaz, and Jonathan Rodriguez</i>	37

Analysis of Sharing Economy Antecedents for Recent Spectrum Sharing Concepts

Seppo Yrjölä
Nokia
Oulu, Finland
e-mail: seppo.yrjola@nokia.com

Marja Matinmikko
University of Oulu
Oulu, Finland
e-mail: mmatinmi@ee.oulu.fi

Miia Mustonen
VTT Technical Research Centre of Finland
Oulu, Finland
e-mail: miia.mustonen@vtt.fi

Petri Ahokangas
Oulu Business School
Oulu, Finland
e-mail: petri.ahokangas@oulu.fi

Abstract—The exponential growth of wireless services with diversity of devices and applications depending on connectivity has inspired the research community to come up with novel concepts to improve the efficiency of spectrum use. Recently, several spectrum sharing system concepts have been introduced and widely researched to cope with spectrum scarcity, though, to date, only a few have reached the policy and standardization phase. Moreover, only a subset of these concepts has gained industry interest with pre-commercial deployments and lucrative business model characteristics. This paper analyzes sharing economy business antecedent factors of the three topical regulatory approaches for spectrum sharing: global TV White Space (TVWS), Licensed Shared Access (LSA) from Europe, and Citizens Broadband Radio Service (CBRS) from the US. A comparison is made between these concepts to identify similarities and differences for developing a successful scalable sharing concept. Key factors for a sharing economy enabled scalable business model are introduced including platform, reduced need for the ownership, leverage of underutilized assets, adaptability to different policy regimes, trust, and value orientation. The results indicate that all analyzed sharing concepts meet basic requirements to scale, TVWS radically lowering entry barrier, LSA leveraging key existing assets and capabilities of mobile network operators, and CBRS extending the business model dynamics. The Sharing Economy provides a dynamic framework for analyzing and developing the spectrum sharing business models.

Keywords—business model; Citizens Broadband Radio Service; cognitive radio; sharing economy; spectrum management; Licensed Shared Access; TV White Space.

I. INTRODUCTION

We have seen the exponential growth of wireless services, applications and devices, requiring connectivity. Furthermore, the number of mobile broadband (MBB) subscribers and the amount of data consumed is set to grow significantly [1], leading to increasing spectrum demand. Both the European Commission (EC) [2] and the US President's Council of Advanced Science & Technology

(PCAST) [3] have recently emphasized the need for novel thinking within wireless industry to cope with the growing capacity crunch in spectrum allocation, utilization and management. The prominence of dynamic spectrum access and spectrum sharing has been emphasized in improving the efficiency of the spectrum utilization through balancing across domains with different spectrum dynamics. For any spectrum sharing framework to emerge and scale, close cooperation between research, regulation and across industry domains is essential. The collaboration between research and industry plays a central role in validating enabling platforms, technologies and innovations. The spectrum regulation and standardization has played a central role in enabling current multibillion business ecosystems: For the MBB via exclusive Quality of Service (QoS) spectrum usage rights, and at the same time for unlicensed wireless local area network (Wi-Fi) ecosystem drawing from the public spurring innovations. Without sound and sustainable business models for all the key industry stakeholders, new concepts will not become deployed in a large scale.

To date, only few of the Dynamic Spectrum Access (DSA) concepts from research have crossed the threshold into policy domain. Furthermore, several spectrum sharing concepts supported by National Regulatory Authorities (NRA) and standardization have not to date scaled up in the wireless services market, the TV White Space (TVWS) being the latest example. After a decade of profound unlicensed TVWS concept research, standardization and trials in the US [4] and the UK [5] with their key learnings, license based sharing models have recently emerged and are under regulatory discussion, standardization and pre-commercial trials. The most prominent novel spectrum sharing concepts are the Licensed Shared Access (LSA) [6] from Europe and the three-tiered Citizens Broadband Radio Service (CBRS) from the US [7].

Development of business models for spectrum sharing can benefit from the previous work on business models in the Internet business domain. Scalable business model analysis has been developed by Amit and Zott [8] as a model of e-business based on four independent dimensions:

efficiency, complementarities, lock-in, and novelty. Rappa [9] classified the Web-based business models as brokerage model, advertising model, information-intermediary model, merchant model, manufacturer direct model, affiliate model, community model, subscription model, and utility and hybrid models. Bouwman et al. [10] differentiate in their business model analysis business model effects: organizational structure, services, technology, revenue, and environmental factors: regulation, technology, market. Hallowell [11] stated a scalability paradox that while the reduction of scalability is often caused by human intervention, the competitive advantage based on differentiation is also gained by human intervention. Stampfl identified and categorized the antecedents of business model scalability into five mutually exclusive factors in the explorative business model scalability model [12], which Stephany adapted into his sharing economy definition [13].

For all of the three spectrum sharing concepts there is no prior work available in particular regarding their business model design comparative analysis. An initial evaluation of the general spectrum sharing concept from the business modeling point of view can be found in [14]. Business modelling for the TVWS network was discussed in [15], and the LSA focused strategy and business model analysis in [16][17]. Business model typology and scalability analysis for the LSA and the CBRS were done in [18]. We extend that work by focusing on analyzing and comparing the viability and attractiveness of all three spectrum sharing concepts using sharing economy [19] antecedent factors. This paper investigates:

How do recent spectrum sharing concepts support the antecedents for business model scalability in the sharing economy framework?

The rest of the paper is organized as follows. First, the TVWS, the LSA and the CBRS sharing concepts are introduced in Section II. Theoretical background for the sharing economy is introduced in Section III. The business model characteristics and sharing economy antecedents for the TVWS, the LSA, and the CBRS spectrum sharing concepts are derived and analyzed in Section IV. Finally, conclusions are drawn in Section V.

II. OVERVIEW OF RECENT SPECTRUM SHARING CONCEPTS

This section presents the three prominent spectrum sharing frameworks and system concepts under discussion in regulatory domain: the TVWS, the LSA and the CBRS. The common intention of the concepts is to improve spectrum usage efficiency by allowing new users to access a spectrum on the space or time basis when not being used by the incumbent system(s) currently holding the spectrum usage rights. Detailed description and the status of the TVWS, the LSA, the CBRS, and the concepts and technologies, under continuous revision can be found for example in [4][5], [20][21], and [22][23], respectively.

A. TV White Space

In this section, the opportunistic TV White Space concept utilizing terrestrial broadcasting Ultra High Frequency

(UHF) spectrum is discussed in general level. TVWS standardization is spread to several organizations around the world, and there is no single dominant standard, technology or solution to date. In addition to Wi-Fi based technologies focused on in this paper, also other radio technologies like Long Term Evolution (LTE) and Worldwide Interoperability for Microwave Access (WiMAX) have been experimented for TVWS.

The TVWS aims to improve spectrum efficiency through utilizing the unused and underutilized spectrum in space and time based on databases. In this concept, license-exempt White Space Devices (WSDs) obtain the available channel information via a certified Geo-Location Database (GLDB), which optimizes the effective reuse of the spectrum, and ensures interference free operation for the incumbent licensed users. The GLDB stores and periodically updates TV licensees' Digital Terrestrial TV (DTT) network infrastructure and channel occupancy information, and in the case of the UK, the Program Making and Special Events (PMSE) service usage data. In the operations phase, to access the TVWS spectrum, WSD base stations reports locations to a GLDB, which computes and returns the available TV channels for WSDs. Figure 1 below depicts an overview of the TVWS framework, and how access to white spaces based on the GLDB would work in the UK case. In the preparatory phase, the GLDB will deploy the basic operational dataset provided by the Office of Communications (Ofcom) consisting of DTT coexistence data, location agnostic data, PMSE data, and unscheduled adjustments data. A master WSD would first consult a list of DBs provided by Ofcom hosted Website. Then, it would select its preferred GLDB from the list, and send to it its location and device parameters. The GLDB would then return details of the allowed frequencies and power levels [5].

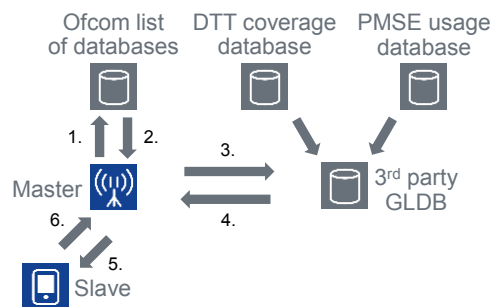


Figure 1. Overview of TV White Spaces framework in the UK.

In the US, the FCC has finalized the TVWS regulation [24], followed by the Infocomm Development Authority (IDA) of Singapore [25] in 2014 and Ofcom from the UK in 2015 [5]. The ECC prepared European level technical framework in the European Conference of Postal and Telecommunications (CEPT) FM53 working group [26]. The TVWS regulatory frameworks to date have been unprotected and license-exempt, applicable for deploying the most prominent TVWS Wi-Fi version of IEEE 802.11af [27]. The FCC has temporarily certified several companies

including Google, Microsoft, and Spectrum Bridge as geolocation database operators. In UK, Fairspectrum, Nominet UK, Sony Europe, and Spectrum Bridge are qualified to provide database services for the TVWS. The first use cases of the TVWS in the US have been fixed Wireless Internet Service Provisioning (WISP) for rural communities and industry verticals, where another connection technology, typically Wi-Fi, is needed between the User Equipment (UE) and the TVWS Customer Premises Equipment (CPE).

B. Licensed Shared Access (LSA)

The EC communication based on an industry initiative promoted spectrum sharing across wireless industry and different types of incumbents [28]. In 2013, the Radio Spectrum Policy Group (RSPG) of the EC defined LSA as [2] “a regulatory approach aiming to facilitate the introduction of radio communication systems operated by a limited number of licensees under an individual licensing regime in a frequency band already assigned or expected to be assigned to one or more incumbent users. Under the LSA framework, the additional users are allowed to use the spectrum (or part of the spectrum) in accordance with sharing rules included in their rights of use of spectrum, thereby allowing all the authorized users, including incumbents, to provide a certain QoS.”

The recent development in policy, standardization and architecture has focused on applying the LSA to leverage scale and harmonization of the Third Generation Partnership Project (3GPP) ecosystem. This would enable MBB systems to gain shared access to additional harmonized spectrum assets not currently available on exclusive basis, particular the 3GPP band 40 (2.3-2.4 GHz) as defined by the CEPT [29]. The European Telecommunications Standards Institute (ETSI) introduced related system reference, requirements and architecture documents [21][30][31] from the standardization perspective. In the LSA concept, the incumbent spectrum user, such as a PMSE video link, a telemetry system, or a fixed link operator, is able to share the spectrum assigned to it with one or several LSA licensee users according to a negotiated *sharing framework* and *sharing agreement*. The LSA model guarantees protection from harmful interference with predictable QoS for both the incumbent and the LSA licensee.

The LSA architecture consists of two new elements to protect the rights of the incumbent, and for managing dynamics of the LSA spectrum availability shown in Figure 2: the LSA Repository (LR) and the LSA Controller (LC). The LR supports the entry and storage of the information about the availability, protection requirements and usage of spectrum together with operating terms and rules. The LC located in the LSA licensee’s domain grants permissions within the mobile network to access the spectrum based on the spectrum resource availability information from the LR. The LC interacts with the licensee’s mobile network in order to support the mapping of LSA resource availability information (LSRAI) into appropriate radio transmitter configurations via Operation, Administration and

Management (OAM) tools, and to receive the respective confirmations from the network.

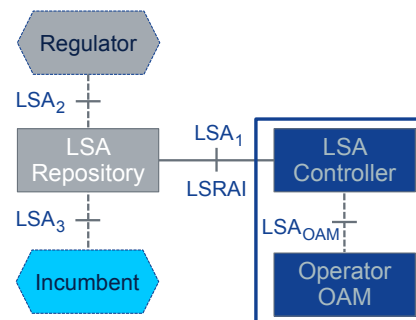


Figure 2. The LSA architecture reference model.

The LSA system for 2.3-2.4 GHz band has been validated in field trials in Finland, Italy and France. Architecture, implementation and field trial results are presented, e.g., in [32] – [35]. The second use case currently being considered in European regulation is the application of LSA to the 3.6-3.8 GHz band [36]. For this band, the incumbent usage is less dynamic, and the LSA band availability is guaranteed in the license area for a known period. This allows extension to more innovative use cases, such as local networks using small cells, as there is no need for additional frequency resource or existing infrastructure to support dynamic handover.

C. Citizens Broadband Radio Service (CBRS)

As the LSA policy discussion started in Europe, in the US the CBRS concept started to gain interest as a complementary spectrum management approach. In the US, the PCAST report [3] in 2012 suggested a dynamic spectrum sharing model as a new tool to the US wireless industry to meet the growing crisis in spectrum allocation, utilization and management. The key policy messages of the document were further strengthened in 2013 with Presidential Memorandum [37] stating “...we must make available even more spectrum and create new avenues for wireless innovation. One means of doing so is by allowing and encouraging shared access to spectrum that is currently allocated exclusively for Federal use. Where technically and economically feasible, sharing can and should be used to enhance efficiency among all users and expedite commercial access to additional spectrum bands, subject to adequate interference protection for Federal users.”

In Figure 3, the US three-tier authorization framework with the FCC’s spectrum access models for 3550-3650MHz and 3650-3700MHz spectrum segments is illustrated. While the general CBRS framework could be applied to any spectrum and between any systems, the current regulatory efforts in the Federal Communications Commission (FCC) are concentrated on the 3550-3700 MHz band as the first use case [7]. The standardization process for the CBRS is ongoing in the Wireless Innovation Forum (WinnForum)

[23], and for the specific spectrum band in the 3GPP [38]. The three tiers are:

1) Incumbent Access (IA) layer consists of the existing primary operations including authorized federal users and Fixed Service Satellite (FSS) earth stations. The IA is protected from harmful interference from the CBRS users by geographic exclusion zones and interference management conducted by the dynamic Spectrum Access System (SAS),

2) Priority Access (PA) layer includes critical access users like hospitals, utilities, governmental users, and non-critical users, e.g., Mobile Network Operators (MNOs). PA users receive short-term priority authorization (currently, a three year authorization is considered) to operate within designated geographic census track with Priority Access Licenses (PALs) in 10 MHz unpaired channel. PALs will be awarded with competitive bidding, and with ability to aggregate multiple consecutive PALs and census tracks in order to obtain multi-year rights and to cover larger areas. Any entity eligible to hold a FCC license could apply for a PAL and is protected from harmful interference from the General Authorized Access (GAA) layer.

3) General Authorized Access layer users, e.g., residential, business and others, including Internet service providers are entitled to use the spectrum on opportunistic *license-by-rule* regulatory basis without interference protection. In addition to the 50% GAA spectrum availability floor specified to ensure nationwide GAA access availability, the GAA could access unused PA frequencies. GAA channels are dynamically assigned to users by a SAS. The addition of the third tier is intended to maximize spectrum utilization, and to extend usage from centralized managed Base Stations (BSs) to stand-alone GAA access points (CBSDs).

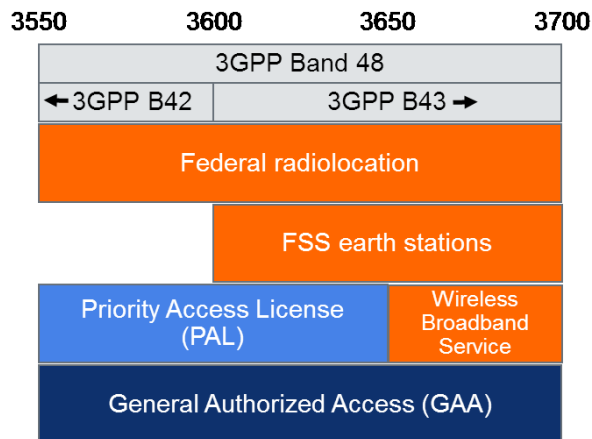


Figure 3. The US 3-tiered CBRS spectrum access model and band plan.

The SAS dynamically determines and assigns PAL channels and GAA frequencies at a given geographic location, controls the interference environment, and enforces exclusion zones to protect higher priority users as well as takes care of registration, authentication and identification of user information. In 2016, the FCC finalized rules for CBRS [7], and introduced the *light-touch leasing* process to make

the spectrum use rights held by PALs available in secondary markets. Under the light-touch leasing rules, PA Licensees are free to lease any portion of their spectrum or license outside of their PAL protection area (PPA) without the need for the FCC oversight required of partitioning and disaggregation. This allows lessees of PALs to provide targeted services to geographic areas or quantities of spectrum without additional administrative burden. Coupled with the minimum availability of 80 MHz GAA spectrum in each license area, these rules will provide the increased flexibility to serve specific or targeted markets. Furthermore, the FCC will let market forces determine the role of a SAS, and as such, a stand-alone exchanges or a SAS-managed exchanges are permitted.

In the dialog between industries [39], the FCC and the main incumbent user, United States Department of Defense (DoD), it is assumed that in addition to informing database approach, there is a need to introduce a Non-Informing Approach, requiring *Environmental Sensing Capability* (ESC). The ESC architecture and implementation scenarios discussed include a dedicated sensing network for a SAS, collaborative sensing by commercial network BSs, or their combination. According to the FCC rules [7], the SAS must either confirm suspension of the CBSD's operation or its relocation within 300 seconds after the ESC detection communication, or other type of notification from the current federal user of the spectrum band.

III. BUSINESS MODEL AND SHARING ECONOMY ANTECEDENTS

Business models in general are built to exploit a business opportunity [40], in connection with the company and its external business environment [41]. In order to gain and sustain competitive advantage, companies must continuously develop and renew their business models. In the development of any new spectrum sharing concept, it is essential to consider the underlying business opportunities and the business model elements that are attractive and feasible for all the key stakeholders. Authors in [42] define business model in general as a framework across three analytical building blocks: a) focus of the business (activities that provide the basis for value creation and capture), b) locus of the business (i.e., defining the potential and scalability of business), and c) modus of business (simplicity and dynamism of business). The discussed spectrum sharing concepts confront the MBB and the wireless industry with strategic environmental changes, such as emerging competitive market structures, policy and regulatory changes as well as technology complexity, which all require companies to adapt or reinvent one or more aspects of their business model designs. In the following, the theoretical frameworks used to analyze how business models and their key elements could evolve and scale in response to novel spectrum sharing models are introduced.

Potential for scalability is an important aspect when developing a business model, and synchronizing it to the respective business opportunity is crucial. The scalability of the business model and its key elements has been shown to be the primary driver for the venture growth [43], and the

attractor towards venture capital investments [44]. Vertical scalability approach scales-up a system by adding more resources into the system nodes, while the horizontal scale-out approach adds more nodes to the whole system. Stampfl identified and categorized the antecedents of business model scalability into five mutually exclusive factors in the explorative business model scalability model [12]: technology, cost and revenue structure, adaptability to different legal regimes, network effects, and user orientation.

The emerging *sharing economy framework* has leveraged these scalability factors with focus on resource efficiency and on-demand platform [45]. Through studying recent early adopters of the framework, Stephany [13] defined sharing economy as “*the value in taking the underutilized assets and making them accessible online to a community, leading to a reduced need for ownership of those assets.*” Furthermore, the framework originated from collaborative individual peer-to-peer community consumption has lately evolved to corporations and governments participating in the ecosystem as buyers, sellers or lenders [46]. Proposed sharing economy antecedent factors used in assessing business model characteristics of the spectrum sharing concepts are:

- a) *Platform for online, on-demand accessibility,*
- b) *Reduced need for the ownership,*
- c) *Utilization of underutilized assets,*
- d) *Adaptability to different legal and policy regimes,*
- e) *Communities and trust, and*
- f) *Value creation and user orientation.*

Each of these antecedent factors relate to the specificities of the focus, locus and modus of the business in question.

IV. ANALYSIS OF THE SPECTRUM SHARING CONCEPTS

The three spectrum sharing models, the TVWS, the LSA, and the CBRS, introduced and discussed in Section II are next analyzed and compared against the sharing economy criteria presented in Section III. The summary of the sharing economy antecedent analysis is given in Table 1.

A. Platform

Sharing economy business models are hosted through platforms and automatized processes that enable a more precise, real-time measurement of available capacity, and the ability to dynamically making that capacity accessible. This dynamic adaptability to short-term changes, and automatic configuration of radio infrastructure and user equipment is the key differentiator to static sharing concepts, e.g., in the Industrial, Scientific and Medical (ISM) spectrum bands. The global 3GPP ecosystem with scale and harmonization will be the common technology scalability factor for the LSA and the CBRS approaches, while the TVWS has heritage on the Institute of Electrical and Electronics Engineers (IEEE) Wi-Fi ecosystem at the ISM bands.

Compared to the LSA and the CBRS, regulatory and standardization actions for the TVWS have been concluded. However, to date the TVWS platform has not reached a tipping point, in spite of support from several major IT

companies providing the GLDB. Interference constraints and strict technical requirements entail dedicated radio designs. Furthermore, radio ecosystem has not scaled due to scattered standardizations, lack of mobile operators’ interest, and the lack of certainty for the long-term availability of white spaces.

The deployment of the LSA system will require relatively small changes to the existing mobile broadband infrastructure. MNOs can utilize existing network off-the-shelf, and build additional LSA controller as an added Self Organizing Network (SON) functionality on top of the OAM system. In the LSA system, envisaged for the 2.3-2.4 GHz band, spectrum control is inside the MNO domain, and diffusion towards cognitive networks, in large, could be retained within MNOs control. Furthermore, the LR has low complexity compared other sharing concepts as sharing will be static or semi-static and binary between the incumbent and the licensee.

In the CBRS model with higher dynamics, the third opportunistic GAA layer and sensing function will require a more complex SAS system. In managing a higher volume of dynamic transactions, big data analytics capabilities of Internet players could become of need and bring competitive advantage. In the radio access side, higher dynamics in the spectrum control across the PA and the GAA layers and operator service areas will necessitate advanced spectrum analytics and horizontal co-existence management. Furthermore, with tight response time requirements this could also affect radio design of base stations. On the other hand, the PAL and the GAA layers with the common SAS will offer opportunities to common markets for licensed and licensed-by-rule equipment, and services across customer segments. Higher frequency and the small cell focus layer enables CBRS operators to utilize their fixed optical infra assets in backhauling. In addition to this, the GAA layer has an optimal opportunity to leverage emerging LTE unlicensed and Wi-Fi ecosystems to scale and complement LTE operator and stand-alone solutions.

B. Reduced Need for the Ownership

The second factor deals with the superior value proposition and transactions that offer access over ownership, and ability to realize more choices with rapidity and lower initial costs. Sharing economy are spawning a variety of efficient new as-a-service (aaS) business models.

In the unlicensed TVWS concept, only device authorization is needed before starting operations on practically free spectrum, which radically lowers the entry barrier compared to two other concepts. Unlimited number of users are administratively imposed, rather than voluntarily chosen. Concept scores well in terms of efficiency of frequency bands utilization and rapidity of access. In the UK TVWS concept, the unlicensed approach is complemented with a licensed option for devices that must be manually configured.

The LSA concept offers lower cost spectrum without coverage obligations, with QoS guaranteed by licensing. For a greenfield operator, the up-front investment in spectrum license combined with needed infrastructure continues to set

an entry barrier. Therefore, the second use case of LSA on the band 3.6-3.8 GHz envisaged for more local licenses and deployment without need for existing mobile infrastructure or specific network management tools provides opportunities that are more prominent for new entrants. Extra capacity could in addition offer a scale-out opportunity with a wholesale service. The PAL operator in the CBRS could deploy similar kind of business model designs.

The CBRS three-tiered regulatory approach could disruptively unbundle investment in spectrum, network infrastructure and services. Access to low cost spectrum with lower initial annuity payments for spectrum rights enables local 'pro-competitive' deployments, and further expands sharing mechanism for infra resources between operators. Furthermore, the light-touch leasing process will make the spectrum use rights held by a PA licensee available in secondary markets. The CBRS concept has potential on a longer term to reduce the need for parallel network infrastructure when spectrum, and related radio access infra assets are tradable, and hosted and shared on-demand and as-a-Service.

C. Utilization of Underutilized Assets

Access and deployment of the underutilized assets on-demand is essential to generate continuous revenue early. The value of the shared spectrum resources is highly dependent on the availability, liquidity and predictability.

Future availability of the shared TVWS spectrum assets is uncertain particularly in the dense urban areas. In rural area, TVWS operators are optimally positioned to create revenues from savings in spectrum costs, extended coverage and increased relative capacity. Coverage has potential to extend the customer base, while capacity could increase the Average Revenue Per User (ARPU). On the other hand, non-guaranteed QoS, heterogeneous incumbent users, and TV channel properties limit usability and the scope of services of the shared resources.

In the LSA approach, a sharing framework and binary sharing agreement negotiated between regulator, incumbent and licensee guarantee QoS and statistically known availability in advance. The LSA sharing framework could be initiated on a voluntary basis, but the regulator also may impose it. Availability of spectrum assets is highly dependent on the regulation, and the LSA was studied in the context of 2.3 GHz spectrum band as the starting point. The second use case currently under discussion is the 3.6-3.8 GHz band, in which case the predictability of spectrum availability is even higher, as dynamic changes in spectrum availability do not occur. Similar predictability is possible for the second tier PAL operator in the CBRS. Utilizing extra capacity established MNOs could create differentiating value proposition around QoS and Quality of Experience (QoE), and have option to expand to capacity wholesale and hosting services.

While the third opportunistic GAA layer offers the Wi-Fi ecosystem type innovation environment, the availability, and particularly the QoS is not guaranteed. This has limited MNOs interest, based on traditional business models with

need for the high upfront investments. On the other hand, both traditional MNOs and alternative operators could use the GAA layer with free spectrum resource for offloading and nomadic Wi-Fi type of Internet access. On dense urban environment, new business model designs and revenue structures could emerge combining spectrum with other shared assets, e.g., small cell hosted solution as-a-service (SCaaS), advertisement & transaction based models, and enabling new vertical segments within Internet of Things (IoT). Furthermore, the three-tier model offers network operators unprecedented flexibility and scalability through the ability for to move between the PA and the GAA tiers. This allows for the use of much shorter leasing periods, 3 years, without requiring a lessee to forgo their investment if their lease does not renew via simply converting from PA to GAA tier. For a new market entrant, this enables to try out their new service utilizing the GAA tier without having to invest in spectrum with future option to choose buy a PA license when / where needed depending on the market and interference protection needs. In the system level, this flexibility and scalability between tiers combined with the secondary market provisions will improve spectrum efficiency in capacity, and particularly in value as spectrum can be regularly re-allocated to the most valuable use. The complexity of the CBRS introduces new independent or integrated roles to the ecosystem related to SAS administration, sensing operator and future spectrum broker that could increase transaction costs in early development. New technology introduction should be continuously assessed in relation with added complexity and transaction costs.

D. Adaptability to Different Legal and Policy Regimes

The harmonization of spectrum management is indispensable to unlock a wide range of positive externalities throughout the entire value chain. Scalability of all sharing concepts could be limited by fragmented national incumbent use cases, related different incumbent protection mechanisms, and regulatory differences affecting repository/database and spectrum management system architectures and implementations.

The TVWS concept is regulated and standardized the US and Europe / the UK with variants, e.g., in Singapore and Canada. While having a negative impact on the platform scale, the low administrative burden approach of the TVWS offers low entry barrier to the market.

Existing European LSA regulatory framework offers legal certainty and security with relatively high initial administrative burden. This protects the turf for established players, but limits the scalability through high entry barrier during the early macro deployments on the 2.3 GHz band. While the LSA offers visibility and predictability needed for high up-front investments in spectrum and infrastructure, both the CBRS and the TVWS regulatory approaches are pro-competitive targeting to lower administrative burden and entry barrier. The higher frequency small cell use cases of the LSA envisage opportunities that are more prominent for new entrants, and similar kind of business model designs than the PAL layer in the CBRS.

The CBRS will have advantage on leveraging the common US market. Sharing concepts in Europe require a harmonized framework in regional standardization and regulation to reach economies of scale. The regulatory and standardization actions needed with regulated or highly political incumbents' ecosystem (like defense, media and broadcasting) will potentially limit the scalability of all the frameworks. Uncertainty is introduced with the short PA licensing terms, and the GAA with opportunistic access only.

E. Communities and Trust

Making spectrum accessible is not enough; the underutilized assets need to move within the community. The trust is the trigger of collaborative shared consumption that makes the system grow and scale. The creation of a critical mass ecosystem with positive network effects is important for all three approaches with new context model based spectrum administrator and broker roles.

The TVWS concept rules out the possibility of decentralized agreement over accepted interference levels and is prone to the tragedy of the commons as number of competitive users grows. Heterogeneous GLDB operators in terms of services and business models may have additional negative impact to the community and the trust factor.

The repository or database is the vehicle to accomplish trust in all the models. Trust in the predictability of QoS and pragmatic incumbent protection is built on binary agreements and implemented in LSA Repository. In the CBRS, the database approach is complemented by the ESC for defense incumbents. Additional challenge for the CBRS is protection of MNOs business critical information assets in a SAS, and to meet stringent DoD's Operational Security (OPSEC) requirements.

In network externalities, business model designs represent a co-opetitive situation between MBB, wireless Internet and Internet domains. TVWS operators leverage their niche through tailoring according to local customer segment they serve benefiting of extended coverage. Furthermore, particularly in rural use cases, communication bit rates could be increased to level that enables access to Internet and media services to new user group.

In case LSA licensees have existing infrastructure and dedicated resources in other mobile bands, they can utilize their connectivity scale and customer base to achieve instant critical mass, and use existing consumer ownership on connectivity for lock-in. New entrants in the case of LSA and CBRS could build their critical mass and lock-ins using Internet 'innovation' ecosystems, and consumer and customer data ownership on apps and services.

Shared spectrum local small cell deployments in all the sharing concepts scale out ecosystems from legal and real estate aspects to radio planning and site camouflaging, as small cells will attach to structures and building assets not owned by traditional operator. This creates additional opportunities for sharing and collaboration between operators and various specialist companies like infrastructure owners and providers, real estate and street furniture owners, utility service companies and backhaul providers.

F. Value Creation and User Orientation

Sharing economy platforms create reciprocal economic value. Simplicity of the offer built around user knowledge driven 'demand pull' is critical in differentiating with existing service, as well as in scaling new spectrum sharing enabled services.

In the TVWS concept, unlicensed users' QoS is not protected. To date, the primary commercial 'niche' use case has been the non-competitive Fixed Wireless Access (FWA) WISP, in which a single GLDB serves a set of unlicensed WSDs belonging to local WISP providing Internet access to unserved rural areas. Free spectrum facilitates local niche services, e.g., for various IoT vertical start-ups. FWA use cases need specialized devices seen as extra complexity by users.

MNOs could utilize the surplus LSA spectrum in strengthening customer satisfaction through fulfilling existing need pull with familiar services and simplicity of the offer built on existing customer data via customer experience management tools. In general, spectrum sharing technologies should only be visible to end user through benefits offered in availability, coverage, capacity, data rates, or as decreased service costs. Both the LSA and the CBRS can also facilitate introduction of innovative local business model designs. For MNOs, they enable differentiation opportunities in serving more heterogeneous customer segments, e.g., consumers and enterprises, and for alternative type operators like Internet players faster efficient access to new systems and services. Local and Internet players are uniquely positioned to offer differentiation around existence of their extensive user knowledge. On one hand, operators prefer specialized services, or enhanced QoS traffic delivery for a fee to content, application, or over-the-top service providers. On the other hand, new entrants from Internet domain, in particular, on the GAA layer would like to see broadband as a utility, transparent and non-exclusive basis.

In addition to provide mandatory spectrum availability information brokerage, the LSA repository, the SAS, and the GLDB administrators can capture value through selling advanced information regarding the quality of the shared spectrum based on information from both the incumbents and other sharing users. These value added services will be framed by regulatory action, and their value will increase with the number of service users, creating a positive network externality. On the other hand, for operators the added complexity of the spectrum management can be seen as increased transaction and opportunity costs.

V. CONCLUSION AND FUTURE WORK

The exponential growth of wireless broadband services with diversity of devices and applications has inspired research community to come up with novel concepts to improve the efficiency of spectrum use. Recently, several spectrum sharing system concepts have been introduced and widely studied to cope with spectrum scarcity, though to date only a few has developed into pre-commercial deployments.

TABLE I. SPECTRUM SHARING BUSINESS MODEL ANTECEDENT FACTORS

Antecedents	Sharing model		
	TVWS	LSA	CBRS
a) Platform	<ul style="list-style-type: none"> + Technology platform standardized and may thus be adopted quickly - Based on evolving technologies scores on flexibility, but may lack scale and harmonization - Interference constraints and strict technical requirements requires specialized radios - Uncertainty of spectrum assets has limited interest of major technology vendors and MNOs. 	<ul style="list-style-type: none"> + Utilizes existing 3GPP ecosystem assets and scale + Network management system automatization based spectrum control function (LC) + Simple repository function (LR) fullfills static and semi-static use cases + Protects and leverages MNOs infrastructure investments 	<ul style="list-style-type: none"> + Extend 3GPP ecosystem to unlicensed and standalone LTE unlicensed + Dense urban deployments have additional utility and infra assets to share, e.g., fixed optical infra - Requires new intelligent and near real time SAS and ESC sensing functions. - New capabilities in big data & spectrum analytics needed to manage horizontal interference, co-existence and transactions - New spectrum band and introduced dynamism impacts BS and UE radios
b) Reduced need for the ownership	<ul style="list-style-type: none"> + Offers access to practically free spectrum + Scores well in terms of efficiency of frequency bands utilization and rapidity of access - Unlimited number of users administratively imposed, rather than voluntarily chosen 	<ul style="list-style-type: none"> + Enables faster access to lower cost capacity spectrum without coverage obligations + Protects the turf on existing MNO infra with radio upgrades +/- Based on traditional exclusive licensing model with relatively high up front license payment + Expands sharing into other assets, e.g., with local venue owners 	<ul style="list-style-type: none"> + Unbundles investment in spectrum, network infrastructure and services + Spectrum access with low initial annuity payments + Access to local spectrum driven by business needs, when and where + Expands sharing into other assets, e.g., with local venue owners.
c) Utilization of underutilized assets	<ul style="list-style-type: none"> - Future availability of the shared UHF spectrum assets is uncertain particularly in dense urban areas - Heterogeneous incumbent users and TV channels properties - Non-guaranteed QoS may limit scope of services 	<ul style="list-style-type: none"> + Availability of spectrum assets dependent on regulation, currently LSA considered for 2.3 GHz and 3.6 GHz spectrum band. + MNO connectivity model as is + Differentiation through extra data capacity and high speed enabling QoS and QoE pricing + Option to expand to capacity wholesale service 	<ul style="list-style-type: none"> + For MNOs low cost offloading + Nomadic Wi-Fi type of Internet access on dense urban environment hot spots + PAL – GAA tier flexibility + Spectrum and small cell hosted solution (SCaaS) + Enables new vertical segments: IoT - Concerns over the QoS predictability particularly with and at GAA layer and neighboring users across census tracks - Transaction costs increase in early development with increased complexity
d) Adaptability to different legal and policy regimes	<ul style="list-style-type: none"> +/- Regulated and standardized the US and Europe / UK with variants, e.g., in Singapore and Canada. + Low administrative burden + Low entry barrier enables quick access to the market 	<ul style="list-style-type: none"> + Legal certainty and security with existing regulatory framework + Requires a harmonized framework in regional standardization and regulation in order to reach economies of scale + Initial European focus but very generic concept adaptable to other regimes - National regulation with incumbent ecosystem 	<ul style="list-style-type: none"> + Low administrative burden with low entry barrier on GAA - Uncertainty with short PA license term and GAA with opportunistic access only - Need regulation and standardization with incumbent ecosystem (DoD) - Initially US federal specific, need adaptability to other regimes
e) Communities and trust	<ul style="list-style-type: none"> + Geo-location database is trust vehicle to protect incumbent users' QoS - Heterogeneous GLDB operators in terms of services and business models - Rules out the possibility of decentralized agreement over accepted interference levels - The tragedy of the commons - Business model uncertainty limits incentives to invest 	<ul style="list-style-type: none"> + Trust in predictability of QoS and pragmatic incumbent protection build on binary agreements and implemented in LR. + Protection of LSA licensee business critical information guaranteed + Use existing consumer ownership on connectivity with existing known services for lock-in + Small cell ecosystem could introduce new players & shared asset opportunities 	<ul style="list-style-type: none"> + Trust implemented using the SAS + Internet giants 'innovation' ecosystems to trigger communities + Customer data ownership on apps and services for customer lock-in + Small cell ecosystem introduces new players and shared asset opportunities +/- Complemented by sensing as defense incumbents lack of trust in GLDB - Protection of MNOs business sensitive information assets in SAS uncertain - DoD OPSEC requirements
f) Value and user orientation	<ul style="list-style-type: none"> + Main current use case is to provide Internet to rural unserved areas + Free spectrum facilitates local niche services, e.g., for various IoT vertical start-ups +/- Spectrum market related new value added service opportunity for database providers utilizing positive network externality - Unlicensed users' QoS not protected - Requires special user equipment 	<ul style="list-style-type: none"> + Clear business model as is + Additional capacity to serve customers with improved QoS and QoE + Customer experience management as a tool for value differentiation + Can open the market to new players with local licenses 	<ul style="list-style-type: none"> + Flexible regulatory framework allows facilitates introduction of innovative local business model designs + Local and Internet players offer differentiation based on user knowledge. + Enables heterogeneous segments, e.g., consumers, enterprises, IoT + Introduces new roles: SAS admin, broker and sensing + Local services, e.g., media broadcasting and advertisement

This paper discussed business model characteristics and sharing economy scalability criteria, and evaluated recent spectrum sharing concepts, the TV Whites Space, the European Licensed Shared Access and the US Citizens Broadband Radio Service, with respect to these criteria.

For a spectrum sharing concept to be adopted, it is essential not just to develop technology enablers to meet regulatory criteria but also to provide a scalable business model design for all the stakeholders. Harmonization and scalability of the platform and automation of processes will drive economies of scale and trigger early market opening. The model must be able to offer superior value proposition that offer access over ownership and ability to realize more choices with lower initial transactions costs compared to exclusive models. Value of the shared spectrum resources are highly dependent on its availability, liquidity and the predictability. Access and deployment of the underutilized assets on-demand is essential to generate continuous revenue early. Scalability of all sharing concepts could be highly impacted by fragmented national incumbent use cases, related different incumbent protection mechanisms and regulatory differences. Trust is the trigger of all collaborative shared consumption that makes system grow and scale. The creation of a critical mass ecosystem with positive network effects is important for all three approaches with new database spectrum administrator and broker roles. Simplicity of the offer built around user knowledge driven 'demand pull' is critical in value differentiation for existing services as well as in scaling new spectrum sharing enabled services.

The analysis indicates that the TVWS concept actively promoted by the US and the UK administrations, benefits from practically free spectrum and low entry barrier. However, to date the level of market acceptance has remained low mainly due to uncertainties related to the available spectrum assets, platform scale, and predictability. Moreover, unlicensed non-guaranteed QoS has limited the scope of services and business model designs. The LSA provides high predictability and certainty for both the incumbent and the LSA licensee, leverages existing platforms and capabilities, and preserves low impact to the ecosystem and business models. The opportunistic third tier of the CBRS concept lowers entry barrier to new alternative operators, scale out ecosystem with new roles, and foster service innovation particularly. Similarly, the higher frequency small cell use cases of the LSA envisages more flexible and scalable opportunities for new entrants, and novel business model designs. On the other hand, introduced dynamism will increase system complexity, and requires novel technology enablers in building trust and ensuring pragmatic predictability in the spectrum management platform while minimizing additional transaction costs.

The Sharing Economy provides a dynamic framework for analyzing and developing the spectrum sharing business models. In the future, spectrum sharing concept business modelling studies will need to be expanded to cover novel ecosystem roles and stakeholders. In particular, co-operative business model with traditional mobile network operators and local alternative operators will be an important aspect to research.

ACKNOWLEDGMENT

This work is supported by Tekes – the Finnish Funding Agency for Technology and Innovation. The author would like to acknowledge the 5thGear CORE++ and JoiNtMaCS project consortia.

REFERENCES

- [1] Cisco white paper. Cisco Visual Networking Index: Global Mobile Data Traffic Forecast Update, 2015-2020. [Online]. Available from: <http://www.cisco.com/c/en/us/solutions/collateral/service-provider/visual-networking-index-vni/mobile-white-paper-c11-520862.pdf> 2017.02.27
- [2] RSPG Opinion on Licensed Shared Access. RSPG13-538, Radio Spectrum Policy Group, Nov. 2013.
- [3] The White House, Realizing the Full Potential of Government-Held Spectrum to Spur Economic Growth, President's Council of Advisors on Science and Technology (PCAST) Report, July 2012.
- [4] FCC, Second Memorandum Opinion and Order (FCC 08-260), FCC, Washington, DC, USA, Sep. 2010.
- [5] Ofcom, Statement on Implementing TV White Spaces. [Online] Available from: <http://stakeholders.ofcom.org.uk/binaries/consultations/white-space-coexistence/statement/tvws-statement.pdf> 2017.02.27
- [6] ECC, Licensed Shared Access (LSA), ECC Report 205, Feb. 2014.
- [7] FCC, FCC 16-55: The Second Report and Order and Order on Reconsideration finalizes rules for innovative Citizens Broadband Radio Service in the 3.5 GHz Band (3550-3700 MHz). [Online]. Available from: https://apps.fcc.gov/edocs_public/attachmatch/FCC-16-55A1.pdf 2017.02.27
- [8] R. Amit and C. Zott, "Value creation in e-business," *Strategic Management Journal*, vol. 22, no. 6/7, pp. 493-520, 2001.
- [9] M. A. Rappa, "The utility business model and the future of computing services," *IBM Systems Journal*, vol. 43, no. 1, pp.32-42, 2004.
- [10] H. Bouwman and I. MacInnes, "Dynamic business model framework for value Webs," in the Proceedings of the 39th Hawaii International Conference on System Sciences, Hawaii, USA, vol. 2, p. 43, Jan. 2006.
- [11] R. Hallowell, "Scalability: the paradox of human resources in e-commerce," *International Journal of Service Industry Management*, vol. 12, no. 1, pp.34-43, 2001.
- [12] G. Stampfl, R. Prügl, and V. Osterloh, "An explorative model of business model scalability," *Int. J. Product Development*, vol. 18, nos. 3/4, pp.226-248, 2013.
- [13] A. Stephany, *The Business of Sharing: Making it in the New Sharing Economy*, Palgrave and Macmillan, 2015.
- [14] J. Chapin and W. Lehr, "Cognitive radios for dynamic spectrum access - The path to market success for dynamic spectrum access technology," *IEEE Commun. Mag.*, vol. 45, no. 5, pp. 96-103, 2007.
- [15] Y., Luo, L., Gao, and J., Huang, "Business Modeling for TV White Space Networks," *IEEE Commun. Mag.*, vol. 53, pp. 82 – 88, 2015.
- [16] P. Ahokangas, M. Matinmikko, S. Yrjölä, H. Okkonen, and T. Casey, "Simple rules" for mobile network operators' strategic choices in future spectrum sharing networks," *IEEE Wireless Commun.*, vol. 20, no. 2, pp. 20-26, 2013.
- [17] P. Ahokangas *et al.*, "Business models for mobile network operators in Licensed Shared Access (LSA)," *IEEE International Symposium on Dynamic Spectrum Access Networks (DYSpan)*, pp. 263 – 270, 2014.

- [18] S. Yrjölä, P. Ahokangas, and M. Matinmikko, "Evaluation of recent spectrum sharing concepts from business model scalability point of view," IEEE International Symposium on Dynamic Spectrum Access Networks (DYSPAN), pp. 241-250, 2015.
- [19] A. Sundararajan, "The Sharing Economy: The End of Employment and the Rise of Crowd-Based Capitalism," MIT Press, May 2016.
- [20] M. Mustonen *et al.*, "Cellular architecture enhancement for supporting the European licensed shared access concept," IEEE Wireless Commun., vol. 21, no. 3, pp. 37 – 43, 2014.
- [21] ETSI, System Architecture and High Level Procedures for operation of Licensed Shared Access (LSA) in the 2300 MHz-2400 MHz band. TS 103 235, 2015.
- [22] M. Sohil, M. Yao, T. Yang, and J. Reed, "Spectrum Access System for the Citizen Broadband Radio Service," IEEE Commun. Mag., vol. 53, no. 7, 2015, pp. 18-25.
- [23] The WINNF Spectrum Sharing Committee, "SAS Functional Architecture," [Online]. Available from: <http://groups.winnforum.org/d/do/8512.2017.02.27>
- [24] FCC, White Spaces. [Online]. Available from: <http://www.fcc.gov/topic/white-space> 2017.02.27
- [25] Info-Communications Development Authority of Singapore. "Regulatory framework for TV White Space operations", June 2014.
- [26] CEPT, the regulatory framework for TV WSD (White Space Devices) using a geolocation database and guidance for national implementation, ECC report 236, May 2015.
- [27] IEEE Standards Association. "Part 11: Wireless LAN Medium Access Control (MAC) and Physical Layer (PHY) Specifications, Amendment 5: Television White Spaces (TVWS) Operation", 2013.
- [28] EC, Promoting the shared use of radio spectrum resources in the internal market, COM (2012) 478, European Commission, Sept. 2012.
- [29] CEPT, Harmonised technical and regulatory conditions for the use of the band 2300-2400 MHz for Mobile/Fixed Communications Networks (MFCN), CEPT, ECC Decision (14)02, June 2014.
- [30] ETSI, Mobile Broadband services in the 2300-2400 MHz frequency band under Licensed Shared Access regime. ETSI TR 103.113, 2013.
- [31] ETSI, System requirements for operation of Mobile Broadband Systems in the 2300 MHz -2400 MHz band under LSA. ETSI TS 103 154, 2014.
- [32] M. Matinmikko *et al.*, "Cognitive radio trial environment: First live authorized shared access-based spectrum-sharing demonstration," IEEE Veh. Technol. Mag., vol. 8, no. 3, pp. 30-37, Sept. 2013.
- [33] S. Yrjölä *et al.*, "Licensed Shared Access (LSA) Field Trial Using LTE Network and Self Organized Network LSA Controller," Wireless Innovation Forum European Conference on Communication technologies and Software Defined Radio (WinnComm-Europe), pp. 68-77, Oct. 2015.
- [34] Italy, "World's first LSA pilot in the 2.3-2.4 GHz band," Input contribution to ECC PT1 #51, ECC PT1(16)028, Jan. 2016.
- [35] RED Technologies, "Ericsson, RED Technologies and Qualcomm Inc. conduct the first Licensed Shared Access (LSA) pilot in France," [Online]. Available from: <http://www.redtechnologies.fr/news/ericsson-red-technologies-and-qualcomm-inc-conduct-first-licensed-shared-access-lsa-pilot-france> 2017.02.27
- [36] ECC PT1, "Operational guidelines for spectrum sharing to support the implementation of the current ECC framework in the 3 600-3 800 MHz range", ECC PT1(16)82 Annex 20, Apr. 2016.
- [37] The White House, Expanding America's Leadership in Wireless Innovation, Presidential Memorandum, June 2013.
- [38] The 3GPP R4-168006: Relevant requirements for Band 48 introduction in 36.104, TSG-RAN4 Meeting #80bis, Ljubljana, Slovenia, Oct. 2016.
- [39] FCC, Amendment of the Commission's Rules with Regard to Commercial Operations in the 3550-3650 MHz Band, FCC, Docket 12-354, 14-49, 2014.
- [40] C. Zott and R. Amit, "Business model design: An activity system perspective. Long Range Planning, vol. 43, no. 2-3, pp. 216-226, 2010.
- [41] D. Teece, "Business models, business strategy and innovation," Long Range Planning, vol. 43, no. 2-3, pp. 172-194, 2010.
- [42] A. Onetti, A. Zucchella, M.V. Jones, and P. P. McDougall-Covin, " (2012) Internationalization, innovation and entrepreneurship: business models for new technology-based firms. J Manag Gov, vol 16, pp. 337-368, 2012.
- [43] L. Berry, V. Shankar, J. Parish, S. Cadwallader, and T. Dotzel, "Creating new markets through service innovation," MIT Sloan Management Review, vol. 47, no. 2, 2006, pp.56-63.
- [44] N. Franke, M. Gruber, D. Harhoff, and J. Henkel, "Venture capitalists' evaluations of startup teams: trade-offs, knock-out criteria, and the impact of VC experience," Entrepreneurship: Theory & Practice, vol. 32, no. 3, pp.459-483, 2008.
- [45] S. Choudary, M. Van Alstyne, and G. Parker, "Platform Revolution: How Networked Markets Are Transforming the Economy--And How to Make Them Work for You," John Wiley & Sons, Inc., Mar. 2016.
- [46] A. Sundararajan, "From Zipcar to the Sharing Economy" HBR, June 2013.

New Spectrum Sensing based on Goodness of Fit Testing for Cognitive Radio

Djamel Teguig,
 Communication Systems Laboratory
 Polytechnic Military School
 Algiers, Algeria
 Email: djamel_teg@yahoo.com

François Horlin
 OPERA-Wireless Communication Group
 Universit Libre de Bruxelles
 Brussels, Belgium
 Email: fhorlin@ulb.ac.be

Abstract—Recently, the Goodness of Fit Test (GoF) has been applied for hypothesis testing in the case of spectrum sensing for Cognitive Radio (CR). GoF sensing has the desirable feature of needing only a few samples to perform sensing. In this paper, we first compare the existing GoF sensing methods in the literature. Secondly, we study some typical impairment for spectrum sensing, i.e., the effect of a non Gaussian noise, noise uncertainty and Rayleigh fading channel on the performance of GoF based sensing. Thirdly, we propose two GoF sensing methods and compare them against the conventional Anderson Darling (AD) sensing. The first proposed method is the IQ (In-phase and Quadrature components) GoF sensing method, which consists in testing the real and the imaginary part of the received samples against the Gaussian distribution to make a decision. In the second method, we propose a new GoF test statistic by taking into account the physical characteristic of spectrum sensing. The derived GoF sensing method results in significant improvement in terms of sensing performance.

Keywords—Cognitive Radio; Spectrum Sensing; Goodness of Fit test; Test Statistic.

I. INTRODUCTION

Due to the rapid development of wireless communications services, the requirement of spectrum is growing dramatically. The Federation Communications Commission (FCC) has stated that some allocated frequency bands are largely unoccupied (under-utilized) most of the time [1]. Cognitive Radio has emerged as a novel approach to enable Dynamic Spectrum Access (DSA) by allowing unlicensed users to access the under-utilized licensed spectra when/where licensed Primary Users (PU) are absent and to vacate the spectrum immediately once a PU becomes active without causing harmful interference [2] [3]. This ability is dependent upon Spectrum Sensing. Spectrum Sensing is a key component of dynamic spectrum sensing paradigm to find spectrum opportunities [4]. For practical dynamic spectrum sensing and access, power detectors are required. Generally, in CR environments, sensing algorithms are expected to be able to detect the presence of signals at very low Signal to Noise Ratio (SNR) levels within a limited observation time. Moreover, it is necessary that they are robust to practical impairments and parameter uncertainties. Therefore, spectrum sensing is a difficult task in CR and to design detection algorithms that are capable to work under very harsh conditions is of fundamental importance.

Many studies have focused on spectrum sensing algorithms in literature. The Matched Filter (MF) is considered as the optimum detector based on the classical detection theory but it has the disadvantage that it requires the knowledge of the signal to be detected [5], condition that in general is not satisfied in cognitive radio applications. The Energy Detector

(ED) is the most used detector when the signal is unknown [6]. The ED exhibits a low computational complexity and is widely used because it has a simple implementation. The main disadvantage of the ED is that it requires knowledge of the noise power to properly set the threshold. This requirement is often critical, in particular in low SNR environments, in which an imperfect knowledge of the noise power can cause severe performance losses. Moreover, the ED cannot distinguish between interference and signal [7].

When the signal to be detected has some known characteristics, the detection of such features is an effective method to identify such kind of signal. The cyclostationary method can be an appropriate sensing technique to recognize a particular transmission and/or extract its parameters [8]. This technique enables separation between signal and noise components and it can be adopted for signal classification. This spectrum sensing method has high computational and implementation requirements. It is worth to mention that the cyclostationary method outperforms the ED method if the noise power is wrongly estimated [9].

To the above mentioned spectrum sensing algorithms, we can also add other algorithms derived from spectral analysis, such as: multi-taper spectral analysis [10], wavelet transforms [11] and filter banks receivers based sensing methods [12].

There are several important characteristics to be considered in order to decide on a specific sensing method such as : prior knowledge, sensing time, computational complexity and noise rejection. To make trade-offs between these different characteristics, we propose in this paper the study of a spectrum sensing method based on statistic test ((GoF) test). In literature, many GoF sensing methods are proposed. The most important ones are the Anderson-Darling based sensing [13], Kolmogorov-Smirnov based sensing [14], the Cramer-Von Mises based sensing [15] and Order Statistics [16]. All these GoF sensing methods are based on the same hypothesis test, but differ in the way the distance between the empirical cumulative distribution of the observations made locally at the CR user and the noise distribution is calculated. The calculated distance is compared with a threshold to decide whether the signal is present or not, given a certain probability of false alarm. The first GoF sensing was presented in [13]. It is based on the Anderson-Darling GoF test to decide whether the received samples are drawn from the noise distribution F_0 (Gaussian distribution) or a different distribution. In [17], the authors reformulate the AD sensing to a Students t-distribution testing problem and propose a method which does not require any knowledge of the transmitted signal. The performance of the proposed method is better than ED sensing but less than AD sensing proposed in [13]. Kurtosis GoF sensing is proposed

in [18] in which the kurtosis is calculated from the absolute values of the Fast Fourier Transform (FFT) of the received samples. The value of the kurtosis statistic is then compared to a predefined threshold to decide about the presence of the signal. Skewness and Kurtosis GoF sensing, Goodness of fit High Order Statistic Testing (GHOST) is proposed in [19]. The method is based on the kurtosis and skewness computed from the received signal. Jarque-Bera (JB) GoF sensing is presented in [20]. Moreover, detection methods based on Tietjen-Moore (TM) and Shapiro-Wilk (SW) tests are proposed to detect and suppress Spectrum Sensing Data Falsification (SSDF) attacks by malicious user in cooperative spectrum sensing [21]. Most of the above methods take a normal noise distribution for the GoF test, and they all assume that the samples of the received signal are real valued. As CR is based on the Software Defined Radio (SDR) technology, the received base-band samples in the digital domain are complex in nature. Therefore, the most practical approach to apply the GoF test for spectrum sensing is to consider the squared magnitude of the complex samples (i.e., energy of the samples) and to test their empirical distribution against the hypothetical noise energy distribution [22]. In [23], and based on our new model in [22], we have proposed a blind spectrum sensing method based on GoF test using Likelihood Ratio (LR). Motivated by its desirable feature of needing only a few samples to perform sensing, in [24], the narrowband spectrum sensing based on GoF is used for a Nyquist wide-band sensing also known as a conventional wide-band sensing. Besides, we have studied in [25] the GoF sensing methods under noise uncertainty.

In this paper, we propose a new GoF based spectrum for cognitive radio. The first proposed method is the IQ GoF sensing method, which consists in testing the real and the imaginary part of the received samples against the Gaussian distribution to make a decision. In the second method, we propose a new GoF test statistic by taking into account the physical characteristics of spectrum sensing. Besides, we evaluate the GoF based sensing methods under some typical impairment such as the effect of a non Gaussian noise, noise uncertainty and Rayleigh channel.

The paper is organized as follows. In Section II, we explain the Goodness of Fit tests and we mention the most important among them. We present some existing GoF sensing methods and compare their detection performances in Section III. In Section IV, the GoF based spectrum sensing is investigated under non Gaussian noise, noise uncertainty and Rayleigh channel. In Section V, two new spectrum sensing methods are proposed and evaluated. We conclude this paper in Section VI.

II. GOODNESS OF FIT TESTS

GoF tests were proposed in mathematical statistics by measuring a distance between the empirical distribution of the observation made and the assumption distribution. In CR, GoF sensing is used to solve a binary detection problem and to decide whether the received samples are drawn from a distribution with a Cumulative Distribution Function (CDF) F_0 , representing the noise distribution, or they are drawn from some distribution different from the noise distribution. The hypothesis to be tested can be formulated as follows:

$$\begin{aligned} H_0 : F_n(x) &= F_0(x) \\ H_1 : F_n(x) &\neq F_0(x), \end{aligned} \quad (1)$$

for a random set of n independent and identically distributed observations and where $F_n(x)$ is the empirical CDF of the received sample and can be calculated by:

$$F_n(x) = |\{i : x_i \leq x, 1 \leq i \leq n\}|/n, \quad (2)$$

where $|\bullet|$ indicates cardinality, $x_1 \leq x_2 \leq \dots \leq x_n$ are the samples under test and n represents the total number of samples.

Many goodness of fit tests are proposed in literature. The most important ones are the Kolmogorov- Smirnov test [14], the Cramer-von Mises test [15], the Shapiro-Wilk [21] test and the Anderson-Darling test [13]. In the following, we briefly recall these GoF tests.

A. Kolmogorov- Smirnov test (KS test): In this test, the distance between $F_n(x)$ and $F_0(x)$ is given by:

$$D_n = \max|F_n(x) - F_0(x)|, \quad (3)$$

where $F_n(x)$ is the empirical distribution which is defined in (2). If the samples under test are coming from $F_0(x)$, then, D_n converges to 0.

B. Cramer-Von Mises (CM test): In this test, the distance between $F_n(x)$ and $F_0(x)$ is defined as:

$$T_n^2 = \int_{-\infty}^{\infty} [F_n(x) - F_0(x)]^2 dF_0(x). \quad (4)$$

By breaking the integral in (4) into n parts, T_n^2 can be written as:

$$T_n^2 = \sum_{i=1}^n [z_i - (2i - 1)/2n]^2 + (1/12n), \quad (5)$$

with $z_i = F_0(x_i)$

C. Anderson-Darling test (AD test): This test can be considered as a weighted Cramer-Von Mises test where the distance between $F_n(x)$ and $F_0(x)$ is given by:

$$A_n^2 = \int_{-\infty}^{\infty} [F_n(x) - F_0(x)]^2 \frac{dF_0(x)}{F_0(x)(1 - F_0(x))}. \quad (6)$$

The expression of A_n^2 can also be simplified to:

$$A_n^2 = -n - \frac{\sum_{i=1}^n (2i - 1)(\ln z_i + \ln(1 - z_{(n+1-i)}))}{n}, \quad (7)$$

with $z_i = F_0(x_i)$.

III. GOF SENSING METHODS

We formulate the spectrum sensing problem as a binary hypothesis testing problem as follows:

$$\begin{aligned} H_0 : X_i &= W_i \\ H_1 : X_i &= S_i + W_i, \end{aligned} \quad (8)$$

where S_i are the received complex samples of the transmitted signal and W_i is the complex Gaussian noise. We now consider the random variable $Y_i = |X_i|^2$ which corresponds to the received energy. It is known that, if the real and the imaginary part of X_i are normally distributed, which is the case under H_0

hypothesis, the variable $Y_i = |X_i|^2$ is chi-squared distributed with 2 degrees of freedom.

As mentioned before, we will consider a normal noise, in order to be able to compare the different GoF sensing methods. This assumption is not limiting. The performance of the GoF sensing is independent of the noise distribution, as the distribution of GoF test statistic $(A_n^2, T_n^2, D_n, \dots)$ under H_0 is independent of the $F_0(y)$ [26] [27].

The spectrum sensing problem can now be reformulated as a hypothesis represented in (8) where we test whether the received energy $Y_i = |X_i|^2$ samples are drawn from a chi-square distribution with 2 degrees of freedom or not. The CDF of the chi-square distribution is given by:

$$F_0(y) = 1 - e^{-y/2\sigma_n^2} \sum_{k=0}^{m-1} \frac{1}{k!} \left(\frac{y}{2\sigma_n^2}\right)^k, y > 0, \quad (9)$$

where m is the degree of freedom (in our case $m = 1$) and σ_n^2 is the noise power.

In summary, GoF sensing methods follow these steps:

- Step1 From the complex received samples X_i , calculate the energy samples $Y_i = |X_i|^2$
- Step2 Sort the sequence $\{Y_i\}$ in increasing order such as $Y_1 \leq Y_2 \leq \dots \leq Y_n$
- Step3 Calculate the GoF test statistic T^* , with F_0 given in (9).
use (3) for KS GoF sensing
use (5) for CM GoF sensing
use (7) for AD GoF sensing
- Step4 Find the threshold λ for a given probability of false alarm such that:

$$Pfa = P\{T^* > \lambda | H_0\}. \quad (10)$$

- Step5 Accept the null hypothesis H_0 if $T^* \leq \lambda$, where T^* is the GoF test statistic (KS, CM or AD). Otherwise, reject H_0 in favor of the presence of the signal.

The value of λ is determined for a specific value of P_{fa} . Tables listing values of λ corresponding to different false alarm probabilities P_{fa} are given according to the test considered [26]. Otherwise, these values can be computed by Monte Carlo approach [23] [25].

A. Performance comparison of existing GoF sensing methods

In this subsection, we will analyze and compare the performance of existing GoF sensing methods.

Thereafter, simulation results are presented to show the sensing performance of various GoF sensing methods compared to the conventional ED sensing. In Fig. 1, we show the ROC (Receiver Operating Characteristic) curves of GoF sensing methods (AD, CM and KS) and ED sensing for a fixed number of 80 samples and a given SNR equal to -6 dB. It is clear that ED sensing outperforms the considered GoF sensing methods. Likewise, AD sensing is the best among the considered GoF sensing methods. This is indeed confirmed in the simulation results as shown in Fig.2, where the detection probability versus SNR is plotted for a fixed number of 80 samples and at given false alarm probability $P_{fa} = 0.05$. ED sensing has better performance than the three GoF sensing methods. To achieve 90 % of detection probability, ED sensing outperforms AD sensing by about 1 dB, and AD sensing

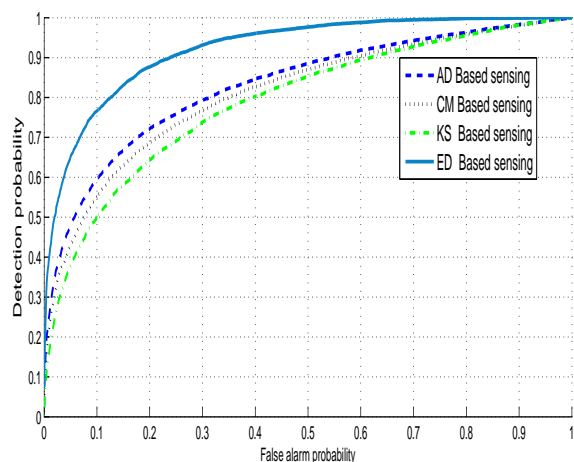


Figure 1. Detection probability versus false alarm probability of various GOF test based sensing at $SNR = -6dB$ and $n = 80$ samples

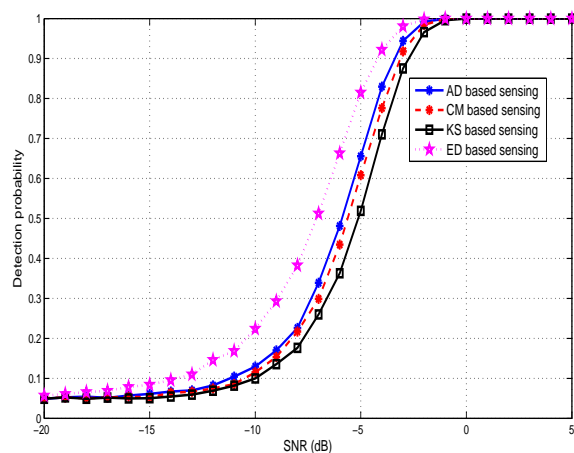


Figure 2. Detection probability versus SNR for different GOF tests based sensing with $P_{fa} = 0.05$ and $n = 80$ samples

presents a slight difference in gain compared to CM sensing and KS sensing of about 0.2 dB and 0.5 dB respectively.

IV. GOF SENSING UNDER NON GAUSSIAN NOISE, NOISE UNCERTAINTY AND RAYLEIGH CHANNEL

Although, its nice feature that it only needs a few samples to perform sensing, we have seen in the previous section that the conventional Energy Detection still outperforms the GoF based sensing (when considering a normal distribution of noise). However, the GoF sensing methods have the merit to be resistant to different impairments. This point is studied in this section.

A. Impact of a non Gaussian noise (GM Model)

It is worth to mention that the existing works on GoF for spectrum sensing [13] [15] [16] and [17] are focusing on detecting a signal in white Gaussian noise. In this paper, we will also focus on detecting signals in white non-Gaussian

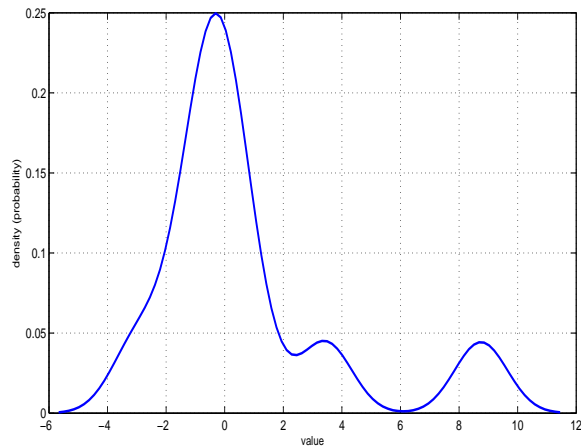


Figure 3. probability distribution function (pdf) of GM noise $\alpha = 0.9$, $\beta = 5$ and $\sigma = 1$

noise. In literature, a lot of models are proposed to pattern a non Gaussian noise. The most used models are the Gaussian Mixture model (GM) and the Generalized Gaussian model (GG). For our spectrum sensing model, we will work with the GM model [28], as it has been used in practical applications in [30] and in radio signal detection applications in [31]. To apply the GoF test for spectrum sensing, we need to know the CDF of the non Gaussian noise (GM CDF). The Probability Density Function (PDF) of GM noise has three parameters α , β , and σ and is defined as [31]:

$$f_w(w) = \frac{c}{\sigma\sqrt{2\Pi}} \left[\alpha \exp\left(-\frac{c^2 w^2}{2\sigma^2}\right) + \frac{1-\alpha}{\beta} \exp\left(-\frac{c^2 w^2}{2\sigma^2 \beta^2}\right) \right] \quad (11)$$

where $c = \sqrt{\alpha + (1-\alpha)\beta^2}$

In Fig. 3, we depict a PDF of a white non Gaussian noise (GM) with the following selected parameters $\alpha = 0.9$, $\beta = 5$ and $\sigma = 1$. The methodology explaining how the GM parameters may be estimated can be found in [29]. The CDF F_0 of the energy of the non-Gaussian noise samples under H_0 hypothesis can be derived from the GM's PDF. For that, we have: if $Y = X^2$ and X is GM noise with CDF $F_X(x)$

$$\begin{aligned} F_0(y) &= P(Y \leq y) = P(-\sqrt{y} \leq X \leq \sqrt{y}) \\ &= F_X(\sqrt{y}) - F_X(-\sqrt{y}) \end{aligned} \quad (12)$$

Once we get the CDF of the non Gaussian noise, we apply the proposed algorithm in section III. Note that the knowledge of F_0 is required to apply the GoF test, therefore, if the parameters of the GM model are unknown, they must be estimated first.

To evaluate the effect of a non Gaussian noise on the sensing performance, we have performed simulations with the selected GM noise. We set the parameters of the non Gaussian noise as: $\alpha = 0.9$, $\beta = 5$ and $\sigma = 1$. Fig. 4 presents the results of the AD GoF sensing under Gaussian noise and non Gaussian noise. It is shown that the effect of considering a non Gaussian noise is to slightly decrease the performance of the AD GoF sensing. However, it can be seen in Fig. 5 that the performance of the ED is significantly influenced by the

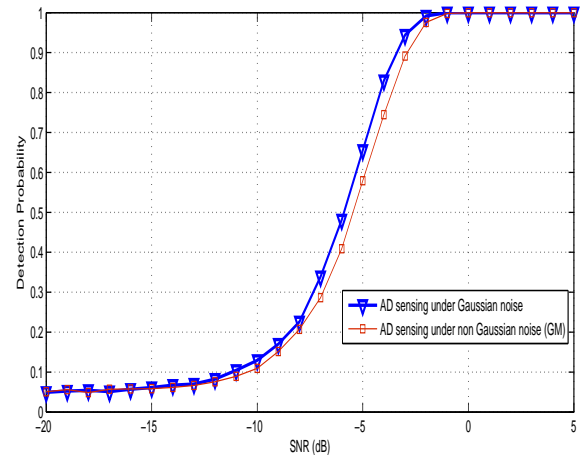


Figure 4. Detection probability versus SNR under Gaussian and non Gaussian noise for AD-GoF, with $P_{fa} = 0.05$ and $n = 80$ samples

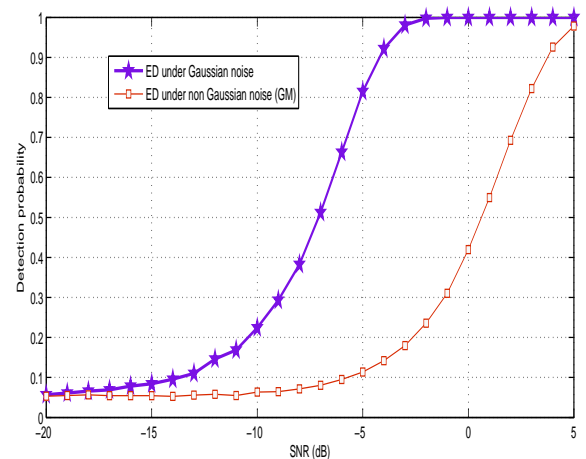


Figure 5. Detection probability versus SNR under Gaussian and non Gaussian noise for ED, with $P_{fa} = 0.05$ and $n = 80$ samples

considered non Gaussian noise. It has to be noted that the considered non Gaussian noise ($\alpha = 0.9$, $\beta = 5$ and $\sigma = 1$) is very unfavorable for ED. In order to obtain a $P_{fa} = 0.05$, the threshold λ in the binary hypothesis test needs to be shifted to the right at a certain level. GoF sensing is less affected by the non Gaussian noise, as the test is performed on the mismatch between the measured CDF and the reference CDF F_0 .

B. Impact of a noise uncertainty

One of the main issues with ED is the impact of noise uncertainty on the detection performance. It is shown in [33] and [32] that ED is very sensitive to noise uncertainty. The aim of this subsection is to study the effect of noise uncertainty on GoF sensing methods compared to ED.

Through simulation, we have compared the impact of noise uncertainty on both methods, ED based spectrum sensing and GoF sensing. The noise uncertainty is modeled by letting the actual noise variance be limited within a set given by a nominal noise variance and an uncertainty parameter ρ such

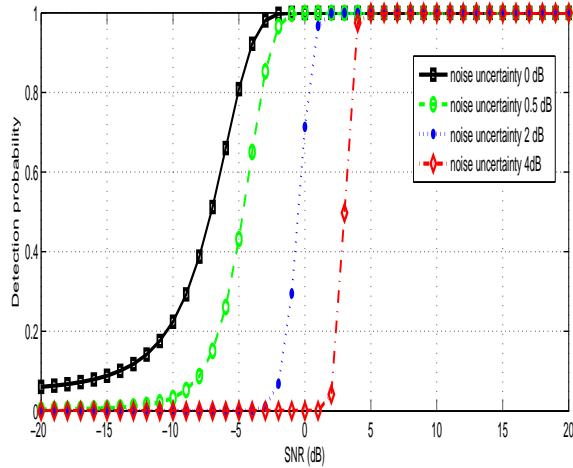


Figure 6. Impact of noise uncertainty on ED with $P_{fa} = 0.05$ and $n = 80$ samples

that $\sigma_n^2 \in [\frac{1}{\rho}\sigma^2, \rho\sigma^2]$.

There is a fundamental difference between ED and GoF sensing when it comes to noise uncertainty. The energy detector suffers under noise uncertainty because computing the threshold λ for the binary test requires knowledge of the underlying noise variance. In order to guarantee a given false alarm rate P_{fa} , the threshold λ will be calculated for the worst case, i.e., a noise variance of $\rho\sigma^2$, leading to higher values of λ and hence to a decrease in detection probability.

In GoF sensing, the distribution of the test statistic A_n^2 under the H_0 hypothesis is independent of the noise distribution. As a consequence, the value of the threshold λ for the GOF binary test will not be influenced by the noise uncertainty. However, the calculation of the test statistic (A_n^2) requires the exact knowledge of the underlying theoretical noise CDF F_0 . In summary, for GoF sensing, noise uncertainty will, via F_0 , indirectly affect the value of the test statistic, but not the detection threshold. For the simulation of the GoF sensing under noise uncertainty, we will also follow a worst case approach, by considering a reference noise CDF F_0 given in (9) based on the highest noise variance $\rho\sigma^2$, which will eventually lead to a reduction of the detection probability.

In Fig. 6, we have plotted the detection probability versus SNR for several values of noise uncertainty (0 dB, 0.5 dB, 2 dB, 4 dB) in the case of the ED spectrum sensing method. It is shown that the performance of the ED is significantly decreasing when the noise uncertainty level is increasing. At 80 % of detection probability, due to noise uncertainty of 0.5 dB, the SNR drops to about 2 dB.

In a similar way, in Fig. 7, we have plotted the detection probability as a function of SNR when considering a noise uncertainty for GoF based spectrum sensing. It can be seen that under uncertainty in the noise statistic of the CDF under hypothesis H_0 (F_0), the impact on the performance of the GoF based spectrum sensing is significantly less than the impact on energy detection. Intuitively, this can be explained by the fact that in ED, the values of P_{fa} and P_d are directly affected by the noise uncertainty. In case of GoF based sensing the statistic such as: A_n^2 , is indirectly affected by the noise uncertainty via the CDF F_0 under hypothesis H_0 .

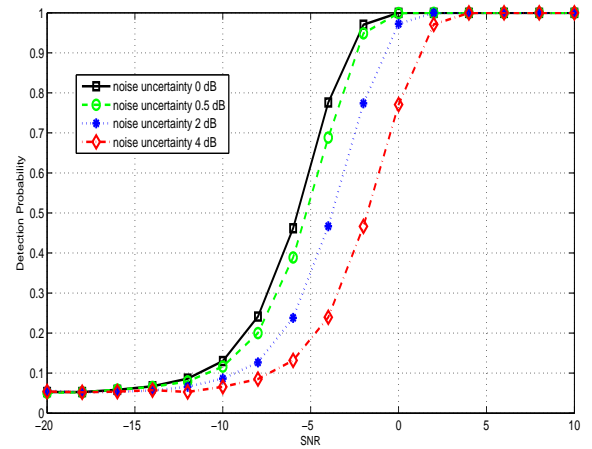


Figure 7. Impact of noise uncertainty on GoF test based sensing with $P_{fa} = 0.05$ and $n = 50$ samples

Note also that, in Fig. 6, for high values of noise uncertainty, the P_d drops to 0. This effect is known as the SNR wall [33]. This effect is not observed in GoF based spectrum sensing for the given simulation parameters.

C. Impact of a Rayleigh fading channel

Under fading, the value of SNR may vary. In this case, the probability of detection must be given for the instantaneous SNR. This means that the resulting probability of detection may be derived by averaging over the fading statistics. Under Rayleigh fading, SNR has an exponential distribution [34].

In Fig. 8, we provide a plot of the ROC curve, under AWGN (Additive White Gaussian Noise) and Rayleigh fading scenarios. SNR_{avg} (the average over SNR values) and n are assumed to be -5 dB and 60 samples, respectively. It is shown that Rayleigh fading significantly degrades the performance of the energy detector.

To evaluate the impact of Rayleigh channel on GoF sensing methods, we have plotted in Fig. 9, the detection probability versus SNR_{avg} under AWGN and Rayleigh fading channel for AD GoF sensing with P_{fa} fixed to 0.05 and $n = 80$ samples. According to Fig. 9, it can be observed that the effect of considering a Rayleigh fading channel has a slight decrease in the performance of the AD GoF sensing.

V. NEW GOF SPECTRUM SENSING METHODS

A. IQ GoF based spectrum sensing

We have proposed in [22] to calculate the energy samples $Y_i = |X_i|^2$, and then test the sequence Y_i against the chi-square distribution to determine if there exists a primary signal.

However, we could also form another sequence from the same observed complex samples by using its real and imaginary part, i.e., $(Re(X_i), Im(X_i))$ and then test it against the Gaussian distribution to make a decision. The authors in [13] have considered a model (the received signal is real and $S_i = constant$) which does not reflect a realistic scenario for spectrum sensing in cognitive radio, as normally the received signal is complex and varies in time. Compared to the proposed

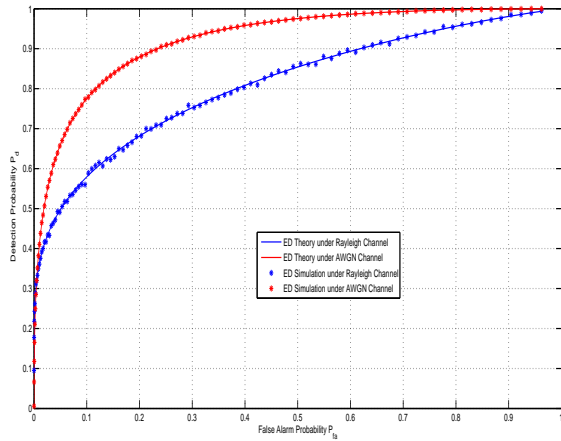


Figure 8. ROC curves for the energy detection under AWGN and Rayleigh fading channels

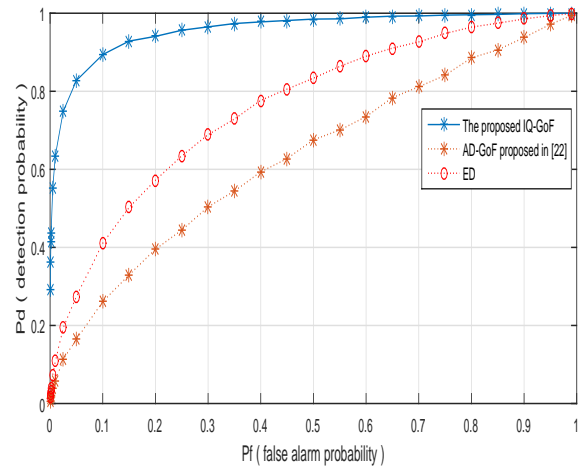


Figure 10. Detection probability versus false alarm probability with $SNR = -6 \text{ dB}$

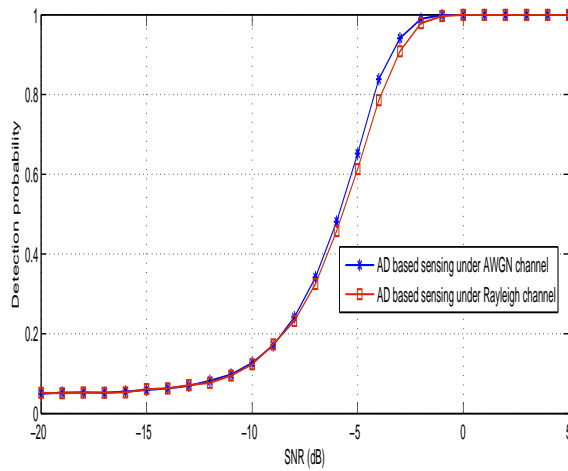


Figure 9. Detection probability versus SNR_{avg} under AWGN and Rayleigh fading channels for AD-GoF sensing, with $P_{fa} = 0.05$ and $n = 80$ samples

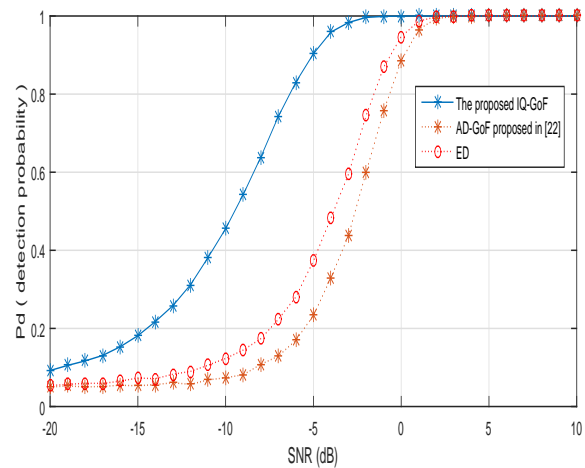


Figure 11. Detection probability versus SNR with $P_{fa} = 0.05$

method in [13], we proposed in this method to start from the more general model as in (8) and test the IQ samples against the Gaussian distribution to make a decision.

In summary, the proposed IQ GoF sensing methods follow these steps:

- Step1 From the complex received samples X_i , separate the X_i to $(Re(X_i), Im(X_i))$.
- Step2 Sort the sequence $\{Re(X_i)\}$ in increasing order such as $Re(X_1) \leq Re(X_2) \leq \dots \leq Re(X_n)$. Perform the same thing for $Im(X_i)$.
- Step3 Calculate the GoF test statistic using (7) for AD GoF sensing, with F_0 given in (9). We use the function 'Adtest' of Matlab, which combines the GoF from both real and imaginary parts, into a single GoF.
- Step4 Find the threshold λ for a given probability of false alarm such that:

$$P_{fa} = P\{T^* > \lambda | H_0\}. \quad (13)$$

Step5 Accept the null hypothesis H_0 if $T^* \leq \lambda$, where T^* is the GoF test statistic (KS, CM or AD). Otherwise, reject H_0 in favour of the presence of the signal.

The value of λ is determined for a specific value of P_{fa} . Tables listing values of λ corresponding to different false alarm probabilities P_{fa} are given according to the test considered [26]. Otherwise, these values can be computed by Monte Carlo approach.

The simulation results when $n = 20$ samples are displayed in Fig. 10 and Fig. 11. In both figures, 'IQ-GoF' denotes our proposed method and AD-GoF denotes the method proposed in [22]. The simulation results are obtained via 10000 Monte Carlo runs. Fig.10 shows the receiver operating characteristic (ROC) curves (detection probability against false alarm probability) with a SNR equal to -6 dB and the values of the detection probability against SNR are plotted in Fig. 11 with false alarm probability (P_f) set to 0.05. Both figures indicate that the proposed sensing method is more efficient compared to the conventional Energy Detection.

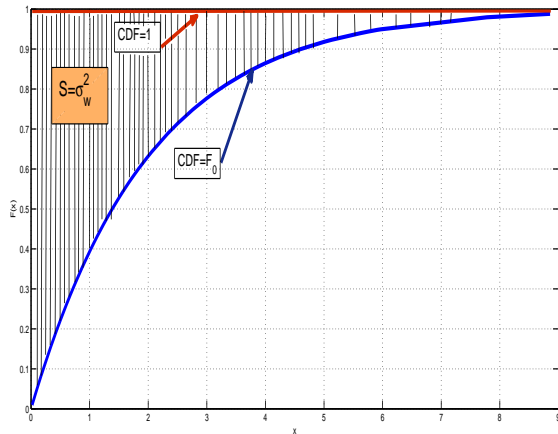


Figure 12. Noise power area

B. Spectrum sensing method based on the new GoF statistic test

The aforementioned GoF tests use the statistical hypothesis testing in (1) (which means testing the hypothesis H_0). However, in the H_1 hypothesis, it can be noted that the overall power of the received signal should always be larger than the noise power, as noise and signal are uncorrelated. This results in having a cumulative distribution function under hypothesis H_1 on the right of the cumulative distribution function of the noise, meaning that the area above the expected continuous CDF of the random variable (energy of samples in our case) will also increase. The above finding is based on the property of the expected value of a non-negative random variable.

$$E[X] = \int_0^{\infty} (1 - F_X(x)) dx \quad (14)$$

In our sensing model as in [22], the received energy $Y_i = |X_i|^2$ is a non negative random variable and equation (14) is applicable. As the received signal $\{X_i\}$ has zero means, $E[Y] = E[|X_i|^2] = \sigma_X^2$. Hence, we find

$$\sigma_X^2 = \int_0^{\infty} (1 - F_Y(x)) dx \quad (15)$$

In other words, the received signal power equals the area of the region lying above the CDF $F_Y(x)$ and below the line at height 1 to the right of the origin. Under H_0 hypothesis, this means that the area above F_0 equals the noise power σ_w^2 as depicted in Fig. 12. Under H_1 hypothesis, the total power in the received signal will increase to $\sigma_s^2 + \sigma_w^2$, meaning that the area above the expected continuous CDF of the random variable Y_i will also increase, shifting this CDF to the right. Therefore, the statistical hypothesis comes down to test one of the following inequalities:

$$\begin{aligned} H_0 &: F_n(y) \geq F_o(y) \\ H_1 &: F_n(y) < F_o(y) \end{aligned} \quad (16)$$

The problem with the AD test (and also with the Von Mises test) is that the deviation of the empirical CDF $F_n(x)$

to the reference CDF $F_0(x)$ can be either to the left and to the right as the test is based on the square of the difference $[F_n(x) - F_0(x)]^2$. For spectrum sensing application, the sign of the difference is significant for the reason cited above. Therefore, the associated expression of the GoF test statistic can be given as:

$$S_n = n \int_{-\infty}^{+\infty} [F_0(y) - F_n(y)] \phi(F_0(y)) dF_0(y). \quad (17)$$

According to the choice of the weight function $\phi(t)$, we can derive the corresponding test statistic of the statistical hypothesis in (16). When $\phi(t) = 1$, the above equation (17) can be simplified as

$$\begin{aligned} S_n &= n \int_{-\infty}^{+\infty} [F_0(y) - F_n(y)] dF_0(y) \\ &= n \int_{-\infty}^{y_1} F_0(y) dF_0(y) \\ &+ \dots \\ &+ n \int_{y^{(n)}}^{+\infty} (F_0(y) - 1) dF_0(y) \\ &= -\frac{n}{2} + \sum_{i=1}^n (F_0(y_i)) \\ &= -\frac{n}{2} + \sum_{i=1}^n (z_i) \end{aligned} \quad (18)$$

When $\phi(t) = \frac{1}{t(1-t)}$, the above equation (17) can be simplified as

$$\begin{aligned} S_n &= n \int_{-\infty}^{+\infty} [F_0(y) - F_n(y)] \phi(F_0(y)) dF_0(y) \\ &= n \int_{-\infty}^{y_1} \frac{F_0(y)}{F_0(y)(1-F_0(y))} dF_0(y) \\ &+ \dots \\ &+ n \int_{y^{(n)}}^{+\infty} \frac{F_0(y) - 1}{F_0(y)(1-F_0(y))} dF_0(y) \\ &= -\sum_{i=1}^n (\ln(1-F_0(y_i)) - \ln(F_0(y_i))) \\ &= -\sum_{i=1}^n (\ln(1-z_i) - \ln(z_i)) \end{aligned} \quad (19)$$

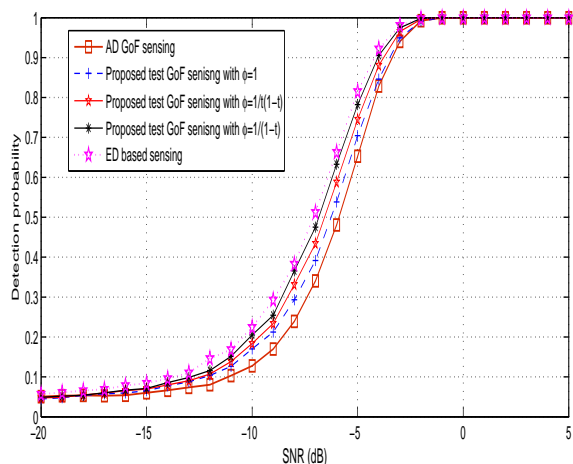


Figure 13. Detection probability versus SNR for the proposed GoF sensing under different weights, with $Pfa = 0.05$ and $n=80$ samples

When $\phi(t) = \frac{1}{(1-t)}$, the above equation (17) can be simplified as:

$$\begin{aligned}
 S_n &= n \int_{-\infty}^{+\infty} [F_0(y) - F_n(y)] \phi(F_0(y)) dF_0(y) \\
 &= n \int_{-\infty}^{y_1} \frac{F_0(y)}{(1-F_0(y))} dF_0(y) \\
 &+ \dots \\
 &+ n \int_{y(n)}^{+\infty} \frac{F_0(y) - 1}{(1-F_0(y))} dF_0(y) \\
 &= -n - \sum_{i=1}^n \ln(1 - F_0(y)) \\
 &= -n - \sum_{i=1}^n \ln(1 - z_i)
 \end{aligned} \tag{20}$$

Once the test S_n is calculated, it will be compared with a decision threshold λ to decide whether to accept H_1 or reject it (accept H_0). The threshold λ can be determined according to the given value of the false alarm probability. The decision threshold λ is computed through Monte Carlo simulation.

In Fig. 13, the performance comparison between the new GoF sensing method, AD GoF sensing [22] and ED sensing is depicted. This figure shows detection performance in terms of detection probability as a function of SNR with $n = 80$ and $Pfa = 0.05$ for different weights. The new GoF sensing method outperforms the AD sensing method. The best performance is obtained with weight $\phi = \frac{1}{1-t}$ corresponding to (20) which has comparable detection performance with ED sensing. Table I gives a corresponding λ for some critical values of Pfa .

The simulations results show that the new GoF sensing method has the best performance and the lowest computational complexity.

TABLE I. THRESHOLD VALUES FOR SOME GIVEN Pfa AND $n = 80$ SAMPLES

$\phi = 1$	Pfa Threshold	0.1	0.05	0.01
		3.536	4.480	6.295
$\phi = \frac{1}{t(1-t)}$	Pfa Threshold	0.1	0.05	0.01
		21.875	28.165	39.484
$\phi = \frac{1}{1-t}$	Pfa Threshold	0.1	0.05	0.01
		12.522	16.136	23.928

VI. CONCLUSION

In this paper, we present GoF sensing methods for CR. The paper has firstly provided a comparative study among existing GoF sensing methods. We have evaluated the performance of the GoF sensing methods through Monte-Carlo simulation. We have secondly studied some typical impairment for spectrum sensing, i.e., the effect of a non Gaussian noise, noise uncertainty and Rayleigh fading channel on the performance of GoF based sensing. As a model for the non Gaussian noise, we have used the Gaussian mixture (GM). It was observed that a non Gaussian noise can noticeably affect the performance of ED, but has only a limited influence on the performance of the GoF sensing methods. The same conclusion can be drawn for the impact of noise uncertainty and Rayleigh fading channel. This is mainly due to the fact that the test statistics in GoF testing is based on the difference of the measured CDF and the reference CDF and hence only indirectly influenced by noise parameters. Thirdly, we have proposed two new methods for GoF sensing. The first proposed method is the IQ GoF sensing method which consists in testing the real and the imaginary part of the received samples against the Gaussian distribution to make a decision. It was shown that this method exhibits better performance compared to ED. In the second method, we propose a new GoF test statistic by taking into account the physical characteristics of spectrum sensing. The derived GoF sensing method results in significant improvement in terms of sensing performance. Finally, this paper has shown the effectiveness of the GoF sensing methods in cognitive radio applications.

REFERENCES

- [1] FCC, "Federal communications commission: Spectrumpolicy task force report" <http://fjallfoss.fcc.gov/>, [retrieved: Mars, 2016], Nov. 2002.
- [2] J. Mitola and G. Q. Maguire, "Cognitive radio: making software more personel" IEEE Personal Commun Mag, vol. 6, pp. 13-18, 1999.
- [3] J. Mitola, Cognitive radio for flexible multimedia communications, IEEE International Workshop on., pp. 3-10, 1999.
- [4] T. Yucek and H. Arslan, "A survey of spectrum sensing algorithms for cognitive radio application", IEEE Communications Surveys and Tutorials, vol. 11, no. 1, pp. 70-78, Dec. 2009.
- [5] D. Cabric, S. M. Mishra, and R. W. Brodersen, Implementation issues in spectrum sensing for cognitive radios, in the 38th Asilomar Conference on Signals, Systems and Computers 2004 (Asilomar), Pacific Grove, CA, USA, 7-10 Nov. 2004, pp. 772-776.
- [6] H. Urkowitz, "Energy detection of unknown deterministic signals," IEEE Proceeding, vol. 55, no. 1, pp. 523-531, 1967.
- [7] A. Sahai and D. Cabric, "Spectrum sensing: Fundamental limits and practical challenges," IEEE International Symposium on New Frontiers in Dynamic Spectrum Access Networks (DySPAN '05), Baltimore, Md, pp. 50-58, USA. 2005.
- [8] M. Ghozzi, F. Markx, M. Dohler and J. Palicot, "Cyclostationarity based signal detection of vacant frequency bands" IEEE Int. Conf. Cognitive Radio Oriented Wireless Netw. Commun. 2006.

- [9] A. Tkachenko, D. Cabric and R. W. Brodersan, Cyclostationary feature detector experiments using reconfigurable BEE2, in Proc. IEEE Int.Symp. New Frontiers in Dynamic Spectrum Access Netw, pp. 216219, Dublin, Ireland, 2007.
- [10] P. S. Reddy and P. Palanisamy, Multitaper Spectrum Sensing Using Sinusoidal Tapers, 2nd International Conference on Advanced Computing, Networking and Security, pp. 47-50, Dec 2013.
- [11] Y. Zhao, Y. Wu, J. Wang, X. Zhong and L. Mei, "Wavelet transform for spectrum sensing in Cognitive Radio networks," 2014 International Conference on Audio, Language and Image Processing, Shanghai, 2014, pp. 565-569.
- [12] B. Farhang-Boroujeny, "Filter Bank Spectrum Sensing for Cognitive Radios," in IEEE Transactions on Signal Processing, vol. 56, no. 5, pp. 1801-1811, May 2008.
- [13] H. Wang and E. H. Yang and Z. Zhao and W. Zhang, Spectrum sensing in cognitive radio using goodness of fit testing, IEEE Trans. Wireless Commun, vol. 8, pp. 5427-5430, 2009.
- [14] G. Zhang and X. Wang and Y. C. Liang and J. Liu., "Fast and robust spectrum sensing via kolmogorov-smirnov test," IEEE Trans. Commun., vol. 58, pp. 3410-3416, 2012.
- [15] T. Kieu-Xuan and I. Koo, "Cramer-von Mises test spectrum sensing for cognitive radio systems," Wireless Telecommunication Symposium, pp. 1-4, 2011.
- [16] S. Rostami and K. Arshad and K. Moessner, "Order-Statistic Based Spectrum Sensing for Cognitive Radio," IEEE Trans. Commun., vol. pp. 592-595.
- [17] L. Shen and H. Wang and W.Zhang and Z. Zhao, "Blind Spectrum Sensing for Cognitive Radio Channels with Noise Uncertainty," IEEE Commun. Lett., vol. 10, pp. 1721-1724, 2011.
- [18] A. Subekti, A Blind Spectrum Sensing Method for DTV Signal Detection, International Conference of Information and Communication Technology (ICoICT), pp. 269-272, 2013.
- [19] D. Denkovski and V. Atanasovski and L. Gavrilovska, GHOST: Efficient Goodness-Of-Fit HOS Testing Signal Detector for Cognitive Radio Networks, IEEE ICC- Cognitive Radio and Networks Simposium., 2012.
- [20] L. Lu and H. C. Wu and S. S. Iyengar, A Novel Robust Detection Algorithm for Spectrum Sensing, IEEE Journal on Selected Areas in Communications., vol. 29, pp. 305-315, 2011.
- [21] S. S. Kalamkar P. K. Singh and A. Banerjee, Block Outlier Methods for Malicious User Detection in Cooperative Spectrum Sensing, IEEE Vehicular Technology Conference-Spring., Seoul, South Korea, 2014.
- [22] D. Teguig and V. Le Nir and B. Scheers, "Spectrum sensing method based on goodness of fit test using chi-square distribution," IET Journal. Electronics Letters, vol. 50, pp. 713715, 2014.
- [23] D. Teguig, V. Le Nir and B. Scheers, Spectrum Sensing Method Based on the Likelihood Ratio Goodness of Fit Test published in IET Journal (Electronics Letters), vol. 51(3), pages 253 - 255, 02 February 2015.
- [24] B. Scheers, D. Teguig and V. Le Nir, Wideband Spectrum Sensing technique based on Goodness-of-Fit testing, in International Conference on Military Communications and Information Systems ICMCIS, Cracow (Poland), May 2015.
- [25] D. Teguig, B. Scheers, V. Lenir, and F. Horlin, "Spectrum sensing Method Based on the Likelihood Ratio Goodness of Fit test under noise uncertainty". International journal of engineering research and technology, 3(9), 488-494, 2014.
- [26] T. W. Anderson and D. A. Darling, Asymptotic Theory of Certain Goodnes of Fit Criteria Based Stochastic Process, Annals of Mathematical Statistics, vol. 23, pp. 193-212, 1952.
- [27] F. Massey, "The Kolmogorov-Smirnov Test for Goodness of Fit," Journal of the American Statistical Association, vol. 69, pp. 730-737, 1974.
- [28] S. Bengio, Statistical machine learning from data: Gaussian mixture models, <http://bengio.abracadoudou.com/lectures/gmm.pdf>, [retrieved: January, 2015] .
- [29] Y. Singer and M. K. Warmuth, "A New Parameter Estimation Method for Gaussian Mixtures," in Advances in Neural Information Processing Systems, MIT Press, 1998.
- [30] A. Saha and G. Anand, Design of detectors based on stochastic resonance, Signal Processing, vol. 83, pp. 11931212, 2003.
- [31] A. Saha and G. Anand, A robust detector of known signal in non-gaussian noise using threshold systems, Signal Processing, vol. 92, pp. 26762688, 2012.
- [32] W. Jouini, Energy detection limits under log-normal approximated noise uncertainty, IEEE Signal Process. Lett., vol. 18(7), pp. 423426, 2011.
- [33] R. Tandra and A. Sahai, "SNR walls for signal detection," IEEE Journal of Selected Topics in Signal Processing, vol. 2, pp. 4-17, 2008.
- [34] J. Li, A. Bose and Y. Q. Zhao, "Rayleigh flat fading channels capacity," 3rd Annual Communication Networks and Services Research Conference (CNSR'05), 2005, pp. 214-217.

Spread Spectrum-Based Underlay Cognitive Radio Wireless Networks

Saed Daoud, David Haccoun, and Christian Cardinal

Department of Electrical Engineering
École Polytechnique de Montréal
Montréal, QC, Canada

Email: saed.daoud@polymtl.ca, david.haccoun@polymtl.ca, christian.cardinal@polymtl.ca

Abstract—In this paper, we investigate the performance of underlay cognitive radio (CR) systems that employ spread spectrum (SS). In particular, we consider a single-user secondary (cognitive) system that coexists with a multiple-user primary system. The quality of service of the primary system is protected by placing a maximum allowable interference power at the primary receiver (PR). We first derive the cumulative distribution function of the signal-to-interference-plus-noise ratio (SINR) at the secondary receiver (SR), which is then used to evaluate the outage probability and average bit error rate (ABER) of the secondary system. Simulation results verified by Monte-Carlo simulations show that SS-based underlay CR systems outperform conventional underlay CR systems by adapting the spreading factor (SF) of the spreading sequences.

Keywords—Cognitive radio; spread spectrum; outage probability; average bit error rate.

I. INTRODUCTION

Cognitive radio (CR) is a new promising technology, that makes an efficient use of the spectrum, by making the spectrum access process more dynamic, by adapting the transmissions' parameters to the surrounding environment, as well as to the users' demands [1]–[4]. In underlay CR mode [5], the adaptation is on the transmitted power from the unlicensed secondary (cognitive) system, such that the aggregate interference at the licensed primary receiver (PR) is below a certain threshold.

In [6], the author studied the capacity of underlay (also called *spectrum-sharing*) secondary system over additive white Gaussian noise (AWGN) channels, where the constraint is placed on the channel output signal, instead of the conventional problem formulation, where the constraint is placed on the channel input signal, mainly because of hardware limitation. In [7][8], the capacity of such system is studied over Rayleigh fading channels under peak and average interference power constraints placed at the primary receiver. In [9], the authors consider a multiuser secondary system which coexists with a primary system with one transmitter-receiver (TX-RX) pair. They found the outage probability at the best secondary receiver (SR) in terms of the received signal-to-interference-plus-noise ratio (SINR). The authors considered the effect of the primary system on the secondary receiver, which was something missing in the previously mentioned works.

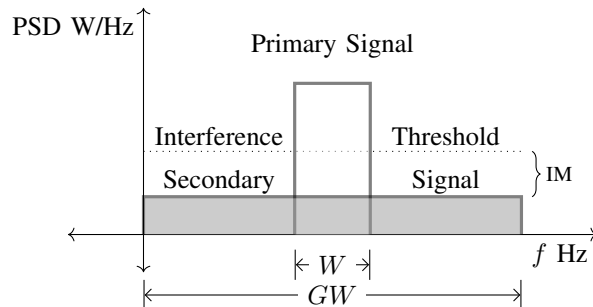


Figure 1. The primary and secondary signals's spectra at the PR.

In [10], the authors studied the problem of distributed frequency spectrum and power allocation and optimization for multicarrier direct sequence code division multiple access (MC DS-CDMA) system in an ad hoc setting. They considered the interweave mode, where the entire available spectrum is sensed, and only the subcarriers that are not being used are assigned to the secondary users. The optimization is done with a target data rate and available power constraints for each secondary user. In [11], the authors considered code division channelization, with joint transmit power and code assignment optimization, such that the interference from the secondary system to the primary system is considered acceptable, while SINR at the secondary receiver satisfies a pre-defined quality of service (QoS). In [12], the authors proposed a MC CDMA secondary system that aggregates non contiguous subbands such that the bandwidth of subbands isn't fixed.

In [13], we investigated the performance of a secondary system when spreading is done by repetition channel coding as a simple means of spreading. Also, we investigated the performance when a combination of channel coding and spread spectrum is used over AWGN channels. In [14], we investigated the problem of maximizing the throughput of a secondary system using CDMA under some idealistic assumptions. In this paper, we consider the coexistence of a primary system with an underlay secondary system, where the secondary system is assumed to be using direct sequence spread spectrum (DS-SS) with a spreading factor (SF) G . See Figure 1. The primary system consists of multiple primary transmitters (PTs) and one primary receiver (PR), while the

secondary system consists of one secondary transmitter (ST) and one secondary receiver (SR). The performance of the secondary system in terms of outage probability and average bit error rate (ABER) is investigated, by taking into account the effect of the primary system on SR. Simulation results verified by Monte-Carlo simulations show that SS-based CR systems outperform conventional underlay systems by adapting the spreading factor (SF) of the spreading sequences, which makes SS a promising technique to be used in such systems.

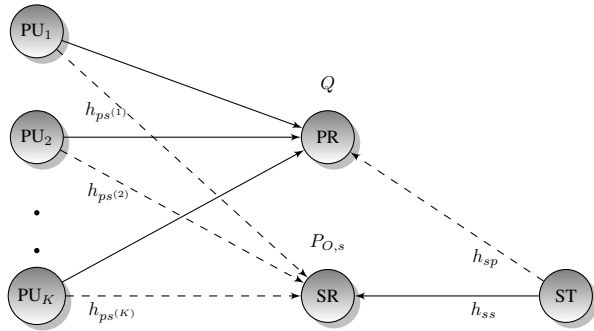


Figure 2. System Model. The dashed lines are interference links.

The rest of the paper is organized as follows: In Section II, the system and channel's model are presented, in Section III, the outage probability and ABER are investigated. In Section IV, simulation results are provided, and finally, we conclude in Section V.

II. SYSTEM AND CHANNEL'S MODELS

We consider the coexistence of a multiple primary user (PU) system with K users and a secondary cognitive system with one user. See Figure 2. It's assumed that all PUs communicate with one PR, i.e., multiple access uplink communication. Also, one secondary transmitter (ST) is communicating with one secondary receiver (SR). ST employs DS-SS with an SF of G , where we assume that $G \geq K$, while the primary system is assumed to employ frequency division multiple access (FDMA) such that there is no interuser interference (IUI) within the primary system. The channel between PU_k and the SR is denoted by $h_{ps}^{(k)}$ for $k = 1, 2, \dots, K$, while the channels between ST and PR and between ST and SR are denoted by h_{sp} and h_{ss} , respectively. All channels are assumed to be complex-valued Gaussian random variables with zero mean and unit variance. To protect the QoS of the primary system, a maximum interference threshold Q is set at the PR. PUs are assumed to transmit using a fixed power P , while ST is assumed to adapt its power such that the interference on PR is below Q .

III. PERFORMANCE ANALYSIS: OUTAGE PROBABILITY AND AVERAGE BIT ERROR RATE

In this section, the performance of SS-based underlay CR system in the presence of multiple-user primary system is evaluated in terms of outage probability and ABER.

A. Outage Probability

Outage probability of the CR system is defined as, the probability that the instantaneous SINR falls below a certain threshold, γ_{th} . Hence, first, SINR at SR will be quantified mathematically and statistically. The statistics of SINR then will be used to evaluate the outage probability (and ABER in the next subsection). Since it is assumed that $G \geq K$, the SINR at SR is given by

$$\Gamma_s = \frac{|h_{ss}|^2 S(h_{sp})}{\frac{P}{G} \sum_{k=1}^K |h_{ps}^{(k)}|^2 + \sigma_n^2}, \quad (1)$$

where $S(h_{sp})$ is the transmit power from ST, and σ_n^2 is the AWGN power. The transmit power $S(h_{sp})$ must be adjusted such that the total interference at PR is less than or equal to the maximum allowable interference power. Mathematically, we need

$$\frac{1}{G} |h_{sp}|^2 S(h_{sp}) \leq Q, \quad (2)$$

where the factor $1/G$ is due to spreading the secondary signal's power over a bandwidth that is G times larger than the minimum required bandwidth. Since we didn't place any physical power budget on ST, we can set it to its maximum allowable value, which is given by

$$S(h_{sp}) = \frac{GQ}{|h_{sp}|^2}. \quad (3)$$

Substituting (3) into (1) yields to

$$\Gamma_s = \frac{\frac{|h_{ss}|^2}{|h_{sp}|^2} G \gamma_Q}{\frac{\gamma_P}{G} \sum_{k=1}^K |h_{ps}^{(k)}|^2 + 1}, \quad (4)$$

where $\gamma_Q = Q/\sigma_n^2$ and $\gamma_P = P/\sigma_n^2$. Having the SINR expression at SR as in (4), the outage probability at SR can be expressed as

$$\begin{aligned} P_{O,s} &= \Pr[\Gamma_s \leq \gamma_{th}] \\ &= \Pr\left[\frac{\alpha_1 G \gamma_Q}{\frac{\gamma_P}{G} \alpha_2 + 1} \leq \gamma_{th}\right], \end{aligned} \quad (5)$$

where γ_{th} is the threshold below which the system will be in outage, $\alpha_1 = \frac{|h_{ss}|^2}{|h_{sp}|^2}$ and $\alpha_2 = \sum_{k=1}^K |h_{ps}^{(k)}|^2$. Let $\alpha_{XY} = |h_{XY}|^2$, then the CDF of α_1 can be expressed as

$$\begin{aligned} F_{\alpha_1}(x) &= \Pr\left\{\frac{\alpha_{ss}}{\alpha_{sp}} \leq x\right\} \\ &= \int_0^\infty \Pr\{\alpha_{ss} \leq x\beta | \alpha_{sp} = \beta\} f_{\alpha_{sp}}(\beta) d\beta, \end{aligned} \quad (6)$$

where $F_Y(y)$ and $f_Y(y)$ are the CDF and probability distribution function (PDF) of the random variable Y . Since the channels' coefficients are assumed to be complex-valued Gaussian random variables with zero mean and unit variance,

the channels' magnitude squares are exponentially distributed with unit mean, i.e.,

$$F_{\alpha_{ss}}(x) = 1 - \exp(-x) \quad (7a)$$

$$f_{\alpha_{sp}}(x) = \exp(-x). \quad (7b)$$

It is straightforward to show that the CDF of the random variable α_1 , denoted by $F_{\alpha_1}(x)$ to be

$$F_{\alpha_1}(x) = \Pr[\alpha_1 \leq x] = 1 - \frac{1}{x+1}. \quad (8)$$

Also note that α_2 is the summation of K squared *complex-valued* Gaussian random variables with variance $1/2$ per dimension, i.e., α_2 is central Chi-square random variable with $2K$ degrees of freedom. Thus, its PDF is given by [15]

$$f_{\alpha_2}(\alpha_2) = \frac{1}{(K-1)!} \alpha_2^{K-1} e^{-\alpha_2}. \quad (9)$$

Then, the outage probability in (5) can be re-written as

$$\begin{aligned} P_{O,s} &= \int_0^\infty F_{\alpha_1} \left(\frac{\gamma_{th}}{G\gamma_Q} \left[\frac{\gamma_P}{G} \alpha_2 + 1 \right] \right) f_{\alpha_2}(\alpha_2) d\alpha_2 \\ &= 1 - \frac{1}{(K-1)! \frac{\gamma_{th}\gamma_P}{G^2\gamma_Q}} \underbrace{\int_0^\infty \frac{\alpha_2^{K-1} e^{-\alpha_2}}{\alpha_2 + \frac{G^2\gamma_Q}{\gamma_{th}\gamma_P} \left[\frac{\gamma_{th}}{G\gamma_Q} + 1 \right]}_I d\alpha_2, \end{aligned} \quad (10)$$

where $F_{\alpha_i}(\cdot)$ and $f_{\alpha_i}(\cdot)$ are the CDF and PDF of the random variable α_i . From [16, eq. 3.353.5], the integral I can be expressed as

$$I = (-1)^{n-1} \beta^n e^{\beta\mu} \text{Ei}(-\beta\mu) + \sum_{k=1}^n (k-1)! (-\beta)^{n-k} \mu^{-k}, \quad (11)$$

where $n = K - 1$, $\mu = 1$, and $\beta = \frac{G^2\gamma_Q}{\gamma_{th}\gamma_P} \left[\frac{\gamma_{th}}{G\gamma_Q} + 1 \right]$.

B. Average Bit Error Rate (ABER)

Another useful performance metric is the ABER, which will be derived next. Toward that end, let

$$X = \frac{\alpha_1 G \gamma_Q}{\gamma_P \alpha_2 + 1}. \quad (12)$$

Without any loss of generality, and for simplicity of exposition, coherent binary phase shift keying (BPSK) is assumed. In this case, the conditional BER is given by

$$\begin{aligned} \varepsilon_s(x) &= Q \left[\sqrt{2x} \right] \\ &\leq \frac{1}{2} e^{-x}, \end{aligned} \quad (13)$$

where we used the Chernoff upper bound of the Gaussian Q -function in the second line of (13). Then the ABER is upper bounded as

$$\varepsilon_s \leq \frac{1}{2} \int_0^\infty e^{-x} f_X(x) dx \quad (14)$$

where $f_X(x)$ is the PDF of the random variable X . It can be shown by integration by parts that

$$\int_0^\infty e^{-x} f_X(x) dx = \int_0^\infty e^{-x} F_X(x) dx, \quad (15)$$

where $F_X(x)$ is the CDF of the random variable X . This implies that we don't need to derive the PDF of the random variable X , but instead, we can use the CDF directly in evaluating the ABER. The ABER in (14) can be re-written as

$$\varepsilon_s \leq \frac{1}{2} \int_0^\infty e^{-x} F_X(x) dx. \quad (16)$$

The CDF to evaluate the ABER has the same expression as the outage probability in (10) by replacing γ_{th} with x . The ABER can be re-written then as

$$\varepsilon_s = \frac{1}{2} - \frac{G^2\gamma_Q}{2(K-1)!\gamma_P} \int_0^\infty \frac{1}{x} e^{-x} I(x) dx, \quad (17)$$

where

$$\begin{aligned} I(x) &= (-1)^{n-1} \left[\frac{G}{\gamma_P} + \frac{G^2\gamma_Q}{x\gamma_P} \right]^n e^{\frac{x}{\gamma_P} + \frac{G^2\gamma_Q}{x\gamma_P}} \text{Ei} \left(- \left[\frac{G}{\gamma_P} + \frac{G^2\gamma_Q}{x\gamma_P} \right] \right) \\ &\quad + \sum_{k=1}^n (k-1)! \left(- \left[\frac{G}{\gamma_P} + \frac{G^2\gamma_Q}{x\gamma_P} \right] \right)^{n-k}, \end{aligned} \quad (18)$$

where $n = K - 1$.

IV. NUMERICAL RESULTS

In this section, numerical evaluation verified by Monte-Carlo simulations are provided for the above mathematical derivations.

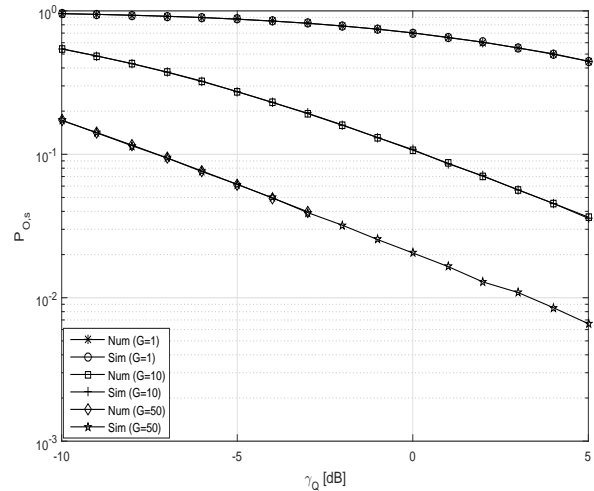


Figure 3. Outage probability at SR vs. γ_Q [dB] for $\gamma_P = 3$ dB, $\gamma_{th} = 0$ dB, $G = \{1, 10, 50\}$, and $K = 1$.

In Figure 3, outage probability vs. γ_Q in [dB] is shown for single user system (i.e., $K = 1$), and for $G = \{1, 10, 50\}$, $\gamma_P = 3$ dB, and $\gamma_{th} = 0$ dB. Monte-Carlo simulations are

also shown, where 10^5 channel realizations were generated for each γ_Q point. Two observations can be made. First, underlay cognitive radio system that employs spread spectrum (i.e., $G > 1$) has better performance than conventional systems that don't employ SS (i.e., $G = 1$). This is because of two reasons, a) by spreading the secondary signal's spectrum over larger bandwidth using spreading sequences, the interference caused at PR is reduced per unit bandwidth, and that allows ST to transmit at higher power (see Figure 1), and b) the interference caused by PT at SR is also reduced, because deprecating the secondary received signal by a synchronized replica of the spreading sequence has the effect of spreading the primary signal's power over larger bandwidth, and thus its effect within the secondary signal's bandwidth is significantly reduced, which contributed more to better performance. That is why the performance as seen in Figure 3 is improved as G increased. In conventional systems, the secondary system cannot do anything beyond adapting its power to meet the interference threshold requirement at PR. Because of this, secondary systems usually don't have enough interference margin that allows the secondary system to be operational, by transmitting at an acceptable power level. On the other hand, in SS-based underlay CR systems, SF G can be adapted such that the interference threshold at PR is met, and making the secondary system operational. The second observation is that, Monte-Carlo simulations are in agreement with the numerical evaluation, which implies that our mathematical derivations are correct.

In Figure 4, outage probability vs. γ_Q in [dB] is shown for multiple primary user system for $K = 5$, and for $G = \{10, 50\}$ (note that we didn't include $G = 1$ for non SS systems, because it is assumed that $G \geq K$, such that the effect of the secondary system is the same for all primary users), $\gamma_P = 3$ dB, and $\gamma_{th} = 0$ dB. Monte-Carlo simulations are also shown, where 10^5 channel realizations were generated for each γ_Q point. The same observations as before can be made.

In Figure 5, outage probability vs. γ_Q [dB] is shown for $K = \{1, 5, 10\}$, $G = 50$, $\gamma_p = 10$ dB, and $\gamma_{th} = 5$ dB. In this case, when G is fixed, and K is variable, we note that, as K is increased, the performance deteriorates. Which is expected, because, although the primary signals' power are despread at SR, the interference from the primary system at SR is the sum of the interference from all primary users. We notice that, the difference in performance as K is increased is not significant. Maybe this due to that fact that G is large enough to make the interference from the primary system to be small, and in the limit when $G \rightarrow \infty$, the system performance approaches that of point-to-point system with no interference.

In Figure 6, ABER vs. γ_Q [dB] is shown for $K = 2$ users, and $G = \{10, 100\}$. The corresponding Monte-Carlo simulation curves are shown as well. It can be observed that there is an error floor. This is due to the fact that, although the primary signals are spread at the SR, the interference is the sum of the primary spread signals. However, as G is increased,

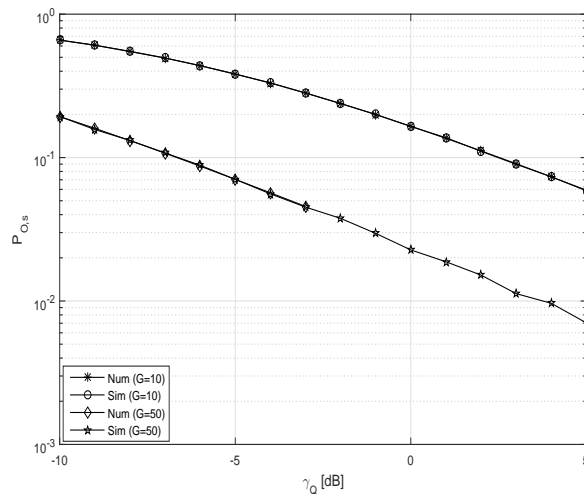


Figure 4. Outage probability at SR vs. γ_Q [dB] for $\gamma_P = 3$ dB, $\gamma_{th} = 0$ dB, $G = \{10, 50\}$, and $K = 5$.

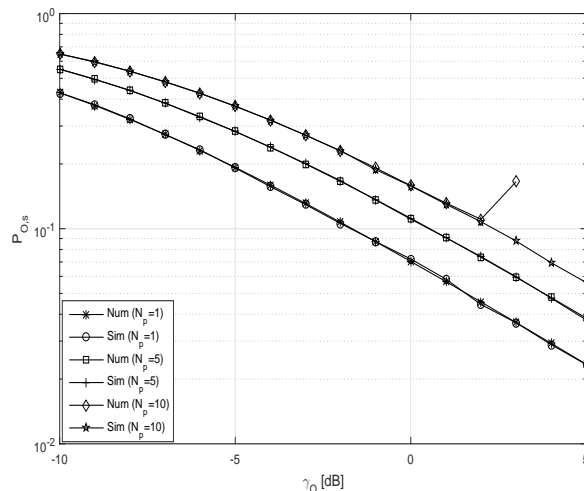


Figure 5. Outage probability at SR vs. γ_Q [dB] for $\gamma_P = 10$ dB, $\gamma_{th} = 5$ dB, $G = 50$, and $K = \{1, 5, 10\}$.

the performance is improved, which is again attributed to the fact that the interference level from each PU is decreased within the secondary signal's bandwidth of interest. We can also observe that there is a small constant difference between the numerical evaluation and Monte-Carlo simulations, which we believe is due to an inherit error in the numerical evaluation of the integral (17).

V. CONCLUSIONS AND FUTURE WORK

In this paper, we considered SS-based underlay cognitive radio systems, and the performance of such systems was evaluated. In particular, first the CDF of the SINR at SR was derived, which was then used to evaluate the outage probability and ABER of the secondary system. Numerical results verified by Monte-Carlo simulations showed that, deploying SS in

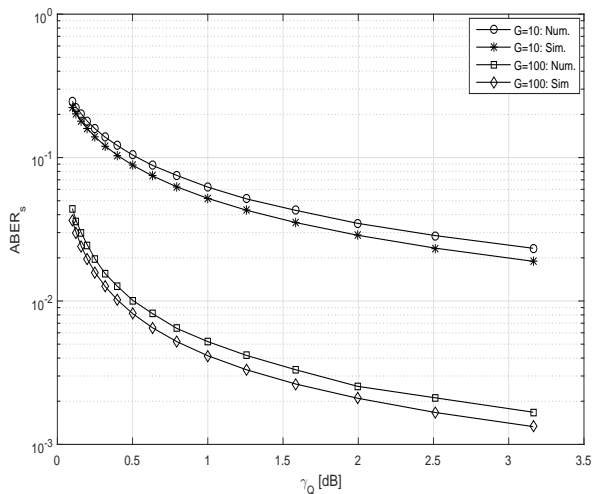


Figure 6. ABER vs. γ_Q [dB] for $\gamma_P = 5$ dB, $G = [10 \ 100]$, and $K = 2$.

underlay CR systems, can improve the performance significantly compared to non-SS underlay CR systems. This study showed that underlay CR systems can be considered a viable option besides the interweave mode, because a limiting factor in underlay systems was that the transmit power is too low for the secondary system to be operational. Spread spectrum can alleviate this limitation.

As a future work, we will consider the case when both the primary and secondary systems consist of multiple users. Furthermore, the effect of channel estimation and synchronization for the spreading sequences will be considered.

REFERENCES

[1] J. Ma, G. Li, and B. H. Juang, "Signal processing in cognitive radio," *Proc. IEEE*, vol. 97, no. 5, pp. 805–823, May 2009.

[2] M. Buddhikot, "Understanding dynamic spectrum access: Models, taxonomy and challenges," in *2nd IEEE International Symposium on New Frontiers in Dynamic Spectrum Access Networks, 2007. DySPAN 2007.*, April 2007, pp. 649–663.

[3] S. Haykin, D. Thomson, and J. Reed, "Spectrum sensing for cognitive radio," *Proc. IEEE*, vol. 97, no. 5, pp. 849–877, May 2009.

[4] Q. Zhao and B. Sadler, "A survey of dynamic spectrum access," *IEEE Signal Processing Mag.*, vol. 24, no. 3, pp. 79–89, May 2007.

[5] A. Goldsmith, S. Jafar, I. Maric, and S. Srinivasa, "Breaking spectrum gridlock with cognitive radios: An information theoretic perspective," *Proc. IEEE*, vol. 97, no. 5, pp. 894–914, May 2009.

[6] M. Gastpar, "On capacity under receive and spatial spectrum-sharing constraints," *IEEE Trans. Inform. Theory*, vol. 53, no. 2, pp. 471–487, Feb. 2007.

[7] A. Ghasemi and E. S. Sousa, "Fundamental limits of spectrum-sharing in fading environments," vol. 6, no. 2, pp. 649–658, Feb 2007.

[8] L. Musavian and S. Aissa, "Capacity and power allocation for spectrum-sharing communications in fading channels," *IEEE Trans. Commun.*, vol. 8, no. 1, pp. 148–156, Jan 2009.

[9] C. Kabiri, H. J. Zepernick, and H. Tran, "Outage probability and ergodic capacity of underlay cognitive radio systems with adaptive power transmission," in *2013 9th International Wireless Communications and Mobile Computing Conference (IWCMC)*, vol. 2, 2013, pp. 785–790.

[10] Q. Qu, L. B. Milstein, and D. R. Vaman, "Cognitive radio based multi-user resource allocation in mobile ad hoc networks using multi-carrier CDMA modulation," *IEEE J. Select. Areas Commun.*, vol. 26, no. 1, pp. 70–82, 2008.

[11] M. Li *et al.*, "Cognitive code-division links with blind primary-system identification," *IEEE Trans. Wireless Commun.*, vol. 10, no. 11, pp. 3743–3753, Nov. 2011.

[12] A. Attar, M. R. Nakhai, and A. H. Aghvami, "Sequence design for cognitive cdma communications under arbitrary spectrum hole constraint," *IEEE Trans. Wireless Commun.*, vol. 7, no. 4, pp. 1157–1162, 2008.

[13] S. Daoud, D. Haccoun, and C. Cardinal, "Underlay cognitive radio wireless networks using repetition coding and spread spectrum," in *The Sixth International Conference on Advances in Cognitive Radio, COCORA 2016*, Lisbon, Portugal, Feb. 2016. (Best paper award).

[14] —, "On the achievable rate and average sum capacity of spread spectrum underlay cr networks," in *2016 IEEE 84th Vehicular Technology Conference: VTC2016-Fall*, Montreal, Canada, Sept. 2016.

[15] J. Proakis, *Digital Communications*, 4th ed. McGraw-Hill, 2000.

[16] I. S. Gradshteyn and I. M. Ryzhik, *Table of Integrals, Series, and Products*, sixth edition ed. San Diego, CA: Academic Press, 2000.

Experimentation with Radio Environment Maps for Resources Optimisation in Dense Wireless Scenarios

Rogério Pais Dionísio

Escola Superior de Tecnologia
Instituto Politécnico de Castelo Branco
Avenida do Empresário, S/N
6000-767 Castelo Branco, Portugal
Email: rdionisio@ipcb.pt

Tiago Ferreira Alves, Jorge Miguel Afonso Ribeiro

Allbesmart, Lda
Centro de Empresas Inovadoras
Avenida do Empresário, n.º1
6000-767 Castelo Branco, Portugal
Email: (talves, jribeiro)@allbesmart.pt

Abstract—The rapidly increasing popularity of WiFi has created unprecedented levels of congestion in the unlicensed frequency bands, especially in densely populated urban areas. This results mainly because of the uncoordinated operation and the unmanaged interference between WiFi access points. Recently, Radio Environment Maps (REM) have been suggested as a support for coordination strategies that optimize the overall WiFi network performance. Despite some theoretical work done in this area, there are no clear experimental evidences of the benefit brought by WiFi coordination. In this context, the main objective of this experiment is to assess the benefit of a coordinated management of radio resources in dense WiFi networks using REMs for indoor scenarios. This experiment has used the w-iLab.t test environment provided by iMINDS, a cognitive-radio testbed for remote experimentation. It was shown that REMs are capable of detecting the presence of interfering links on the network (co-channel or adjacent channel interference), and a suitable coordination strategy can use this information to reconfigure Access Points (AP) channel assignment and reestablish the client connection. The coordination strategy almost double the capacity of a WiFi link under strong co-channel interference, from 6.8 Mbps to 11.8 Mbps, increasing the aggregate throughput of the network from 58.7 Mbps to 71.5 Mbps. However, this gain comes with the cost of a relatively high density network of spectrum sensors (12 sensors for an area of 60×20 m), increasing the cost of deployment.

Keywords—Radio Environment Map; Radio Test-bed; Radio Resource Management; Experimentation.

I. INTRODUCTION

During the last fifteen years, the WiFi technology, as a last mile access to Internet, has experienced global explosion. Nowadays, the WiFi networks carry more traffic to and from end-users terminals (PCs, tablets, and smartphones) than Ethernet and cellular networks combined. The success of this technology is owed to its introduction in unlicensed spectrum (ISM bands), which has furthermore allowed unprecedented innovation in the wireless technology. However, as the penetration of WiFi continues, the unlicensed bands are becoming overcrowded. Unpredictable user-deployed hot spots (smartphone) are a new source of interference and instability that can undermine the network performance. Moreover, many Internet of Things (IoT) devices also share the unlicensed spectrum with WiFi, which further increases the problem scale. In fact, interference is a limit factor of WiFi densification; this

is a result mainly because of the uncoordinated operation and the unmanaged interference between the WiFi Access Points (AP). In WiFi, each Access Point can only access locally available sensing information within single cell coverage. It cannot access global knowledge on a multi-AP network and the deployment environment, leading to a sub-optimal network configuration.

In this context, the design of the WiFi networks is complex because of the high-density of users and significant variability of capacity requirements that can be strongly dependent on location and time. The variability of the capacity demand can be faced by deploying a dynamic network infrastructure, in which WiFi access points can be switched on and off, can work on different bands, and can tune their coverage range according to the network status and QoS requirements.

Several research works have claimed that a coordinated approach of the Radio Resource Management (RRM) of channel frequency and power can increase the performance of WiFi networks in dense deployment scenarios [1], and have recently demonstrated the potential economic value of WiFi coordination in dense indoor Experiments [2]. Other research work claims that an important input for interference management and coordination strategies is the Radio Environment Map (REM) of the target coverage area. The REM is a dataset of spectrum occupancy and interference levels computed based on raw spectrum measurements, propagation modelling and spatial interpolation algorithms [3]. RRM algorithms can use REMs to optimize the overall network performance. In spite of several theoretical studies on the coordinated management of WiFi networks [1], there is no experimental evidences of the benefits promised by the academic or industrial research studies.

The main objective of this experiment is to assess the benefit of a coordinated approach in dense WiFi networks that make use of realistic Radio Environment Maps, using an implementation-oriented approach in a wireless testbed environment. An important performance metric is the gain in terms of average throughput, comparing the coordinated approaches with the legacy uncoordinated approach. In particular, we are interested in measuring the average capacity gain, when using market available and low cost spectrum sensors in very dense indoor scenarios. The results of this experiment are very useful from a business perspective and industrial

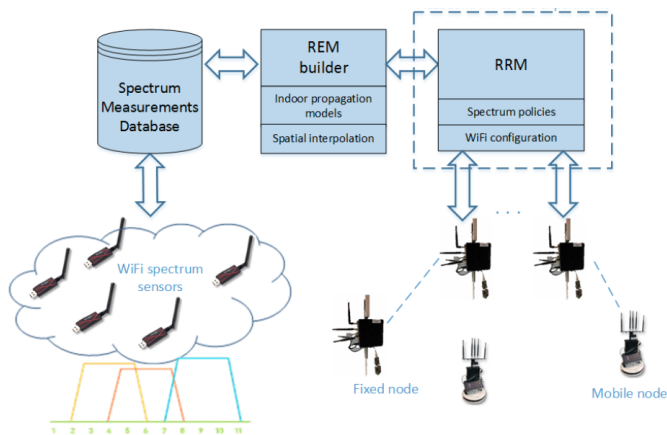


Figure 1. Generic Setup diagram for the experiment.

research, in order to realize if the actual coordination gain is sufficient enough to justify the investment in the sensing and the signalling infrastructure needed to implement a WiFi coordination scheme in realistic scenarios [3].

This paper is organised in four sections. The first section introduces the background and describes the motivation of the work. In Section II, we describe the testbed and define the setup environment of the experiments. The third section presents the experimental results with different measurements. Conclusions and future work are drawn in Section IV.

II. SETUP OF THE EXPERIMENT

This section defines and describes in detail the setup environment of the experiment.

A. Setup architecture

The setup diagram of the demonstrator, depicted in Figure 1, encompasses four major components, as briefly explained in the following:

- A network of spectrum sensors (energy detectors) that report spectrum measurements to a database.
- A REM builder module that computes the radio environmental maps based on measurements stored in the spectrum database, the positions/configurations of radio transmitters (AP), indoor propagation models and spatial interpolation algorithms.
- The RRM that optimizes the overall WiFi network in terms of channel and power allocation based on the REM.
- WiFi APs that receive the configuration settings and reports performance metrics to the RRM module.

B. Testbed and resources allocation

All experiments took place in a shielded environment in the W-iLab.t testbed (Ghent – Belgium). The nodes are installed in an open room (66 m by 21 m) in a grid configuration. Figure 2 shows the testing area and the locations of the nodes, represented by blue numbered circles. Each node has one embedded PC (ZOTAC) with two wireless IEEE 802.11 a/b/g/n cards (Spartklan WPEA-110N/E/11n), a spectrum sensor (Wi-Spy USB spectrum analyzer), one Gigabit LAN,

and also a Bluetooth USB 2.0 Interface and a ZigBee sensor node.

We have selected 5 equidistant links in a Client – Server configuration, represented by a black arrow in Figure 2. The distance between adjacent links is 12 m, and for each link, the distance between the client node and the AP node is 3.6 m. The red arrow represents the interfering link, with a separation of 12.53 m between nodes.

Besides the available WiFi hardware, the testbed offers several software tools to setup, control and gather radio measurements. We used the java-based framework jFed [4] to configure the testbed nodes. jFed is also used to activate nodes, install the Operating System, and SSH into the nodes. OMF6 [5] controls all the experiments, using scripts written with OMF Experiment Description Language (OEDL) [6], which is based on the Ruby programming language. The experiment description with OMF6 is structured in two main steps:

- 1) First, we declare the resources to be used in the experiment, such as applications, nodes, and related configurations, such as Wi-Fi channels and transmitted power;
- 2) In the second step, we define the events that triggers the experiment's execution, and the tasks to be executed.

The Iperf traffic generator tool [7] generates data for each link using a client-server configuration for each link. All links parameters are recorded during 100 seconds for all experiments. This ensures that the radio signals for the links under test are on the air and stable. The measurements data are extracted during the experiment using OML [8]. OML is a stand-alone tool that parses and reports all the measurements to a database (SQLite3 or PostgreSQL) installed on the experiment controller server of the testbed.

C. Radio Environment Map builder

The REM is a dataset of spectrum occupancy computed based on raw spectrum measurements, propagation modelling and spatial interpolation algorithms.

There are several methods to compute REMs available on the literature, with different interpolation approaches and based on space and time spectrum measurements. One of the most commonly used methods is the Inverse Distance Weighted Interpolation (IDW) [3]. Despite the "bull's eyes" effect, this method is relatively fast and efficient, and present good properties for smoothing REM. In order to decrease the sensitiveness to outlier measurements, we have implemented a modified version of IDW method, which calculates the interpolated values using only the nearest neighbour's points.

In order to compute the REM, the exact position of each radio node on the w-iLab.t testbed area is defined as shown in Figure 2. REMs are computed using Matlab to facilitate the integration with the RRM algorithms, also implemented in Matlab.

D. RRM coordinating strategies

The RRM optimizes the overall WiFi network configuration in terms of channel, and power allocation based on the information provided by the REM. The adopted RRM strategies during the experiments are the following [1]:

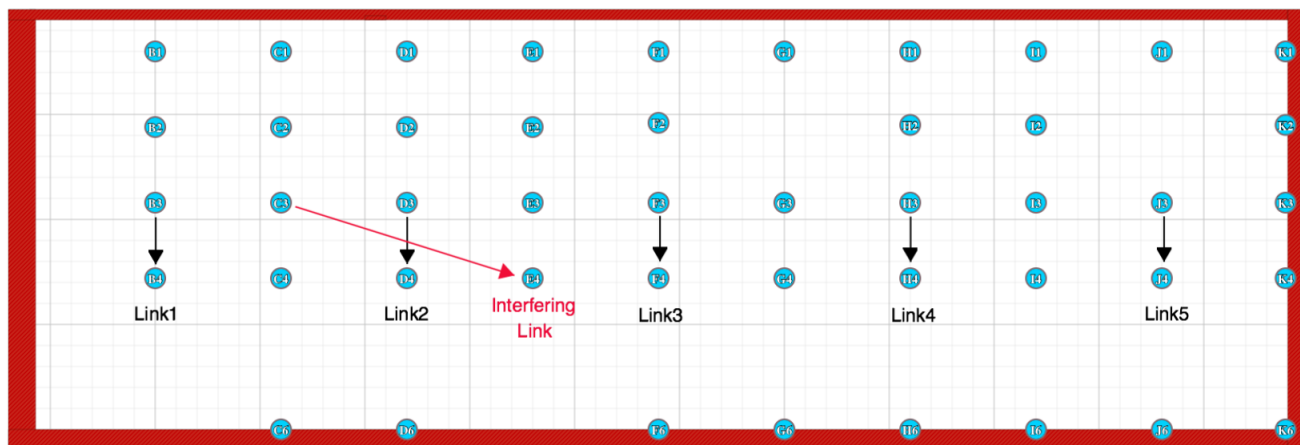


Figure 2. W-iLab.t testbed environment: Distance between AP and client is 3.6m for Links 1, 2, 3, 4 and 5, and 12.53 m for the Interfering Link.

- Strategy 1: Allocate the WiFi links to disjoint, non-overlapping bands and use minimum possible transmit power for each WiFi link;
- Strategy 2: Optimize the transmit power of multiple WiFi links, when interference is detected.

III. EXPERIMENTAL MEASUREMENTS AND RESULTS

After describing the setup architecture and the testbed resources, we will explain the experimental measurement campaigns. Each set of measurement aims at studying the influence of measurable interference characteristics on the throughput of the WiFi network under study. The process was structured in four steps:

- 1) Spectrum measurements from the spectrum sensors in all WiFi frequency channels;
- 2) Compute the REMs based on spectrum measurements and IDW algorithm;
- 3) Measure and record the throughput of the radio links;
- 4) Apply the coordination strategy, e.g., reconfigure the channel allocation or the transmitted power of each APs.

A. Estimation of the path-loss propagation model

Having a suitable propagation model is a key element to build good REMs, therefore before running the experiments, we have measured the path loss between the clients and the APs in the w-iLab.t test environment to estimate the propagation model parameters. Since the majority of the nodes are in Line-of-Sight (LoS) and relatively closed to each other, as shown in Figure 2, we have considered a Free Space Path Loss (FSPL) model:

$$L = n(10\log_{10}(d) + 10\log_{10}(f)) + 32.45 \text{ (dB)} \quad (1)$$

Where L is the path loss in dB, d is the distance in meters, f is the frequency in GHz and n is the path loss exponent, which is 2 in the FSPL model. The path-loss measurement process was implemented as follows:

- 1) Setup one node as an AP with 5 dBm transmit power (P_{Tx}) on WiFi Channel 1 ($f = 2.412$ GHz), and all the other nodes as clients.

- 2) For each client:
 - Measure the Received Signal Strength Indication (RSSI) of the AP, denoted as P_{Rx} .
 - Measure the distance d between the client and the AP.
- 3) Setup a different node as AP and the remaining nodes as clients.
- 4) Repeat steps 1), 2) and 3).

The blue dots on Figure 3 represent the results of the measurement campaign.

Considering Friis transmission equation, $L = P_{Tx}$ (dBm) – P_{Rx} (dBm), combined with (1), we compute an estimate of the path loss exponent n [9],

$$\begin{aligned} P_{Tx} - P_{Rx} &= n(10\log_{10}(d) + 10\log_{10}(f)) + 32.45 \\ \Leftrightarrow \\ n &= \frac{P_{Tx} - P_{Rx} - 32.45}{10\log_{10}(d) + 10\log_{10}(f)} \end{aligned} \quad (2)$$

Using (2) with the Fitting Toolbox provided by Matlab and the measured RSSI (P_{Rx}), the value of n was found to be 2.097, with a 95% confidence bounds [2.084, 2.109]. This experimentally determined value corresponds to what we are expecting for a LoS scenario. The red curve in Figure 3 shows the result of the fitting process.

Appropriate AP power levels are essential to maintaining a coverage area, not only to ensure correct (not maximum) amount of power covering an area, but also to ensure that excessive power is not used, which would add unnecessary interference to the radiating area. Transmitted power can be minimised to reduce interference among the APs.

Considering a typical baseline signal strength of -65 dBm for the WiFi received signals coming from adjacent cells, using (1) and $n = 2.097$, we have computed the optimal transmit power as a function of the distance, as depicted in Figure 4. This study is important to setup the initial APs transmit power to ensure a suitable cell coverage. Considering that 12 m is the separation between adjacent WiFi cells in the experiment set-up (Figure 2), the APs transmit power are set at 0 dBm, unless otherwise noted in the following experiments.

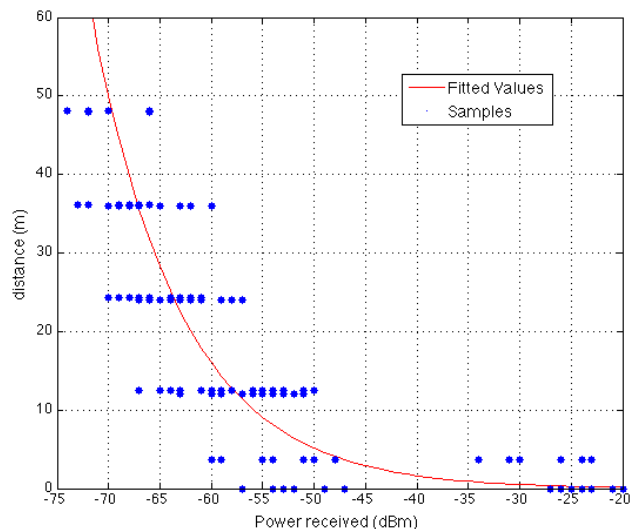


Figure 3. RSSI measurement campaign (blue dots) and corresponding fitting curve (red line).

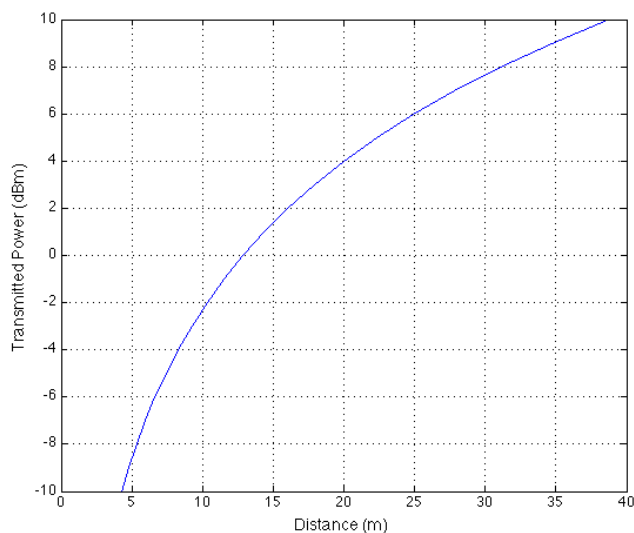


Figure 4. Transmit power as a function of the distance, for -65 dBm received power baseline.

B. Measurement 1: Assessment of the channel distribution influence on the throughput

The aim of this experiment is to assess the influence of channel distribution on the throughput, and verify the worst-case reference scenario in terms of intra-network co-channel interference, e.g., when all APs assigned to the same channel (Channel 1 – 2.412 GHz).

The average values of the measured throughput for each link and the aggregated throughput of the WiFi network are shown in Table I. As expected, the low values of link’s throughput are due to the strong co-channel interference that limits the overall performance of the network. Note that this is a worst-case reference scenario in terms of co-channel

interference.

TABLE I. THROUGHPUT RESULTS FOR MEASUREMENT 1.

Measurement 1	Channel Number	Throughput (Mbps) $P_{Tx} = 0$ dBm
Link 1	1	5.25
Link 2	1	4.02
Link 3	1	3.93
Link 4	1	3.86
Link 5	1	5.28
Aggregated Throughput (Mbps)		22.34

C. Measurement 2: Considering no-overlapping channels assignment – baseline scenario

With this experiment, all APs are configured with non-overlapping channels: Channel 1 (2.412 GHz), Channel 6 (2.437 GHz) and Channel 11 (2.462 GHz). The measured throughput presented in Table II clearly shows the advantage of using non-overlapping channels in the WiFi planning. With a transmitted power set to 0 dBm on each APs, the measured aggregated throughput is 71.50 Mbps, i.e., more than three times higher than the value in Measurement 1 (22.34 Mbps). However, if the transmitted power P_{Tx} is increased to 5 dBm, the aggregate throughput decreases to 66.05 Mbps, because of the higher co-channel interference between Link 1 and Link 4, and between Link 2 and Link 5. Note that according to Figure 4, with 5 dBm, the APs have 22 m coverage radius. This channel configuration is the baseline for the following measurements.

D. Measurement 3: Channel reallocation triggered by co-channel interference

The setup for Measurement 3 has the same non-overlapping channels allocation as in Measurement 2, with an additional interference Link active at Channel 11, placed next to Link 2, as depicted in Figure 2. Three different interference power levels (P_I) were applied during the experiment $\{0, 7, 15\}$ (dBm). The computed REMs at channel 11 for different interference link’s power are shown in Figure 5(a). The color gradient represents the computed power in dBm for a particular channel at location (x, y) . The location of the nodes is added as an additional layer (black circles). The yellow dots are due the ”bull’s eye” effect typical of the IDW interpolation algorithm and should be discarded. It can be seen that by observing the REMs, we can detect not only Link 2 and Link 5, but also the extra radio activity coming from the interfering link. Note that the detection of this interfering link will trigger the coordination strategy in the WiFi network.

The results from Table III shows an overall network throughput decrease, compared with the results from Measurement 2, mainly due to the interference from the interfering link on Link 2 and Link 5. However, the results indicate that the variation on the power level of the interferer doesn’t have a strong impact on the aggregate throughput.

From the REM information, the coordination strategy re-allocates the WiFi channels among the APs, in order to avoid strong co-channel interference. The REM for Channel 11, depicted in Figure 5(b), shows a clear spatial separation between the interference source and Link 4.

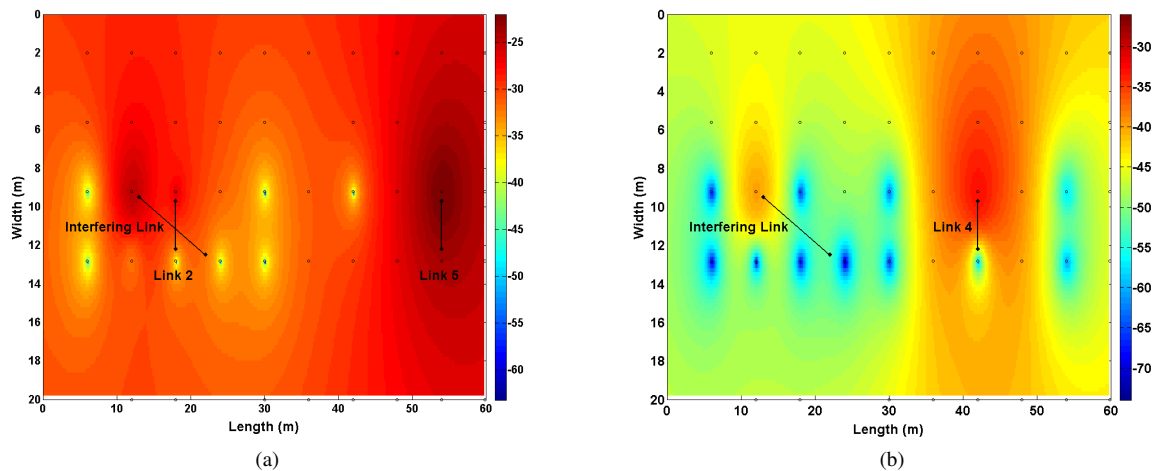


Figure 5. Measurement 3. (a): REMs with Link 2, Link 5 and Interferer Link at Channel 11 with 0 dBm; (b): REMs with Link 4 and Interferer Link at Channel 11 with 0 dBm. Color bar in dBm.

TABLE II. THROUGHPUT RESULTS FOR MEASUREMENT 2.

Measurement 2	Channel Number	Throughput (Mbps)	Throughput (Mbps)
		$P_{Tx} = 0$ dBm	$P_{Tx} = 5$ dBm
Link 1	1	13.27	12.16
Link 2	11	11.76	10.50
Link 3	6	21.54	21.56
Link 4	1	12.57	11.18
Link 5	11	12.36	10.65
Aggregated Throughput (Mbps)		71.50	66.05

TABLE III. THROUGHPUT RESULTS FOR MEASUREMENT 3.

Measurement 3	Channel Number	Throughput (Mbps)	Throughput (Mbps)	Throughput (Mbps)
		$P_I=0$ dBm	$P_I=7$ dBm	$P_I=15$ dBm
Before RRM strategy				
Link 1	1	12.12	12.30	12.3
Link 2	11	6.80	7.08	6.98
Link 3	6	21.59	21.63	21.61
Link 4	1	11.27	11.23	11.07
Link 5	11	6.88	6.83	6.75
Aggregated Throughput (Mbps)		58.67	58.96	58.70
After RRM strategy				
Link 1	6	13.27	13.12	13.10
Link 2	1	11.76	11.62	11.56
Link 3	6	21.53	21.55	21.61
Link 4	11	12.57	12.73	2.70
Link 5	1	12.37	12.41	12.40
Aggregated Throughput (Mbps)		71.47	71.43	71.38

Table III show a significant throughput increase from 58 Mbps to 71 Mbps thanks to the coordination strategy. The aggregate throughput is now close to the values obtained with Measurement 2, i.e., without any interference Link. Once again, the results indicate that the variation on the power level of the interferer doesn't have a strong impact on the aggregated throughput.

E. Measurement 4: Channel reallocation triggered by adjacent channel interference

With this experiment, we want to understand how the WiFi network is affected by strong adjacent channel interference and

TABLE IV. WEIGHTING FACTOR ACCORDING TO THE FREQUENCY SPACING BETWEEN CHANNELS.

n	Frequency Spacing (MHz)	Weight (dB)
1	5	0
2	10	-10
3	15	-19.5
4	20	-28
5	25	36.5

how effective is the coordination strategy under such circumstances. The interfering link is set to operate on Channel 10, while Link 2 uses Channel 11. In the case of adjacent channel interference, the REM generated for channel X has to take into account the power received from adjacent channels $X \pm n \in \mathbb{N}$, weighted according to the spectral mask of the filter present at the WiFi receiver [10]. The weighting factors of the transmit mask are listed in Table IV. Note that each WiFi channel is 22 MHz wide, but the channel separation is only 5 MHz. As an example, the power of the 4th adjacent-channel should be reduced by 28 dB to be correctly used in the computation of the REM.

The results from Table V show an overall network throughput decrease, compared with the results obtained from Measurements 3 and 4. This result shows that the first adjacent-channel interference leads to a higher throughput degradation than a co-channel interference (no-interference: 71.5 Mbps, co-channel interference: 58.6 Mbps and adjacent-channel interference: 56.7 Mbps). Once again, the results also indicate that the variation on the power level of the interferer doesn't have a strong impact on the aggregate throughput.

F. Measurement 5: Automatic power control to overcome co-channel interference

The aim of this experiment is to understand if automatic power control is a good strategy to overcome co-channel interference. The setup of the network under test has five links using non-overlapping channels, with an additional co-channel interference link in Channel 11. The RRM strategy in this experiment keeps the same channel assignment of each

link and increases the power of the victim link (Link 2). The transmitted power increases in steps of 5 dB, from 0 to 15 dBm. The remaining APs of the network under test remains at 0 dBm, and the interfering link is set to transmit 5 dBm in Channel 11. The measured throughput is listed in Table VI.

The results suggest that, despite the increase of transmitted power on Link 2, the overall throughput remains low and approximately constant (roughly 58 Mbps), therefore, power increase alone does not overcome the degradation caused by strong co-channel interference. The WiFi coordination strategy investigated in Measurement 3 is much more effective, leading to an aggregated throughput of 71 Mbps.

IV. CONCLUSION

This paper presented the testing of WiFi coordination strategies that exploits information from Radio Environment Maps, based upon five exploratory measurement campaigns in a pseudo-shielded testbed environment.

The overall performance of the WiFi network depends on a smart channel allocation. As an example, for the network under test, we've got an aggregated throughput of 22.3 Mbps in a full co-channel interference scenario and 71.5 Mbps using a configuration of non overlapping channels. It was shown that based on the observation of REMs, it is possible to detect the presence of interfering links (co-channel and first adjacent channel). First adjacent-channel interference leads to a higher throughput degradation than a co-channel interference with the same power level (no-interference: 71.5 Mbps, co-channel interference: 58.6 Mbps and adjacent-channel interference: 56.7 Mbps). The coordination strategy that automatically reallocates WiFi channels to avoid channel overlapping is very beneficial (e.g., the aggregated throughput goes from 58.7 Mbps to 71.5 Mbps, the link under interference goes from 6.8 Mbps to 11.8 Mbps). however, In case of strong co-channel interference, the strategy of automatically increase the power level of the victim link, when keeping the same channel allocation, does not bring any gain in terms of measured throughput.

For the RRM to be effective, 12 sensor nodes (energy detectors) were needed for an area of 60 m × 20m, to create a REM with enough spatial resolution. The additional hardware required for spectrum sensing, inter-cell signalling and REM building may increase the investment by 50 %, when compared to an uncoordinated WiFi network. However, by implementing an coordinated management of radio resources, the overall throughput in WiFi network was increased more than 200 %, even in the presence of interfering links.

Future research on this work includes testing of the proposed setup architecture in the WiFi 5 GHz band, with

TABLE V. THROUGHPUT RESULTS FOR MEASUREMENT 4 AFTER THE COORDINATION STRATEGY.

Measurement 4	Channel Number	Throughput (Mbps) $P_T=0dBm$	Throughput (Mbps) $P_T=7dBm$	Throughput (Mbps) $P_T=15dBm$
Link 1	6	8.12	8.14	8.16
Link 2	1	7.72	7.75	7.76
Link 3	6	21.53	21.51	21.55
Link 4	11	12.08	11.97	12.2
Link 5	1	11.82	11.06	11.16
Aggregated Throughput (Mbps)		61.13	60.43	60.83

TABLE VI. THROUGHPUT RESULTS FOR MEASUREMENT 5 AFTER AUTOMATIC POWER CONTROL.

Meas. 5	Channel Number	Throughput (Mbps) $P_2=0dBm$	Throughput (Mbps) $P_2=5dBm$	Throughput (Mbps) $P_2=10dBm$	Throughput (Mbps) $P_2=15dBm$
Link 1	6	12.30	12.32	11.47	11.43
Link 2	11	7.08	3.84	6.88	6.97
Link 3	6	21.63	21.33	21.52	21.39
Link 4	1	11.23	11.12	11.60	11.64
Link 5	11	6.83	9.60	6.90	6.83
Aggregated Throughput (Mbps)		58.96	58.13	58.39	58.26

other types of environments, including outdoor scenarios (e.g., public zones with WiFi access).

ACKNOWLEDGMENT

The research and development leading to these results has received funding from the European Union's Seventh Programme for research, technological development and demonstration under grant agreement N.º 612050 (FLEX) and the Horizon 2020 Programme under grant agreement N.º 645274 (WiSHFUL)

REFERENCES

- [1] L. P. Qian, Y. J. Zhang, and J. Huang, "Mapel: Achieving global optimality for a non-convex wireless power control problem," IEEE Transactions on Wireless Communications, vol. 8, no. 3, March 2009, pp. 1553–1563.
- [2] D. H. Kang, "Interference Coordination for Low-cost Indoor Wireless Systems in Shared Spectrum," Ph.D. dissertation, KTH, School of Information and Communication Technology (ICT), Communication Systems, CoS, 2014.
- [3] M. Pesko, T. Jarvonic, A. Kosir, M. Stular, and M. Mohorcic, "Radio Environment Maps: The Survey of Construction Methods," KSII Transactions on Internet and Information Systems, vol. 8, no. 11, November 2014, pp. 3789–3809.
- [4] iMinds. jFed – Java-based framework for testbed federation. [Online]. Available: <http://jfed.iminds.be> [retrieved: January, 2017]
- [5] OMF-6. [Online]. Available: <https://mytestbed.net/projects/omf6/wiki/Wiki> [retrieved: January, 2017]
- [6] OEDL – OMF Experiment Description Language. [Online]. Available: <https://omf.mytestbed.net/projects/omf6/wiki/OEDLOMF6> [retrieved: January, 2017]
- [7] Iperf, The TCP/UDP bandwidth measurement tool. [Online]. Available: <http://iperf.fr/> [retrieved: January, 2017]
- [8] OML. [Online]. Available: <https://oml.mytestbed.net/projects/oml/wiki/> [retrieved: January, 2017]
- [9] A. Goldsmith, Wireless Communications. Cambridge University Press, 2005.
- [10] E. G. Villegas, E. Lopez-Aguilera, R. Vidal, and J. Paradells, "Effect of adjacent-channel interference in IEEE 802.11 WLANs," in 2007 2nd International Conference on Cognitive Radio Oriented Wireless Networks and Communications, Aug 2007, pp. 118–125.

X2-Based Handover Performance in LTE Ultra-Dense Networks using NS-3

Sherif Adeshina Busari, Shahid Mumtaz, Kazi Mohammed Saidul Huq and Jonathan Rodriguez

Instituto de Telecomunicações, Aveiro, Portugal

Email: [sherifbusari, smumtaz, kazi.saidul, jonathan]@av.it.pt

Abstract—Ultra-Dense Network (UDN) has emerged as a key enabler in enhancing the capacity of mobile networks in order to deliver super-speed connectivity and high data rates, provide seamless coverage and support diverse use cases whilst satisfying a wide range of other performance requirements, such as improved reliability, latency, energy and spectral efficiencies. However, the reduced cell size in UDNs poses serious challenges in the areas of inter-cell interference (ICI) coordination and mobility management (due to increased frequency of handovers and signaling overheads). In this study, we simulate scenarios using Network Simulator version 3 (NS-3) to study the impact of cell size on user throughput at the point of handover using pedestrian mobility (3 kmph) as case study. The simulation results show improved spectral (and energy) efficiency with small cells over macrocells but significantly shorter handover times, which translate to more frequent handovers. And since the Long Term Evolution (LTE) and next-generation cellular networks are required to support mobility without serious impact on connectivity and performance, we align with the decoupling of the user and control planes where the macro-layer manages control signals (e.g., handover signaling) while the small cell provides the users with high data rates. By allocating the small cells more bandwidth, preferably in the millimeter wave (mmWave) bands with abundant spectrum, this decoupled framework will guarantee better spectrum management to support the fifth-generation (5G) broadband services and applications.

Keywords—UDN; mobility; handover; small cells; NS-3.

I. INTRODUCTION

Mobile networks have witnessed paradigm shifts in terms of deliverables, architectures and technologies through its evolution from the first-generation (1G) cellular systems announced in the early 1980's to the 5G networks expected to be deployed by 2020. Between 1G and 4G, mobile networks have moved from analogue to digital, voice-only to multimedia (voice and data), circuit-switched to packet-switched networks, and from 2.4 kbps throughput to a peak data rate of 100 Mbps (for highly mobile users) and up to 1 Gbps (for stationary and pedestrian users) [1], [2].

Alongside other performance metrics (data rate, capacity, coverage, latency, cost, spectral and energy efficiencies), mobility is an important feature in cellular systems as it enables users to freely roam across different cells in the network without serious impact on connectivity and performance [3]. While LTE systems standardized by the Third Generation Partnership Project (3GPP) have shown significant improvements in performance, the ever-growing demand for higher data rates and ubiquitous mobility required by new applications continues to pose serious challenges on legacy networks. With 4G networks reaching their theoretical limits, 5G networks are now building momentum to provide the networking solution for the new and smart digital era [4].

In the road towards 5G, the concept of UDN has been identified as the single most effective way to increase network capacity [5], among other enablers, such as massive multiple-input multiple-output (massive MIMO) antenna system, mmWave communication and device-to-device (D2D) communications [6]. Based on its potentials to significantly raise throughput, increase energy and spectral efficiencies, as well as enhance seamless coverage for cellular networks, pockets of dense deployment of low-power base stations (otherwise called small cells - microcell, femtocell, metrocell, picocells - with different levels of power, coverage and capabilities) are being witnessed in LTE systems, and hence the term LTE UDN [5].

The idea of small cells is to get users physically close to their serving base station (BS), thereby bringing down the inter-site distance (ISD) between two cells from 500-1000 m in macro BSs to 100-200 m for micro BSs (small cells) for typical urban deployment scenarios in the 2 GHz band. Hyper-densification of small cells is a promising solution in meeting the capacity, energy and spectral efficiencies expectations of next-generation cellular networks. However, despite the great anticipated benefits, the concept of UDN presents two principal challenges: mobility management and interference coordination. These challenges have drawn the attention of the research community in recent years [5], [7].

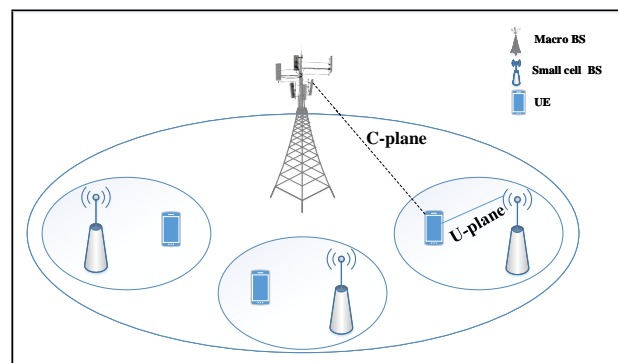


Figure 1. Decoupling of control and user plane in UDN.

Increased ICI resulting from reduced cell size in UDNs is controlled using advanced ICI management and cancellation techniques, while separation architecture (i.e., decoupling of the user plane from the control plane, as illustrated in Figure 1) is being proposed and investigated for mobility management [8]. The topology is such that the macro-layer handles the more efficient control plane functions, such as mobility management, synchronization and resource allocation etc., while the small

cells handle the high-capacity and spectrally-efficient data plane services [2]. This framework will allow more bandwidth to be allocated to the small cells for high data rate user experience. The high-power macro BSs, with much wider coverage, will provide control signaling which has low rate requirements, thereby leading to better spectrum management for next-generation cellular networks.

In this study, we simulate two scenarios to investigate the impact of cell size on user throughput during X2-based handover processes. The first set explores the mobility of a User Equipment (UE) between two macrocells with ISD of 500-1000 m while the second set studies the behavior of small cells with ISD of 100-200 m, which are typical values for urban macrocell and microcell deployment, respectively [5], [7]. The goal is to investigate the decoupled/separation architecture being proposed in literature for user mobility management in UDN deployment for future mobile systems.

The remainder of this paper is organized as follows: Section II gives an overview of related literature; Section III details the simulation procedures. Results and analyses are presented in Section IV and Section V provides the conclusions and direction for future work.

II. LITERATURE REVIEW

Handover algorithms play an important role in LTE networks as they impact on the performance of the systems. Studies have been conducted to investigate the effect of handover on signaling overhead, user throughput, outage probability, cell capacity, load balancing, interference management and energy efficiency, among others, using different scenarios, set-ups and simulators [3], [9]. In this work, we investigate the impact of cell size on user data rate and spectral efficiency at the point of handover. In this section, we present a brief overview on handover in LTE networks and the tool (NS-3) used for the study.

A. Overview of NS-3

NS-3 is an open source, discrete-event network simulator which provides a platform for conducting simulation experiments with packet data networks. It is built as a system of software libraries that work together, with user programs written in either the C++ and/or Python programming languages. For the purpose of education and research, NS-3 serves as a tool to model and study the behavior of networks or systems in a highly controlled, reproducible environment which may be difficult or impossible with real systems [10], [11]. Compared to NS-2, NS-3 has better core architectural features which enable the simulation of realistic packets and development of complex simulation models [12].

B. Evolved Packet System (EPS)

According to 3GPP, EPS is divided into two different functional parts: Evolved Universal Terrestrial Radio Access Network (E-UTRAN) and Evolved Packet Core (EPC) representing the RAN and the core network, respectively. These are also known as LTE and System Architecture Evolution (SAE), respectively [13]. The EPS system architecture is illustrated in Figure 2.

In NS-3, the EPS system is modeled by the LTE-EPC Network Simulator (LENA) model shown in Figure 3, comprising of the UE, evolved NodeB (eNodeB), combined serving

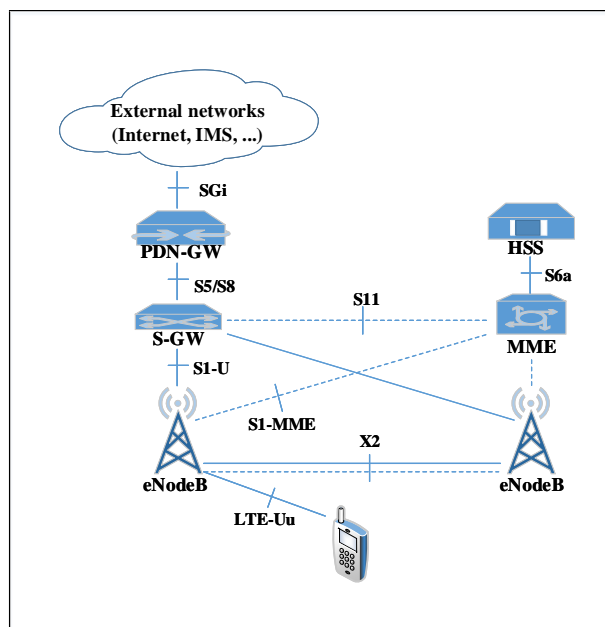


Figure 2. EPS Network Architecture.

gateway (SGW) and packet data network gateway (PGW) and their respective interfaces, mobility management entity (MME) and others. The eNodeBs are responsible for all radio functionalities of the user and control planes, the SGW/PGW serves as router between the user and the network while the MME (in conjunction with the eNodeBs) manages all mobility functionalities [11], [9], [14].

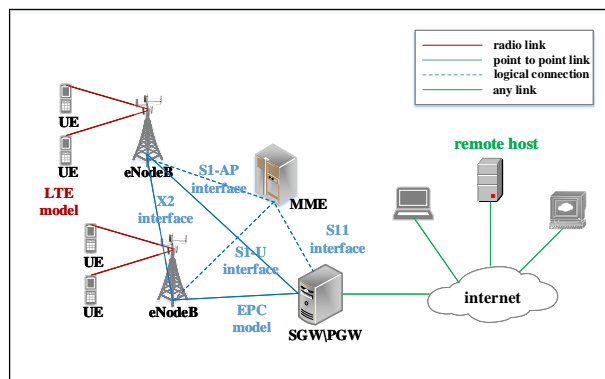


Figure 3. Overview of NS-3 LENA Model.

In EPS, handover decision and implementation are solely undertaken by the eNodeBs. And in contrast with the third-generation (3G) Universal Mobile Telecommunications System (UMTS), handover in LTE is hard handover (i.e.,) the UE has to be first disconnected from the serving eNodeB before being attached to the target/neighbor eNodeB with better signal strength [13].

C. Mobility Management in LTE

LTE networks have simplified architecture, improved user mobility support and higher data rate capability than earlier generations of cellular systems [15]. As users move between the coverage areas of the eNodeBs, they get, process and report

measurements about their serving and neighbor eNodeBs [16]. According to 3GPP LTE, UE measurement reports are the key input for X2-based handover processes [3], which are accomplished in four phases: downlink handover measurements, processing of downlink measurements, uplink reporting and handover decision and execution [16].

Reference Signal Received Power (RSRP) and Reference Signal Received Quality (RSRQ) measured in dBm and dB, respectively, are two types of handover triggering quantities measured by the UE which are reported to the serving eNodeB [11]. As the UEs move away from the serving eNodeB and towards the neighbor eNodeB, the quality of the signal from the serving eNodeB degrades and that of the neighbor eNodeB improves, thus necessitating a handover from the former to the latter. Depending on the handover algorithm, the required condition(s) set out by 3GPP, as presented in Table I, would have to be satisfied in order to trigger the handover process.

TABLE I. LIST OF EVENT-BASED TRIGGERING CRITERIA.

Event	Triggering Condition
A1	Serving cell becomes better than threshold.
A2	Serving cell becomes worse than threshold.
A3	Neighbor cell becomes offset dB better than serving cell.
A4	Neighbor cell becomes better than threshold.
A5	Serving cell becomes worse than threshold 1 and neighbor cell becomes better than threshold 2.

In LTE, there are two types of handover: S1-based handover involving eNodeBs and the MME, and X2-based handover which is entirely handled by the eNodeBs. And according to 3GPP specifications, the X2 interface is a point-to-point interface which inter-connects two eNodeBs and over which X2-based handover is implemented. Handover in LTE is a UE-assisted (i.e., UE provides input to the network in form of measurement reports) and network-controlled process (i.e., dependent on the source and target/neighbor eNodeBs for triggering and execution) [15].

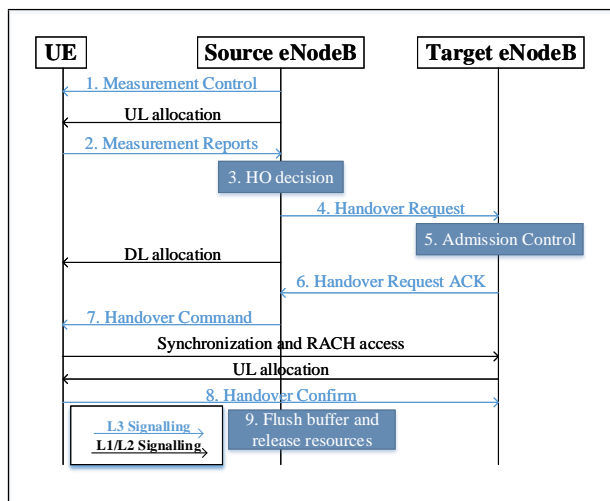


Figure 4. Handover signaling procedure.

In the LENA model, test suites are provided to evaluate three types of X2-based handover algorithms: A2-A4-RSRQ, A3-RSRP and no-op handover algorithms [14]. The no-op algorithm is a special algorithm which disables automatic

handover trigger in order to allow manual handover, while the other two are automatic and based on UE measurement reports satisfying the respective conditions set out in Table I, based on 3GPP specifications [3], [11], [14].

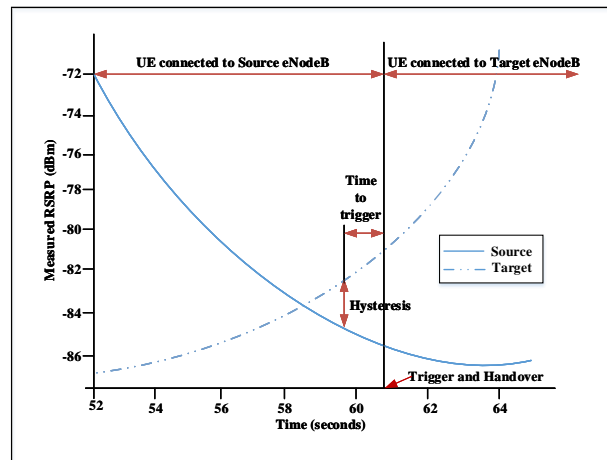


Figure 5. Typical measurement curves for handover scenario.

For the A2-A4-RSRQ algorithm, the threshold and offset parameters respectively represent the RSRQ values and the difference in RSRQ between the serving and target cells that must be surpassed before handover would happen. For the A3-RSRP, the hysteresis value represents the difference in RSRP between the serving and target cells that must be maintained for an amount of time called Time-to-Trigger (TTT) before handover could be triggered [3], [17]. Typical handover signaling and measurement curves indicating the triggering parameters are shown in Figures 4 and 5, respectively.

III. SIMULATION PROCEDURES

In this section, we describe the test scenarios and present the simulation parameters and tools.

A. Test Scenarios and Simulation Parameters

In order to evaluate the effect of cell size on user throughput in LTE UDN during handover scenarios, the implemented cellular network topology is shown in Figure 6. The scenario was simulated using a modified lena-x2-handover-measures.cc script available in the LTE module of NS-3, to implement the A2-A4-RSRQ X2-based handover algorithm.

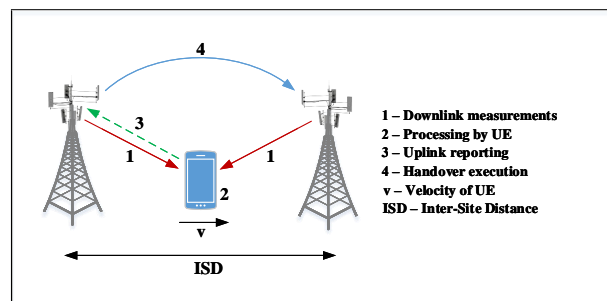


Figure 6. Simulation Network Topology.

For the scenario, a UE moves at a constant speed of 3 kmph (typical pedestrian speed according to 3GPP) between

the serving and target eNodeBs separated at an ISD of 500-1000 m apart (typical urban macrocellular deployment). Then, the cell size was reduced to ISD of 100-200 m (for UDN/small cell/microcellular deployment).

TABLE II. HANDOVER SIMULATION PARAMETERS.

Parameters	Microcell	Macrocell
ISD (m)	100, 150, 200	500, 750, 1000
eNodeB Tx Power (dBm)	44	46
eNodeB Antenna Height (m)	10	15
eNodeB Noise Figure (dB)		5
UE Tx Power (dBm)		24
UE Noise Figure (dB)		9
UE Antenna Height (m)		1.5
UE Speed (kmph)		3
UE mobility	straight line at constant speed	
Thermal Noise (dBm/Hz)		-174
Frequency Band (MHz)		2100
Downlink Freq. (MHz)		2120
Uplink Freq. (MHz)		1930
DL EARFCN		100
UL EARFCN		18100
System Bandwidth (MHz)	5 (25 RBs)	
Number of Users	1	
Antenna Mode	SISO	
Antenna Pattern	Omnidirectional	
Antenna Gain (dBi)	0	
Duplexing Mode	FDD	
Tx Time Interval (ms)	1	
Path Loss Model	COST-231	
Serving Cell Threshold	30	
Neighbor cell offset	1	
Hysteresis (dB)	3 dB	
Time-to-Trigger (ms)	256	
HO Triggering event	A2-A4	

In particular, the parameter that were varied was the ISD, using the different configurations set out in Table II with respect to the UE and eNodeBs (macrocell and microcell), which are broadly in line with ITU-R case study in [7].

B. Tools and Softwares

The simulation was carried out using ns-3.24 version installed on Ubuntu 12.04 LTS operating system via VMware Workstation 12 Player installed on a 4 GB RAM, core i3 HP laptop computer. The Network Animator (NetAnim) software was used for the animation display while the graphs of the simulation results were plotted using MATLAB.

IV. RESULTS AND ANALYSES

In the following subsections, we present the results and analyses of the simulations.

A. Animation of Network Topology

A sample snapshot of the topology obtained from NetAnim is shown in Figure 7. Node 0 is the SGW/PGW, node 1 is the remote host, node 2 is the serving eNodeB, node 3 is the target eNodeB while node 4 represents the UE. It also illustrates the time of the handover, thereby serving as a tool to monitor that the scripts executed as designed.

B. Simulation Results

From the RSRP/RSRQ traces obtained from the simulations, the downlink RSRP and SINR values obtained at the points of handover for both the serving and target cells are presented in Tables III and IV, for the microcell and macrocell, respectively.

Based on the downlink Signal to Interference and Noise Ratio (SINR) values presented in Tables III and IV, the

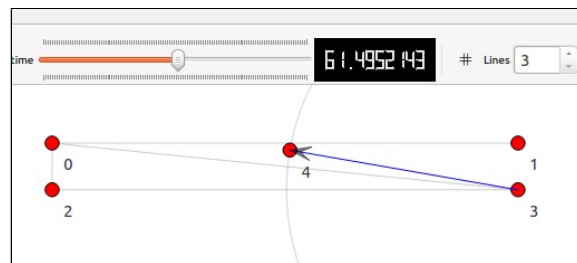


Figure 7. Handover illustration with NetAnim.

downlink spectral efficiencies (η) and data rates (R_d) are obtained using (1) and (2), respectively [14], [18].

$$\eta = \log_2(1 + \frac{\gamma}{\Gamma}) \quad (1)$$

$$R_d (Mbps) = \eta (bps/Hz) \times Bandwidth (MHz) \quad (2)$$

$$\Gamma = \frac{-\ln(5 \times BER)}{1.5} \quad (3)$$

γ is the SINR and Γ is a coefficient (known as SINR gap) which is computed using (3) to account for the difference between the theoretical and model performance of the Modulation and Coding Scheme (MCS), depending on the target Bit Error Rate (BER) [14]. For the simulations, $BER = 5 \times 10^{-5}$ and $Bandwidth = 5 MHz$.

TABLE III. RSRP AT HANDOVER FOR MICROCELL DEPLOYMENT.

ISD (m)	RSRP (dBm)		SINR (Linear)	
	Serving Cell	Target Cell	Serving Cell	Target Cell
100	-83.97	-83.72	8443830	8947470
150	-87.39	-87.21	3844440	4005080
200	-89.85	-89.70	2182600	2256910

TABLE IV. RSRP AT HANDOVER FOR MACROCELL DEPLOYMENT.

ISD (m)	RSRP (dBm)		SINR (Linear)	
	Serving Cell	Target Cell	Serving Cell	Target Cell
500	-95.78	-95.70	556841	566974
750	-99.27	-99.21	249220	252683
1000	-101.76	-101.71	140483	142320

TABLE V. HANDOVER TIME FOR MICROCELL AND MACROCELL DEPLOYMENT.

Microcell		Macrocell	
ISD (m)	Time (s)	ISD (m)	Time (s)
100	60.90	500	301.38
150	90.94	750	451.58
200	121.02	1000	601.98

The handover time for both scenarios is shown in Table V. It shows the time the serving cell executes handover to the target cell, having satisfied both the hysteresis and TTT conditions. The results showing the impact of ISD on the achievable spectral efficiencies and data rates, at the point of handover, are shown in Figures 8-11, for the microcell and macrocell, respectively.

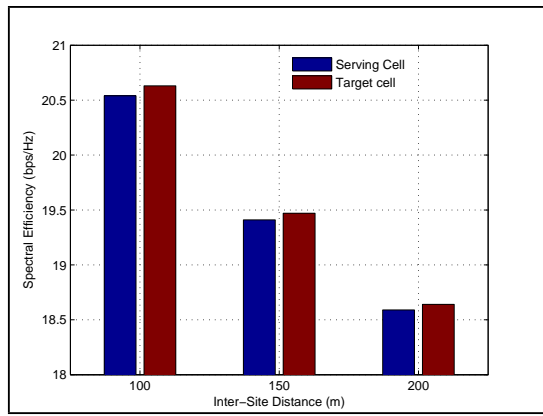


Figure 8. Spectral efficiency for microcell deployment scenarios.

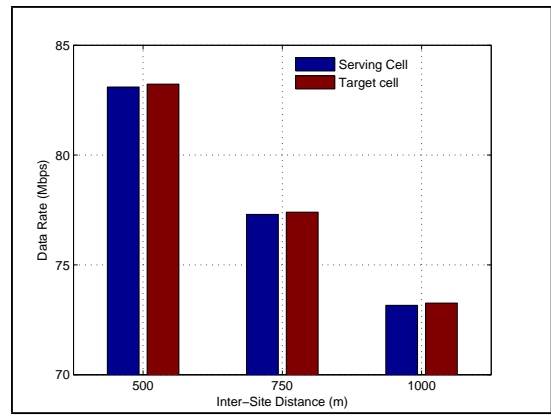


Figure 11. Data rate for macrocell deployment scenarios.

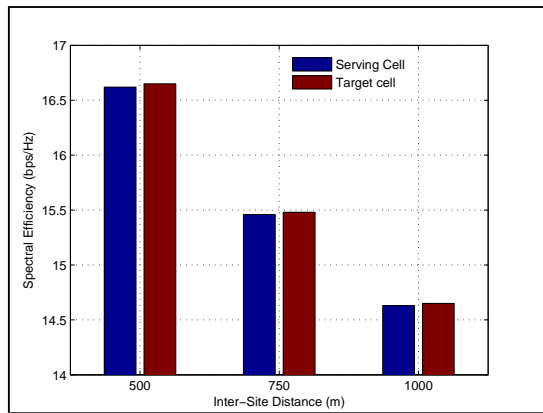


Figure 9. Spectral efficiency for macrocell deployment scenarios.

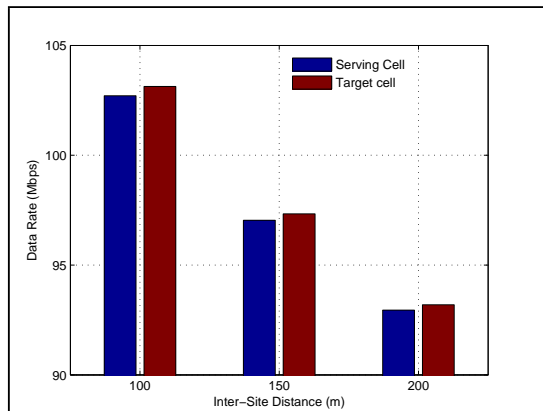


Figure 10. Data rate for microcell deployment scenarios.

In the following subsection, we present the analysis and discussion of the simulation results.

C. Analyses and Discussion

At handover, from the simulations results presented in Tables III-V and plots shown in Figures 8-11,

- 1) the RSRP values, spectral efficiencies and data rates for the serving cells are lower than those of the target cells

for all the scenarios, thus justifying the need for handover. Without handover, the serving cell signal and performance would continue to degrade thereby leading to low quality of experience (QoE) for the end users.

- 2) the RSRP values, spectral efficiencies and data rates for the microcell deployment are better than those of the macrocell deployment for all scenarios. In each case, the performance improves as the ISD reduces, with the best results achieved at ISD of 100 m.
- 3) the performance of the microcell scenarios were better than those of the macrocells, despite the higher transmit power of the macrocells. This implies that the small cells have better energy efficiencies.
- 4) the handover times for the microcells were significantly shorter than those of the macrocell scenarios. This implies an increase in the number of handovers in the small cells.
- 5) the difference in performance between the serving and target cells at the point of handover were higher in the small cell deployments than those of the macrocells. This shows that the macrocells are more stable in handling control signaling than small cells. With small cells handling handover, the hysteresis and TTT values would be achieved much faster, thereby resulting in increased frequency of handover.

Quantitatively, as can be deduced from Table V, the required handover time for macrocells is 5x that of small cells for typical deployment scenarios with ISD of 500 m and 100 m (and 10x for 1000 m and 100 m) for macrocell and small cell, respectively. Very short handover times will result in increased frequency of handover and significantly high measurement overheads, thereby leading to poor spectrum management, which is undesirable for next-generation mobile networks, starting with 5G.

It should however be noted that the scenario considered in the simulation is a single-user, single-input single-output (SISO) system which did not consider the effects of interference from multiple users nor implemented enhancements such as carrier aggregation and advanced MIMO techniques, all of which will impact on the obtained results. Also, other simplifying assumptions have been used in the development of LTE/LENA modules in NS-3, and the interested reader is referred to [14] for the details.

V. CONCLUSIONS AND FUTURE WORK

Densification of small cells has the potential to deliver increased network capacity based on increased cell density and high spatial and frequency reuse, enhanced spectral efficiency based on improved average SINR (with tighter interference control) and improved energy efficiency based on reduced transmission power and lower path loss resulting from smaller cell radii or distance between the small cells and the UEs.

On the other hand, however, UDN presents serious challenges in terms of mobility support, interference management and cost. In the context of mobility, it poses a severe problem due to high frequency of handovers (due to shorter handover time), increased signaling and high measurement overheads that would be incurred if the control signals are from spatially-close small cells. Results from this simulation campaign buttress these outcomes.

The trend and direction for future work in realizing the gains of densification of small cells, therefore, is to decouple the control and user planes such that mobility management (handover and other control signaling) is handled by the macrocell layer where very high data rate is not required, while the data plane functionalities are handled by the closest small cell in order to support the high data rate demands of next-generation services and applications. This framework is an area of growing research interest for 5G and beyond-5G (B5G) systems.

ACKNOWLEDGMENT

This work is part of the Wireless Networks and Protocols course of the MAP-Tele Doctoral Program. Sherif A. Busari would therefore like to thank Profs. Manuel Ricardo, Adriano Moreira and Rui Aguiar for providing guidance and feedbacks, and to acknowledge his PhD grant funded by the Fundação para a Ciência e a Tecnologia (FCT-Portugal) with reference number PD/BD/113823/2015. Also, the research leading to these results received funding from the European Commission H2020 programme under grant agreement no. 671705 (SPEED-5G project).

REFERENCES

- [1] A. Gupta and R. K. Jha, "A Survey of 5G Network: Architecture and Emerging Technologies," *IEEE Access*, vol. 3, 2015, pp. 1206–1232.
- [2] F. B. Saghezchi *et al.*, *Drivers for 5G: The 'Pervasive Connected World'*. John Wiley & Sons Ltd., UK, 2015, chapter 1, pp. 1–27, in Rodriguez J. (Ed.), *Fundamentals of 5G Mobile Networks*.
- [3] B. Herman, N. Baldo, M. Miozzo, M. Requena, and J. Ferragut, "Extensions to LTE Mobility Functions for ns-3," in *Proceedings of the 2014 Workshop on ns-3 (WNS3 '14)*, May 7, 2014, Atlanta, Georgia, USA. ACM, 2014, pp. 1–8.
- [4] Z. S. Bojkovic, M. R. Bakmaz, and B. M. Bakmaz, "Research challenges for 5G cellular architecture," in *Proceedings of the 12th International Conference on Telecommunication in Modern Satellite, Cable and Broadcasting Services (TELSIKS)*, 14–17 Oct., 2015, Serbia. IEEE, pp. 215–222.
- [5] S. Vahid, R. Tafazolli, and M. Filo, *Small Cells for 5G Mobile Networks*. John Wiley & Sons Ltd., UK, 2015, chapter 3, pp. 63–104, in Rodriguez J. (Ed.), *Fundamentals of 5G Mobile Networks*.
- [6] Q. C. Li, H. Niu, A. T. Papathanassiou, and G. Wu, "5G Network Capacity: Key Elements and Technologies," *IEEE Vehicular Technology Magazine*, vol. 9, no. 1, 2014, pp. 71–78.
- [7] "Guidelines for Evaluation of Radio Interface Technologies for IMT-Advanced, Report ITU-R M.2135-1," Tech. Rep., 2009, https://www.itu.int/dms_pub/itu-r/opb/rep/R-REP-M.2135-1-2009-PDF-E.pdf [retrieved: 2017-03-23].
- [8] H. A. U. Mustafa, M. A. Imran, M. Z. Shaker, A. Imran, and R. Tafazolli, "Separation Framework: An Enabler for Cooperative and D2D Communication for Future 5G Networks," *IEEE Communications Surveys & Tutorials*, vol. 18, no. 1, 2016, pp. 419–445.
- [9] N. Baldo, M. Requena-Esteso, M. Miozzo, and R. Kwan, "An Open Source Model for the Simulation of LTE Handover Scenarios and Algorithms in Ns-3," in *Proceedings of the 16th ACM International Conference on Modeling, Analysis & Simulation of Wireless and Mobile Systems (MSWiM '13)*, Barcelona, Spain. ACM, 2013, pp. 289–298.
- [10] NS-3 Tutorial, Release ns-3.24, 2016, <http://www.nsnam.org/documentation> [retrieved: 2017-03-23].
- [11] M. Assyadzily, A. Suhartomo, and A. Silitonga, "Evaluation of X2-handover performance based on RSRP measurement with Friis path loss using network simulator version 3 (NS-3)," in *Proceedings of the 2nd International Conference on Information and Communication Technology (ICoICT)*, 28–30 May, 2014. IEEE, 2014, pp. 436–441.
- [12] G. Carneiro, P. Fortuna, and M. Ricardo, "FlowMonitor: A Network Monitoring Framework for the Network Simulator 3 (NS-3)," in *Proceedings of the 4th International ICST Conference on Performance Evaluation Methodologies & Tools*, 20–22 Oct., 2009, Pisa, Italy. ACM, 2009, pp. 1–10.
- [13] A. Helenius, "Performance of handover in Long Term Evolution," Master's thesis, Aalto University, Finland, 2011, <http://lib.tkk.fi/Dipl/2012/urn100708.pdf> [retrieved: 2017-03-23].
- [14] The LENA ns-3 LTE Module Documentation, Release v8, 2014, <http://networks.cttc.es/wp-content/uploads/sites/2/2014/01/lena-lte-module-doc.pdf> [retrieved: 2017-03-23].
- [15] B. Herman, D. Petrov, J. Puttonen, and J. Kurjenniemi, "A3-Based Measurement and Handover Model for NS-3 LTE," in *Proceedings of the 3rd International Conference on Mobile Services, resources and Users (MOBILITY 2013)*. IARIA, 2013, pp. 20–23.
- [16] M. Anas, F. D. Calabrese, P. E. Ostling, K. I. Pedersen, and P. E. Mogensen, "Performance Analysis of Handover Measurements and Layer 3 Filtering for Utran LTE," in *Proceedings of the 18th International Symposium on Personal, Indoor and Mobile Radio Communications*, Sept., 2007. IEEE, pp. 1–5.
- [17] K. Dimou *et al.*, "Handover within 3GPP LTE: Design Principles and Performance," in *70th Vehicular Technology Conference Fall (VTC 2009-Fall)*, Sept. 2009. IEEE, pp. 1–5.
- [18] G. Piro, N. Baldo, and M. Miozzo, "An LTE Module for the Ns-3 Network Simulator," in *Proceedings of the 4th International Conference on Simulation Tools and Techniques (SIMUTools '11)*, 2011. ACM, pp. 415–422.

Performance Analysis of Downlink CoMP Transmission in Long Term Evolution-Advanced (LTE-A)

Maryem Neyja*, Shahid Mumtaz† and Jonathan Rodriguez ‡

Instituto de Telecomunicações, Campus Universitário de Santiago, AVEIRO - PORTUGAL

* Email: neyja.maryem@av.it.pt

† Email: smumtaz@av.it.pt

‡ Email: jonathan@av.it.pt

Abstract—Coordinated multi-point (CoMP) has evolved as a performance-optimizing technique for cellular networks. In this paper, we investigate two different spectrum allocation schemes for CoMP (i.e., shared and dedicated) within the context of Remote Radio Head (RRH) enabled heterogeneous network (HetNet) topology. The traditional macro cell only layout serves as baseline. Using spectral efficiency and average user throughput as system level performance metrics, our results reveal that CoMP based on shared spectrum outperforms the other two. The scheme, therefore, has great potential for optimizing radio resources and boosting the performance of next-generation mobile networks.

Keywords—Coordinated multi-point (CoMP); Remote Radio Head (RRH); user average spectral efficiency; throughput.

I. INTRODUCTION

The Third Generation Partnership Project (3GPP) Long Term Evolution (LTE) technology, through its periodic releases advances the capabilities of cellular network technology, in order to meet the increasing demands for high-quality and broadband multimedia services. Coordinated multi-point (CoMP) and Remote Radio Head (RRH) have been recently employed to enhance the performance of current wireless systems. With these and other techniques, higher data rates and higher capacity can be attained in LTE-A networks. The main objective of CoMP is to form a cluster of adjacent macro cells to improve User Equipment (UE) throughput and average spectral efficiency [1]. However, the use of dedicated spectrum in wireless network systems is foreseen as the method implemented with CoMP to improve cell edge coverage. Hence in this paper, we shall give a performance analysis of downlink CoMP transmission in LTE-A network by comparing the obtained results of deployed conventional macro cell, CoMP using the shared spectrum (i.e., Frequency Reuse Factor (FRF) one) and CoMP using the dedicated spectrum (i.e., FRF = 3). These results are obtained using the MATLAB Vienna LTE-A Downlink System Level Simulator.

The rest of this paper is organized as follows. Section II provides a basic understanding of CoMP technique benefits used with RRH, and a brief description of the proposed scenario. Section III explains the simulation procedures and methodology of Vienna LTE-A simulator. Section IV outlines the final results obtained, by deploying shared and dedicated spectrum for CoMP and presents an insightful discussion. Finally, Section V concludes this paper and presents the future work.

II. COORDINATED MULTI-POINT (CoMP) IN LONG TERM EVOLUTION-ADVANCED (LTE-A)

CoMP is the foreseen technology that improves not only the cell edge throughput, but also, the coverage and system efficiency by combining and coordinating the desired and interfered signals from multiple transmission points [1]. CoMP increases data rate and ensures consistent service quality and throughput on wireless broadband networks. Hence, the UE gets very consistent service performance and quality. Technically, CoMP allows a signal from another cell to be used as the desired signal. It is an improvement not only for throughput at the cells edges, but also, for the average cell throughput. The UE is served simultaneously by multiple transmission points from the same or different eNBs [2]. Coordinating cells enhance the service quality and the throughput. CoMP reduces the Inter-Cell Interference (ICI) by joining macro cells and eliminating handover effect [3]. Therefore, cooperative communication network improves system resource utilization and data rate. Today's deployed LTE-A networks are mostly based on macro cells. Such networks are homogeneous or HetNet [4]:

- Homogeneous: All the BSs (transmitters) belong to the same type;
- Heterogeneous: The BSs belong to different types.

To improve the cell edge coverage and the cooperative ICI, we will implement CoMP within HetNet, by deploying low power nodes (small BSs) associated with macro cells. These small BSs are formed and typically used to extend coverage in cells edges and to add network capacity in areas with dense data usage. The deployment of low-power nodes within the macro cells is foreseen as the best solution to cover any increased demand in cellular network traffic. Now, the most recent deployment in LTE-A consists of dividing the macro BS functionalities into a Base Band Unit (BBU) responsible for scheduling, and this is placed in a technical room (e.g., near the building). The RRH is the part responsible for all the radio frequency operations such as the power amplifying, filtering and carrier frequency transposition. Hence, it is always placed near to the antenna or it is integrated to it, and it is connected to the BBU via an optical fiber [5]. Figure 1 shows the RRH antenna implementation, which helps the fast coordination between transmission and reception points [6]. The optical link in between guarantee a very high transmission rate. This new system architecture separates the digital radio part BBU from the analog radio part RRH. Thus, it allows to reduce the number of equipment pieces at the site, optimize

the operational cost, decrease the energy demand and increase the efficiency of the network [7].

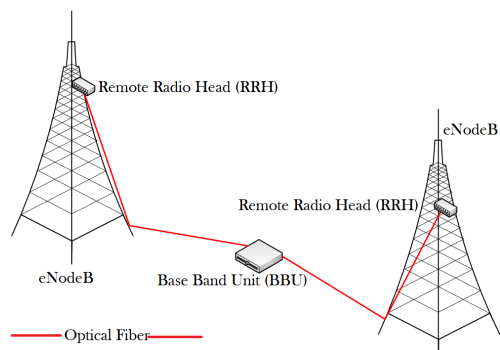


Figure 1. Remote Radio Head (RRH) Deployment

As it is depicted in Figure 2, CoMP technique is classified into coordinated scheduling / coordinated beam-forming (CS/CB) and Joint Point (JP). JP is divided into two different types Joint Transmission (JT) and Transmission Point Selection (TPS).

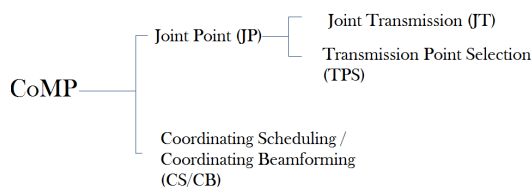


Figure 2. Types of CoMP

As shown in Figure 3, CS/CB is characterized by multiple coordinated transmission points sharing only the Channel State Information (CSI) for multiple UE, while data for a signal user is only available and transmitted from one Transmission Point (TP) [8].

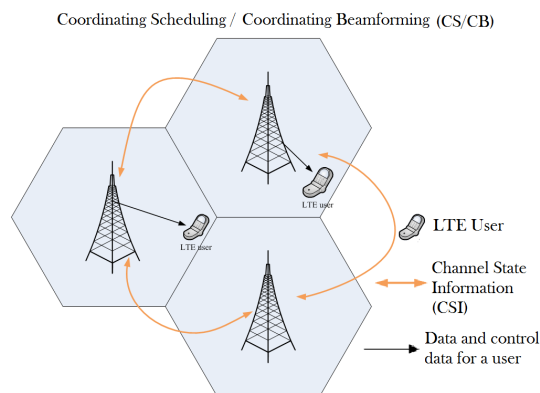


Figure 3. coordinated scheduling / coordinated beam-forming (CS/CB)

Next, we will detail the two parts of CoMP JP scheduling, which is characterized by simultaneous control data transited from multiple points to a single user.

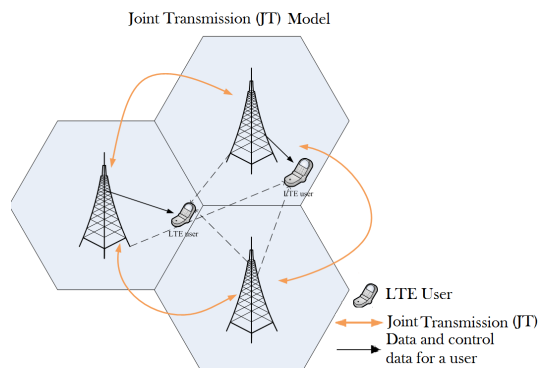


Figure 4. Joint Transmission (JT)

Figure 4 shows that, for JT, the data is simultaneously available at multiple coordinated TPs. Hence, simultaneous data and control data are transmitted from multiple eNBs. JTs convert an interference signal to a desired one [8].

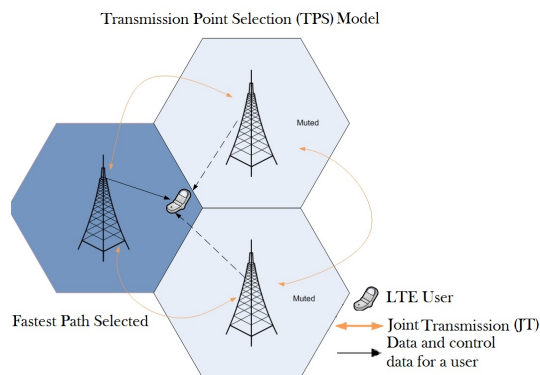


Figure 5. Transmission Point Selection (TPS)

As seen in Figure 5, TPSs transmit data from one TP of CoMP, among multiple TPs at each time instance and only one cell is fast selected to perform the transmission. Thus, the others are muted with simultaneous control data transmission from multiple TPs. To sum up, in this paper we will work with the JT CoMP scheduling.

To study the different possible network topologies and backhaul characteristics of CoMP, 3GPP has focused on different scenarios [9]:

- Scenario 1: The same macro BS controllers coordination between the cells (sectors) where we will not need any backhaul connection.
- Scenario 2: The macro network coordinated cells belonging to different radio sites.
- Scenario 3: The macro cell and the low-power transmit and receive points within its coverage are coordinated and each point controls its own cell (with its own cell identity).
- Scenario 4: The same deployment as the latter, except that the low-power transmit/receive points constitute distributed antennas (via RRH) of the macro cell, thus it is all associated with the macro cell identity.

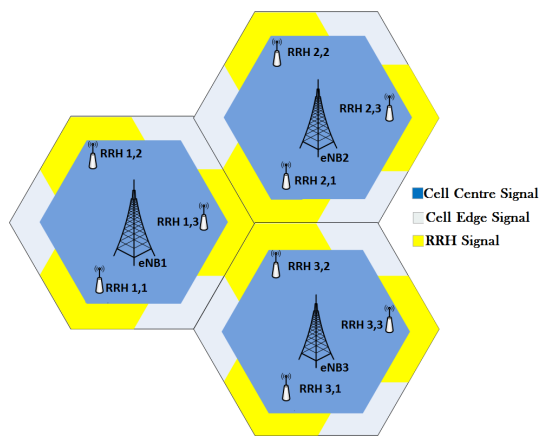


Figure 6. CoMP deploying RRH antennas

As depicted in Figure 6, the deployment of scenario 4, using CoMP, allows each point to be controlled by its own BS and all the RRH are controlled by the same BS. Overall, the implementation of RRH within CoMP extends the cell-edge coverage, thus, the average throughput of each UE increases even in the area with dense data traffic.

III. SIMULATION PROCEDURE

The analysis of single-cell multi-user and multi-cell multi-user scenarios require a large amount of operational and computing effort. Thus, to reduce it, we utilize the freely available Vienna LTE-A simulator version v1.8r1375. Basically, it is composed of LTE physical layer and LTE SLS. As a free simulator under a non commercial open source academic-use license, it enables researchers to implement and test wireless cellular system algorithms in the context of LTE-A [10]. The simulation for mobile communication systems includes the LTE physical layer simulator and LTE SLS. Both are widely employed to evaluate the associated cellular network performances. LTE physical layer simulator focuses on the performance of a transmission between BSs and Mobile Station (MS)s. The performance metrics usually include the Block Error Ratio (BLER), Signal Noise Ratio (SINR) and achievable rate.

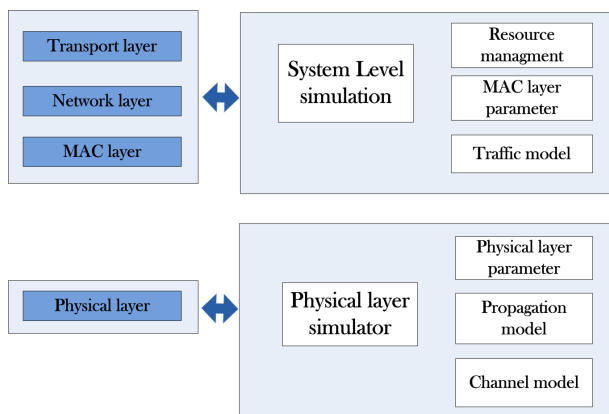


Figure 7. Component layers and model for simulation methodology [2]

Figure 7 shows the relationship between the LTE-A physical layer and other components in communications. For the

purpose of theoretical studies, the performance of modulation and demodulation or coding and decoding schemes in different radio channel models can be obtained from the LTE-A physical layer simulator. The scenario for LTE-A SL Simulator generally consists of a network with multiple BSs and MSs. LTE SLS focuses on the application layer performance metrics as expressed by system throughput, user fairness, user-perceived Quality of Service (QoS), handover delay or success rate. The LTE SLS concentrates on the higher layers above the physical layer, such as the MAC layer, transport layer, network layer, and application layer. Figure 7 shows the component layers related to LTE SLS. For the purpose of theoretical studies, the performance of resource allocation, handover, cell deployment, or other strategies can be obtained from LTE SLS [11].

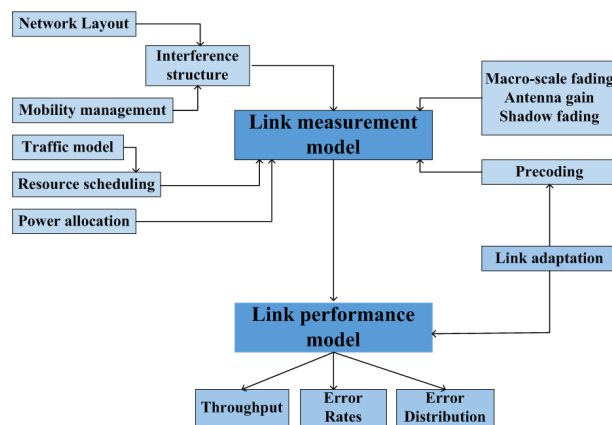


Figure 8. Schematic block diagram of LTE-A SL Simulator [12]

In Figure 8, LTE SLS is done by pre-generating the parameters off-line and using them later during run-time. In this section, we explain the simulation procedure using Vienna LTE-A simulator and LTE SLS. The performances of LTE SLS helps in simulating the totality of radio links between the UE and eNBs, through a vast amount of power that would be required [13]. Thereby, we define a Region Of Interest (ROI) in which the UEs and eNBs are positioned during a simulation length defined by Transmission Time Intervals (TTI)s.

We will analyze the results of three implemented simulation scenarios:

- The basic macro-cell deployment,
- The CoMP with RRH antennas deploying shared spectrum (FRF = 1),
- The CoMP with RRH antennas using dedicated spectrum (FRF >1).

The dedicated spectrum allows UEs to get not only enough resources even at the cell edges, but also an increased average throughput of each UE, no matter where its location. Accordingly, in dedicated spectrum we divide in multiple parts our bandwidth, thus, it can cover all the macro cell's area in moderate way [14]. Also, we focus on dense traffic area by giving it a larger part of the bandwidth compared to others, that may not need such a large part of the spectrum. However, in the case of a shared spectrum, the use of all the bandwidth in the cell center affects the edges coverage, where users are starved of capacity.

After exploring the spectral efficiency and the average throughputs, we will compare the results. This is achieved by setting the optional parameters in the loaded configure file of Vienna LTE-A simulator which provides the inbuilt shared spectrum scheduler. To implement the dedicated spectrum, the concept of 'frrscheduler' is implemented in LTE SLS as a scheduler which allows to specify two independent parts, which are the Fully Reuse (FR) and Partly Reuse (PR)). LTE-config.scheduler is the type of scheduler to use in this case, with the Fractional Frequency Reuse (FFR) parameter which provides FR and PR [15].

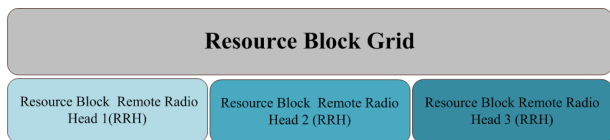


Figure 9. Resource Block Grid Schedule

Figure 9 shows the Resource Block (RB) grid is divided into three equal parts for each RRH antenna using the FFR = 3. Each PR part uses 1/3 of the remaining bandwidth 20 MHz. When simulating, only an integer-valued number of RBs can be scheduled to the FR/PR parts, which means that, for a 20MHz bandwidth (100 RB), the minimum value of FR is 0.01, as 100 is not divisible by 3 (99 is divisible by 3). So, we have 99 RBs and each PR will take 0.33.

IV. RESULTS DISCUSSION

In this section, we present the simulation results and analyze the performance of deployed basic macro-cell, CoMP using shared then dedicated spectrum. Next, we explore various performance metrics to show the effectiveness of the proposed scenario such as:

- The SINR,
- The UE average spectral efficiency (bit/Hz),
- The UE average throughput (Mb/s).

The following results are obtained by deploying basic macro-cell and using Vienna LTE-A simulator.

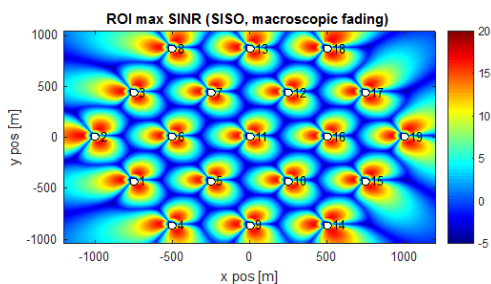


Figure 10. Region Of Interest (ROI) with the different SINR values

Figure 10 shows the values of SINR represented in color code. Blue refers to the lowest SINR value which means bad quality connection for the users at the cell edge. Thereafter, the colors go from blue with minimum SINR value -5 dB to red with maximum SINR value 20 dB. The red signal is in the cell center and it means uninterrupted connection for the desired throughput. However, the cell edges have negligible coverage.

There are 19 tri-sector eNBs, present within the ROI (i.e., the serving area).

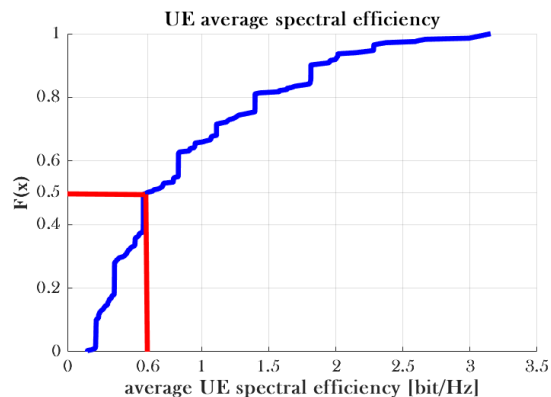


Figure 11. UE Average spectral efficiency (bit/Hz) versus F(x)

From the graph shown in Figure 11, it can be said that for a probability function $F(x)=0.5$, the UE average spectral efficiency is equal to 0.6 (bit/Hz).

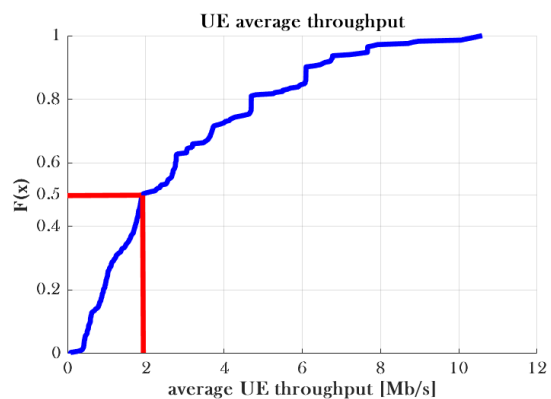


Figure 12. UE Average throughput (Mb/s) versus F(x)

Figure 12 follows the same interpretation as the latter, for $F(x)=0.5$ the UE average throughput is equal to 2 (Mb/s). In the following graphs, we discuss the results of CoMP using shared scheduling spectrum.

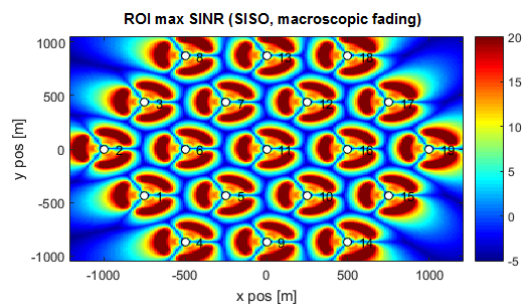


Figure 13. ROI with the different SINR values

Similarly, Figure 13 presents CoMP using shared spectrum footprint. In this proposed scenario, we get SINR values higher in RRH antennas sectors. The propagation of blue is reduced

and almost disappears, while the red is spreading in all the cell area.

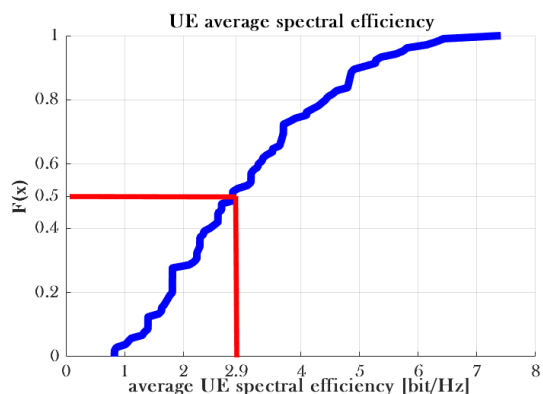


Figure 14. UE Average spectral efficiency (bit/Hz) versus F(x)

From the plot in Figure 14, it can be seen that the UE average spectral efficiency for $F(x) = 0.5$ is 2.9 (bit/Hz). Intuitively, we can say that the implementation of CoMP using shared spectrum increases the average spectral efficiency two times compared to the previous scenario.

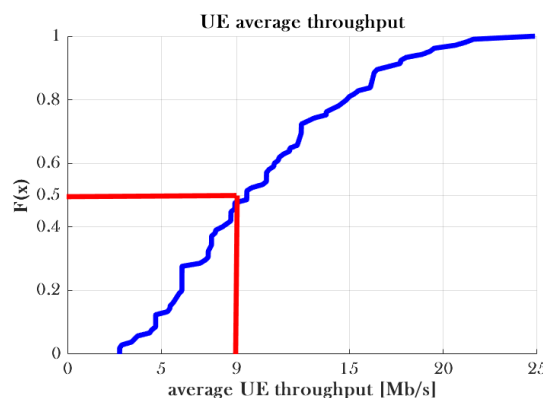


Figure 15. UE Average throughput (Mb/s) versus F(x)

The result plotted in Figure 15 shows that using a shared spectrum combined with CoMP provides higher UE average throughput than using only the conventional scheme. With the conventional scheme, the average throughput is 2 (Mb/s), and when RRH is combined with CoMP techniques, we obtain for $F(x) = 0.5$ the average throughput of 9 (Mb/s).

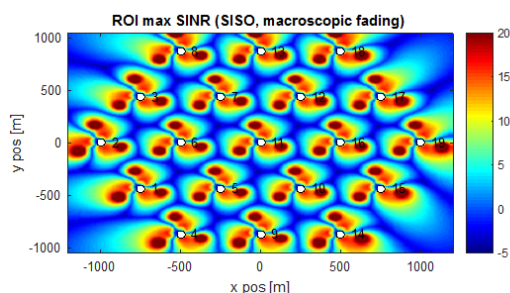


Figure 16. Footprint of ROI with SINR values

Figure 16 is the result from CoMP using dedicated scheduling spectrum. As we can see, implementing CoMP with a

dedicated spectrum scheduler grid makes the SINR values higher in a big part of the cell. However, the SINR performance decreases when we dedicate the spectrum.

As we can see in Figure 16, the effect of dedicating the spectrum is causing a degradation of the SINR. Using shared spectrum combined with CoMP provides higher SINR than using dedicated spectrum.

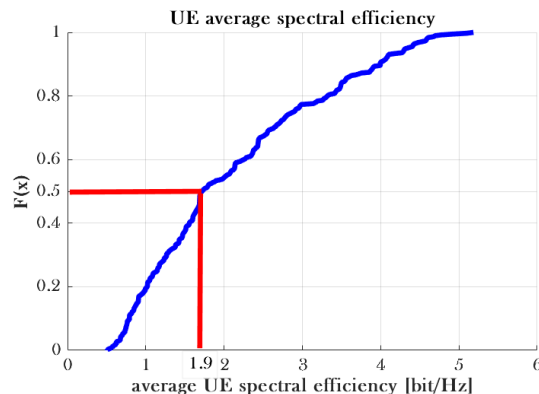


Figure 17. UE average spectral efficiency (bit/Hz) versus F(x)

Figure 17 depicts the UE average spectral efficiency versus $F(x)$. From the graph for $F(x) = 0.5$ the average spectral efficiency is 1.9 (bit/Hz). The performance decreases when compared with previous CoMP results.

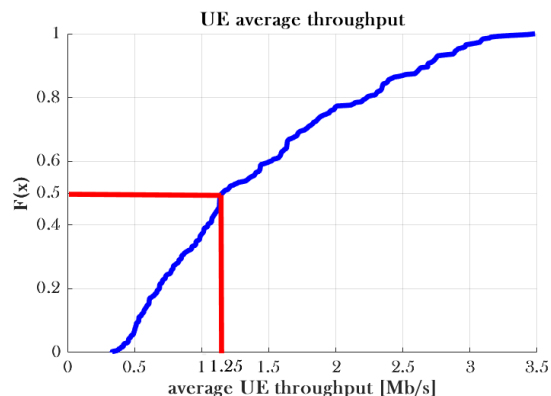


Figure 18. UE average throughput (Mb/s) versus F(x)

The graph of UE average throughput (Mb/s) is depicted in Figure 18. For $F(x) = 0.5$ the average throughput is 1.25 (Mb/s). The throughput performance decreases with dedicating the spectrum.

TABLE I. DIFFERENT MATLAB RESULTS

	UE average spectral efficiency (bit/Hz)	UE average cell throughput (Mb/s)
Basic macro BS	0.6	2
CoMP using shared spectrum	2.9	9
CoMP using dedicated spectrum	1.9	1.25

The performance was evaluated in terms of SINR, average spectral efficiency and average throughput. The results show that the SINR increases when we implement CoMP. The average throughput and the average spectral efficiency are also higher for CoMP using shared spectrum. The use of RRH and

CoMP methods almost double the average spectral efficiency compared to that for conventional scheme. The throughput is also higher when shared spectrum and CoMP are employed simultaneously compared to that when CoMP using dedicated spectrum is employed. This shows that shared spectrum within CoMP methods can reduce the ICI effectively. The SINR performance decreases with increasing the number of FRF in dedicated spectrum. However, the average throughput improves by approximately 9 times when shared spectrum within CoMP techniques are employed.

V. CONCLUSION

In this paper, we had focused on CoMP topology using different frequency spectrum design shared and dedicated for wireless communication systems, namely within the context of RRH antennas, and HetNet scenarios. Performance results are obtained not only in terms of UE average spectral efficiency, but also in terms of UE throughput, that is now increasingly became an important design indicator for planning, deploying and optimizing next generation mobile networks. One of the simplest ways of improving system performance is to enhance the signal power. This goal can be achieved using LTE SLS to joint transmission down link CoMP scheme. As the same frequency bandwidth is used, the system is very sensitive to ICI. The utilized CoMP scheme with dedicated spectrum is introduced to improve the performance of cell edge users by customizing the repartition of bandwidth. The use of shared spectrum increases the cell average throughput. The simulation setup is based on 3GPP Technical Specification Group reports. CoMP plays an important role in improving the system performance and, therefore, this work can be extended such that the optimal parameters are determined for the CoMP and further parameters can be analyzed to optimize the system capacity and end-to-end delay.

ACKNOWLEDGMENT

This research was supported by The European Commission H2020 programme under grant agreement no. 671705 (SPEED-5G) project.

REFERENCES

- [1] D. Lee, H. Seo, B. Clerckx, E. Hardouin, D. Mazzarese, S. Nagata, and K. Sayana, "Coordinated multipoint transmission and reception in lte-advanced: deployment scenarios and operational challenges," *IEEE Communications Magazine*, vol. 50, no. 2, pp. 148–155, February 2012.
- [2] L. Chenand, W. Chen, B. Wang, X. Zhang, H. Chen, and D. Yang, "System-level simulation methodology and platform for mobile cellular systems," *IEEE Communications Magazine*, vol. 49, no. 7, pp. 148–155, July 2011.
- [3] M. Taranetz, T. Blazek, T. Kropfreiter, M. K. Mller, S. Schwarz, and M. Rupp, "Runtime precoding: Enabling multipoint transmission in lte-advanced system-level simulations," *IEEE Access*, vol. 3, pp. 725–736, 2015.
- [4] A. Damnjanovic, J. Montojo, Y. Wei, T. Ji, T. Luo, M. Vajapeyam, T. Yoo, O. Song, and D. Malladi, "A survey on 3gpp heterogeneous networks," *IEEE Wireless Communications*, vol. 18, no. 3, pp. 10–21, June 2011.
- [5] I. L. Cherif, L. Zitoune, and V. Vque, "Performance evaluation of joint transmission coordinated-multipoint in dense very high throughput wllans scenario," in *2015 IEEE 40th Conference on Local Computer Networks (LCN)*, Oct 2015, pp. 426–429.
- [6] Y. Jie, A. Alsharoa, A. Kamal, and M. Alnuem, "Self-healing solution to heterogeneous networks using comp," in *2015 IEEE Global Communications Conference (GLOBECOM)*, Dec 2015, pp. 1–6.

- [7] S. Yi and M. Lei, "Backhaul resource allocation in lte-advanced relaying systems," in *2012 IEEE Wireless Communications and Networking Conference (WCNC)*, April 2012, pp. 1207–1211.
- [8] M. Sawahashi, Y. Kishiyama, A. Morimoto, D. Nishikawa, and M. Tanno, "Coordinated multipoint transmission/reception techniques for lte-advanced [coordinated and distributed mimo]," *IEEE Wireless Communications*, vol. 17, no. 3, pp. 26–34, June 2010.
- [9] Y. N. R. Li, J. Li, W. Li, Y. Xue, and H. Wu, "Comp and interference coordination in heterogeneous network for lte-advanced," in *2012 IEEE Globecom Workshops*, Dec 2012, pp. 1107–1111.
- [10] A. Marotta, K. Kondepu, F. Giannone, S. Doddikrinda, D. Cassioli, C. Antonelli, L. Valcarengi, and P. Castoldi, "Performance evaluation of comp coordinated scheduling over different backhaul infrastructures: A real use case scenario," in *2016 IEEE International Conference on the Science of Electrical Engineering (ICSEE)*, Nov 2016, pp. 1–5.
- [11] S. H. Park, O. Simeone, O. Sahin, and S. Shamaï, "On remote radio head selection for the downlink of backhaul constrained network mimo systems," in *2014 48th Annual Conference on Information Sciences and Systems (CISS)*, March 2014, pp. 1–5.
- [12] J. C. Ikuno, M. Wrulich, and M. Rupp, "System level simulation of lte networks," in *2010 IEEE 71st Vehicular Technology Conference*, May 2010, pp. 1–5.
- [13] D. Matsuo, R. Rezagah, G. K. Tran, K. Sakaguchi, K. Araki, S. Kaneko, N. Miyazaki, S. Konishi, and Y. Kishi, "Shared remote radio head architecture to realize semi-dynamic clustering in comp cellular networks," in *2012 IEEE Globecom Workshops*, Dec 2012, pp. 1145–1149.
- [14] K. Bkowski, M. Rodziejewicz, and P. Sroka, "System-level simulations of selected aspects of 5g cellular networks," in *2015 International Symposium on Wireless Communication Systems (ISWCS)*, Aug 2015, pp. 711–715.
- [15] Y. Wang, J. Xu, and L. Jiang, "Challenges of system-level simulations and performance evaluation for 5g wireless networks," *IEEE Access*, vol. 2, pp. 1553–1561, 2014.